Sediment transport on various depth contours of the 'Holland Coast' shoreface

MSc final project report

ing. P.P.Knook

Delft University of Technology

In cooperation with:

Deltares

January 2013

Sediment transport on various depth contours of the 'Holland coast' shoreface

MSc final project report

Ing. P.P. Knook

Delft University of Technology
January 2013

TUDelft
Technische Universiteit Delft

Faculty of Civil Engineering
Department of Hydraulic Engineering
Section Coastal Engineering

In cooperation with

Deltares
Enabling Delta Life

Graduation committee

Prof. dr. ir. M.J.F. Stive	Delft University of Technology
Ir. D.J.R. Walstra	Delft University of Technology/Deltares
Dr. ir. J.S.M. van Thiel de Vries	Delft University of Technology/Deltares
Dr. A.J.F. van der Spek	Delft University of Technology/Deltares
Dr. J.E.A. Storms	Delft University of Technology

Sediment transport on various depth contours of the 'Holland Coast' shoreface

Understanding sediment transport in coastal regimes is a perplex challenge that in all likelihood will continue to frustrate coastal researchers and engineers for generations to come
(Hughes, 1993)

Voor mijn opa,
Jaap Vijfhoek (1930-2012)

Sediment transport on various depth contours of the 'Holland Coast' shoreface

Preface

This thesis report is written as a final part of the master Hydraulic Engineering, specialization Coastal Engineering, of the faculty Civil Engineering and Geosciences of Delft University of Technology. This project was performed in cooperation with Deltares.

The study concerns an investigation into sediment transport on various depth contours of the 'Holland Coast' shoreface. Morphological investigation into further substantiate the Coastal Foundation (Kustfundament) was the key element (target) in this research, an initiative taken by ir. Walstra and dr. ir. van Thiel de Vries.

Therefore it would only be appropriate to thank ir. Walstra and dr. ir.van Thiel de Vries first, as they were also my daily supervisors. They guided me through the processes of my thesis in good and bad times. I would like to thank professor Stive as well for being chairman of my graduation committee. Furthermore, I would like to thank Dr. van der Spek and Dr. Storms for their remarks, information and given insights. Besides that, I would like to thank the graduation students and employees of Deltares for the exchange of information, ideas and support with Matlab and Unibest-TC.

Last but not least, I would like to thank my parents, my family and friends (especially my parents). Without them I would not have been able to do this. Finally, I would like to thank my girlfriend Novie for everything.

Patrick Knook

Delft, January 2013

Sediment transport on various depth contours of the 'Holland Coast' shoreface

Abstract

The scientific foundation to maintain the Holland Coast shoreward of the -20m depth contour is limited. It is assumed that profile perturbations shoreward of the -20m depth contour influence the coast within a time scale of 50 to 200 years. Hence, seaward of -20m NAP dredging companies are allowed to dredge sand. The dredged material is amongst others applied in nourishments near the beach. In order to naturally preserve the shoreface of the Dutch Coast, coastal policy in The Netherlands prescribes that the sediment volume of Holland Coast should be preserved shoreward of the -20m depth contour. The volume required to accomplish this can be significantly reduced in case a shallower depth contour can be assumed. In order to investigate the influence of perturbations shoreward of -20m NAP and to validate the scientific foundation of the -20m depth contour, cross-shore sediment transport on various depth contours will be analysed. The emphasis of this research will lie on sediment transport on the lower shoreface (deeper than -10m NAP).

Sediment transport will be evaluated with the model Unibest-TC. First, sediment transport sensitivity on a straight slope due to varying parameters (wave height, wave period, grain size, slope steepness, water depth and magnitude of Longuet-Higgins streaming) is analysed. Besides, non-dimensional numbers and transport equations were considered to extend the analysis. In the analysis the dominance, direction and magnitude of the wave related and current related transport of both the bed load and suspended load is investigated. Subsequently, sediment transport due to variable wave conditions on various depth contours is examined from the shoreface profile of Noordwijk. Also the situations with a variable wave angle and a tidal current was considered. Finally, morphological simulations, including a 100-year profile evolution and profile perturbations (e.g. sand pits) located on the lower shoreface, were performed.

Shoreface sediment transport depends on the wave steepness in combination with the slope steepness for every depth contour. This was concluded by analysing sediment transport sensitivity for a range of parameter settings. Sediment transport due to wave action is particular present on the upper shoreface. Although, the onshore directed bed load transport is dominant on the lower shoreface (provided that the orbital velocity induced shear stress exceeds the critical shear stress), its relative contributions is negligible in case a tidal current is included. It was found that low amplitude waves are responsible for the largest profile changes. On the lower shoreface, the tidal current induced offshore sediment transport is dominant. Onshore transport on the upper shoreface and offshore transport on the lower shoreface induce a lower shoreface flattening and an upper shoreface steepening. Perturbations located at the -15m, -20m and -25m NAP depth contours propagate shoreward caused by tidal current induced concentration gradients. Sediment transport induced by waves result in diffusion of profile perturbations and a limited shoreward shifting. Only at -15m NAP a clearly visible propagation is visible. A situation including a tidal current, results in a larger shoreward propagation of the sand pits/artificial ridges at -25m NAP than at -15m NAP. A larger depth dependent tidal velocity induced sediment transport gradient at -25m NAP is responsible for this phenomenon. So, the interaction of waves and tidal currents is of great importance on the entire shoreface profile and may have a large impact on cross-shore sediment transport.

Deltares

Table of contents

1 Introduction

The scientific foundation to maintain the Holland Coast shoreward of the -20m depth contour is limited. It is assumed that profile perturbations shoreward of the -20m depth contour influence the coast within a time scale of 50 to 200 years. Hence, seaward of -20m NAP dredging companies are allowed to dredge, and apply dredged material in nourishments near the beach to naturally preserve the shoreface of the Dutch Coast. It would be economically beneficial for dredging companies to dredge closer to coast, because the -20m NAP depth contour is located 5 -20km offshore. Secondly, as Dutch Coastal policy prescribes the sediment volume of Holland Coast should be preserved shoreward of the -20m depth contour. The required volume to achieve this can be significantly reduced in case a shallower depth contour is assumed. In order to investigate the influence of profile perturbations shoreward of -20m NAP and to validate the scientific foundation of the -20m depth contour, sediment transport on various depth contours will be analysed in this thesis. The emphasis will lie on sediment transport on the lower shoreface (deeper than -10m NAP).

1.1 The Dutch Coast

The Netherlands is a low-lying country, which is adjacent to the North Sea and the main part of this land is located below mean sea level. Therefore, there is a constant threat of inundation, unless the coastal protection is sufficient. The Dutch coast is to a large extend protected by a natural 'soft' protection in the form of sand dunes. However, due to relative sea level rise and land subsidence, the safety level of the sandy coast should be adjusted.

To protect the Netherlands from the water, the Dutch government chose the maintenance strategy to 'preserve' the coastal system out of four possible options (Rijkswaterstaat, 1989). The other options were coastline retreat, partly preserving the coastline or seaward extension of the coastline. Because eco-friendly sand nourishments could be used, the decision was made to ''dynamically preserve'' the coastal system. The Dutch government decided that the coastal system should be preserved as it was in 1990 (Rijkswaterstaat 1989). ''Dynamically preserve'' entails the concurrent rise of the coastal profile along with, for instance, relative sea level rise.

Figure 1.1 Coastal Foundation (https://publicwiki.deltares.nl/display/KvdNLK/Beleid+Kustfundament). The yellow hatched area represents the Coastal foundation.

1.1.1 Coastal foundation

The coastal foundation consists of three parts, namely the Holland Coast, the Wadden Sea and the Westerschelde estuary (Stolk, 1989). The coastal foundation is a body of sand along the Dutch coast, stretching from the Belgium border up to the German border (see figure 1.1). The inner boundary is located at the inner side of the dunes and the seaward boundary extends to a depth of -20m NAP. The Holland Coast has an uninterrupted coastline, whereas the Wadden Sea area consists of tidal inlets and the southern deltaic area consists of (closed-off) estuaries.

1.1.2 Research

The -20m NAP seaward border of the coastal foundation has been discussed a lot (Rijkswaterstaat, 1989). The basic assumption is that beyond this border, no significant sediment transport on time scales of 50-200 years occurs, although a physical proof is not yet given. This seaward boundary influences the maintenance strategy to ''dynamically preserve'' the Dutch Coast. With a reduction in depth at the seaward border of only one or two meters, the volume of sand which ought to be preserved and therefore the costs to maintain it will significantly decrease.

In this research, the seaward extend of the morphological active zone will be investigated. Longer time scales will be regarded to include very slow or event driven processes, which contribute to long-term, large-scale net sediment transports. These processes can cause erosion or sedimentation over long time scales, say decades to centuries. Within this research, the sensibility of the -20m NAP will be evaluated, which might affect the presented maintenance strategy.

1.2 Objective and hypotheses

The objective of this master thesis is to gain insight into the dominant physical processes over the middle and lower shoreface along the Dutch coast in consideration of various time scales. Hence, *sediment transport for various depth contours over a period of 100 years* will be examined. The emphasis of this study will lie on the lower shoreface.

1.2.1 Hypotheses

The most important hypothesis should help to obtain insight in the sensibility of the -20m NAP depth contour as the seaward boundary of the coastal foundation for different time-scales. Through various profile perturbations like dredging pits or shoreface nourishments relevant results can possibly be investigated. In the context of investigating sediment transport on several parts of the shoreface, the question arises whether it is the event driven processes or the continuous processes which are responsible for the upper- and lower shoreface morphodynamics. So which (wave) conditions cause morphodynamics on different parts of the shoreface? Furthermore, Stive and de Vriend (1995) concluded that the suspended load is dominant on the lower shoreface and that bed load transport can be disregarded. Finally, an implementation of the tidal current in Unibest-TC will be evaluated. This leads to the following hypotheses:

- Within a time scale of 100 years, there's no substantial sediment transport at -20m NAP that influences the upper shoreface.

- Sand borrow pits between -20m NAP and -18m NAP affect the upper shoreface within a time scale of 100 years.

- Sand pits and sand ridges located on various depth contours have different time scales.

- The continuous processes, in contrast to event driven processes, are responsible for the lower shoreface morphodynamics.

- Implementation of a tidal current in Unibest-TC makes the suspended load transport dominant on the lower shoreface.

1.3 Approach

As a starting point, the historical evolution of the Holland coast and contributory dominant physical processes will be examined. This might entail the evolution of the Holland coast and which processes should be considered investigating sediment transport on the shoreface. It, too, reveals whether the shoreface is steepening or flattening over the last centuries and this should be taken into account examining model results later on. Subsequently, a suitable model will be selected. This model should be able to simulate the profile evolution over a long period and include the most important physical processes. The next step is to obtain better insight in shoreface processes by elaborating on the different components of sediment transport in the model and the wave conditions that are responsible. With gained insight, sediment transport on the shoreface for various depth contours can be classified. Successively, percentages of occurrence will be added to sediment transport patterns that vary with wave and tide conditions, to obtain a realistic representation of the direction and magnitude of the shoreface sediment transports. Finally, morphological simulations will be performed to evaluate the shoreface profile changes. By examining the progress of excavations and nourishments located on selected depth contours, the different behaviour of sediment transport on various depth contours can be examined.

1.4 Scope

1.4.1 Uniform coast

Assessing sediment transport on the shoreface profile for certain depth contours, a simple case scenario with a uniform coast will be regarded. Moreover, the scope of this research is to examine the Holland coast, which is more or less a uniform stretch of coast. Nevertheless, longshore processes might be present (i.e. additional shear to tide and wave driven longshore flow), but gradients in longshore processes are assumed to be zero. Although, some disturbances are present along the Holland coast, which can be taken into account in the modelling by applying boundary conditions. In addition, some assumptions are made which are described in the next section.

1.4.2 Assumptions

To make representative simulations, some assumptions are made. For instance, the dunes will be disregarded as research will be done into the offshore extension of sediment transport. Instead, a boundary condition will be imposed to make the simulations realistic and valid. Furthermore, interruptions will be ignored, which are listed next:

1.4.2.1   Interruptions:

- Tidal channels and ebb tidal deltas enclosing the Holland Coast
- Shipping lanes (e.g. IJ-channel)
- Anthropogenic influences (Harbour moles, groynes, sea dikes, etc.)
- Borrow areas
- Dumping sites
- Plateaus and terraces (artificial in the South and two at the Northern side)
- Rip currents
- Debouching rivers

1.5   Thesis outline

Chapter 2 reveals some background information of the Holland coast with the existing dominant physical processes. Moreover, the selected model will be explained. Subsequently in chapter 3, the model processes will be investigated. A straight profile will be assumed including a variable slope steepness, grains size and wave height and period. The relative importance of several sediment transport components will be examined upon their dominance, direction, magnitude and whether what forcing causing this. Based on the insight in the sediment transport components, a realistic Holland coast profile will be regarded in chapter 4. In this case the dominance of the components will be examined for various parts of the shoreface and a classification will be set up. In chapter 5 the percentages of occurrence of wave conditions will be added and realistic representation of sediment transport on the shoreface, including a sensitivity analysis, will be elaborated. By considering percentages of occurrence of certain wave conditions, the dominant processes (continuous or event-driven) which are responsible for the lower shoreface morphodynamics can be evaluated. Subsequently, morphological simulations will be performed; results will be investigated and discussed in chapter 6. Profiles including and excluding profile perturbations are considered to investigate the shoreface profile evolution and sediment transport on various depth contours. Finally, conclusion and recommendations will be given in chapter 7.

2 Background and model description

To get a better understanding in the evolution of the Holland coast, its geological history will be described next. Physical processes on the shoreface, which are present nowadays, will be discussed afterwards. Finally, the selected model Unibest-TC will be explained. This chapter reviews some background information, which is important to gain insight and a better understanding in sediment transport on various parts of the shoreface.

2.1 The Holland coast

2.1.1 Historical evolution

The Holland coast is located adjacent to the North Sea and has a long history before it became the uninterrupted coastline as presently known. The present day Holland coast (from Hoek van Holland to Den Helder) is enclosed by the entrance channel of the Wadden Sea south of Texel and delta area of Zeeland (see figure 2.1). These interruptions in the Dutch coast (from the south of Zeeland to the border with Germany in the North) still influence sediment transport along the Holland coast.
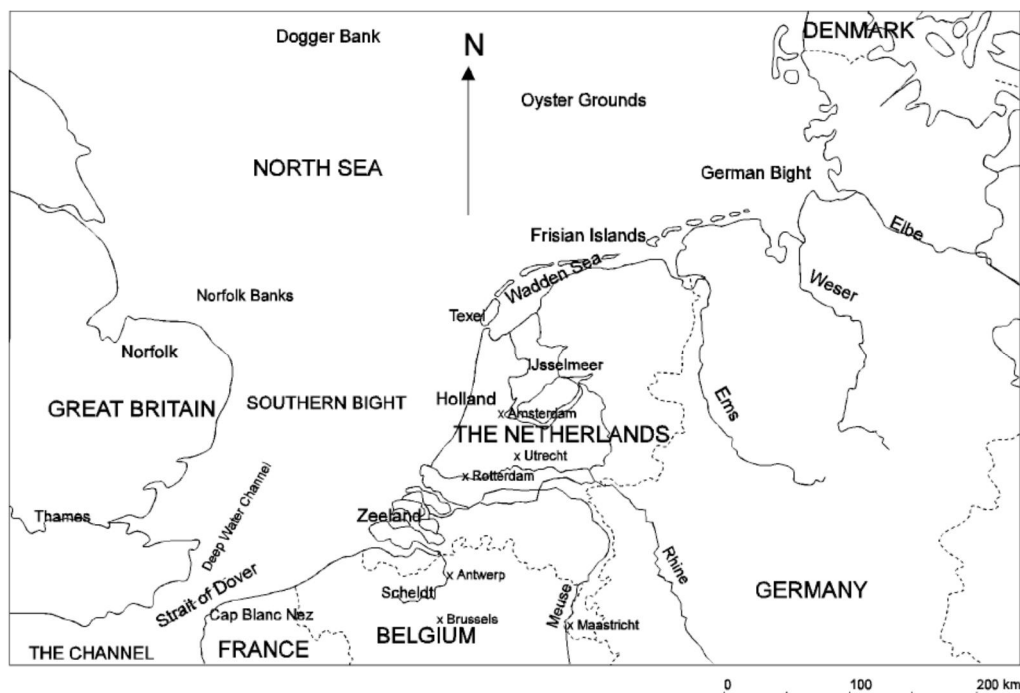
Figure 2.1 Map of the North Sea (from Beets en Van der Spek, 2000)

In the Atlantic (8000-5000 yrs B.P.), the Holland coast was completely different shaped than nowadays. The Holland Coast consisted of two headlands separated by a large tidal basin. Around 6000 yrs B.P., a strong decrease in the rate of sea level rise caused an accumulation of sediments in the basin and silted up the tidal channels. The estuarine deposits near the Holland Coast are depicted in figure 2.2 A. This caused the barrier to propagate seaward and lasted for some thousands of years until it enclosed the two headlands. According to Beets and Van der Spek (2000), the available sediments are thought to originate from reworking of ebb-tidal deltas of former inlets, by erosion of the headlands, by cross-shore transport and a

small amount of alluvial source. Stive and de Vriend (1995) assume that the wave driven alongshore sediment transport is responsible for this redistribution of sediments.

Although the prograding barrier enclosed the headlands, still some rivers debouch in the North Sea. Though it was thought to be the estuarine deposits stated by Beets et al. (1992) which were responsible for transgression of the coastline and not riverine deposits. The Holland Coast barrier including some protruding rivers which are debouching in the North Sea are indicated in figure 2.2 B and C.

Around 2000 yrs B.P. the shoreline was situated near the present shoreline and the progradation proceeded only slowly. Due to a lack of sediment supply the transgression of the coastline slowly diminished. While the Holland Coast already was enclosed, the Wadden Sea remained a tidal basin due to a lack of sediment supply. The still prograding Holland Coast barrier remained and reacted to this decrease in sediment supply by steepening of the upper shoreface (Beets et al., 1992).
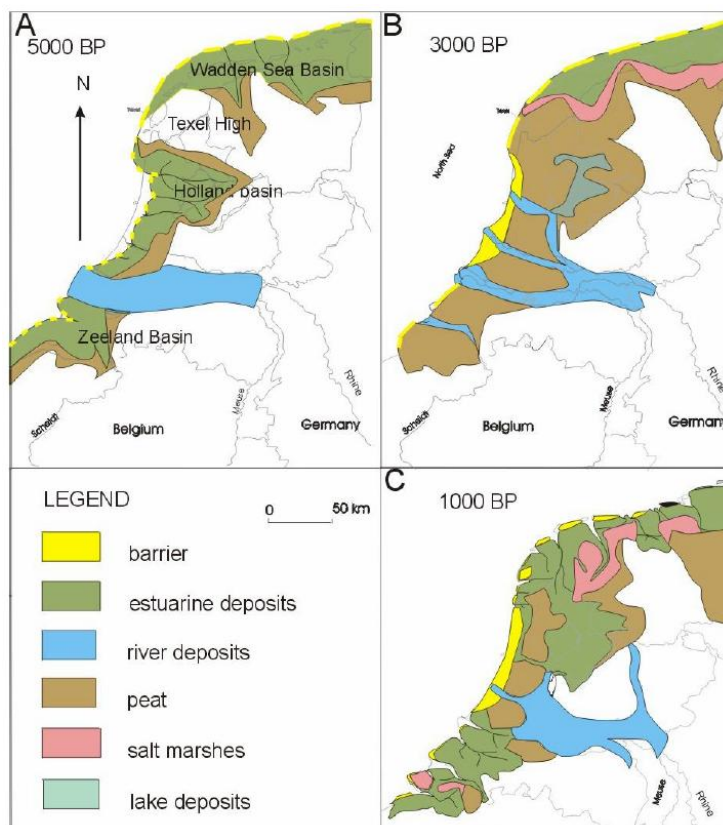
Figure 2.2 Historical evolution Dutch Coast (Beets en Van der Spek, 2000)

Considering the observations that the upper shoreface is steepening (Van der Valk, 1996), the question arises whether is the longshore transport or cross-shore transport causing this, while keeping in mind that the gradients of longshore transport decreased in time. The reducing longshore transport gradients resulted from the retreating headlands, which were eroded and sediment was distributed over the Holland Coast, and the eroding alluvial plain in the south. According to Stive et al. (1990), the longshore net losses in the active zone along the Holland Coast (-8m NAP) are, at present day, so small that the shore normal shoreface feeding, by wave asymmetry and upwelling, can compensate for these losses. This causes the upper shoreface to steepen and the middle and lower shoreface to flatten (Stive and de Vriend, 1995)

2.1.2   Present day

Present day, the Holland Coast has approximately a SW-NE orientation and has a slope of 1:1000 near the -20m NAP depth contour, which steepens towards the coast to about 1:100 near -10m NAP (Van Alphen et al., 1990). According to van Alphen, the -20m NAP depth contour is thought to be the transition of the shoreface to the continental shelf or seafloor. The edge of the shoreface can either be located at 5km to 15km offshore, depending on the location along the Holland Coast. The shoreface, thus, presently has a gentle lower shoreface (1:1000), which becomes steeper when reaching the upper shoreface (shallow than -10m NAP).

According to Stive and de Vriend (1995), the upper shoreface evolves due to the presence of waves and in particular the effect of dissipation of wave energy. The lower shoreface is affected by shoreface currents, like the tide, and shoaling and refracting waves. The upper shoreface, which have often been called the 'active zone' with an offshore extension to the 'depth of closure', stated by Hallermeier (1981). However, this closure depth is conditional and therefore is variable with the time scale considered (Nichols et al., 1998).
A tidal current is present along the Holland Coast, which changes direction during its tidal cycle. The residual tidal current is in south-north direction parallel to the Holland Coast. The tide along the Holland Coast originates from the tide present in the Atlantic Ocean, which enters the North Sea passing the north of Great-Brittan. Due to the geometry of the North Sea basin, an amphidromic system is existing. The tidal current circles counter clockwise around the amphidromic point and therefore have an residual tidal current in SW-NE direction along the coast. In case the vertical tide has reached its maximum at the northern end of the coast and its minimum at the southern end, the horizontal tidal current is in opposite direction, namely NE-SW.

The Dutch Coast predominantly experiences wind waves, due to the adjacent shallow North Sea. Swell waves can only enter the Holland Coast through the entrance between England and Denmark, which is bordering the Atlantic Ocean. The south-west wind direction is dominant. However, regarding normative storms the north-west direction is most important (Roskamp, 1988). The yearly averaged wave height and period are 1m and 5s (Van Alphen et al., 1990).

Although the Holland Coast is an uninterrupted coastline, for which physical processes will be described in the next section, the debouching Rhine at the southern end and the tidal channel at the northern end do influence these processes. The freshwater debouching from the river Rhine into the North Sea and the presence of Coriolis, which is caused by the earth's rotation, cause that the fresh water that enters the North Sea in the south bends towards the north. As a result salinity gradients over depth are present on the shoreface (especially along the southern Holland Coast which may cause an onshore net flow component (De Boer, 2008)). In the north, the tidal channel called Marsdiep is still assumed to experience erosion (Kragtwijk, 2001) and the tidal current through these tidal channels is affecting the processes on the uninterrupted shoreface as well.

2.2   Physical processes

Prior to describing the actual physical processes, a description of the shoreface will be presented. As it will become clear in the next section, the shoreface can globally divided in two parts on which different processes are dominant.

2.2.1   Description shoreface

The shoreface can be divided in two or three parts, namely the upper-, middle- and lower shoreface. Often, the middle- and lower shoreface are considered a unity and one is referring to the 'lower shoreface'. The middle shoreface is, in fact, the transition between the highly active upper shoreface and slow responding lower shoreface (Stive and de Vriend, 1995). The upper shoreface is wave-dominated, whereas the lower shoreface is tide-dominated. Consequently, the middle shoreface is subjected by a mixed wave-tide dominated zone.
The upper shoreface extends from mean low water (MLW) up to the zone where waves start to break. This defines the region where present hydrodynamics control sediment transport directly (within a period of 1 day). This landward boundary is fixed on MLW, in contrast with the seaward boundary of the surf zone, which is variable. Since the seaward boundary of the upper shoreface is variable, a yearly-average boundary is often assumed. This variability is induced by the offshore migration of breaker bars and varying wave conditions. Some of these boundaries are indicated in figure 2.3.

The middle- and lower shoreface zone extends from the seaward boundary of the upper shoreface until the inner shelf or sea floor. The sea floor is defined as the area where the slope is less than 1:1000 (Van Alphen and Damoiseaux, 1987). According to them, this 'flat' sea floor is a different morphological zone and differs from the shoreface zone. Therefore, it can be assumed to be a good distinction. On the middle/lower shoreface, the present hydrodynamics has limited effect on the morphology as it is merely affected by long term and very slow processes.
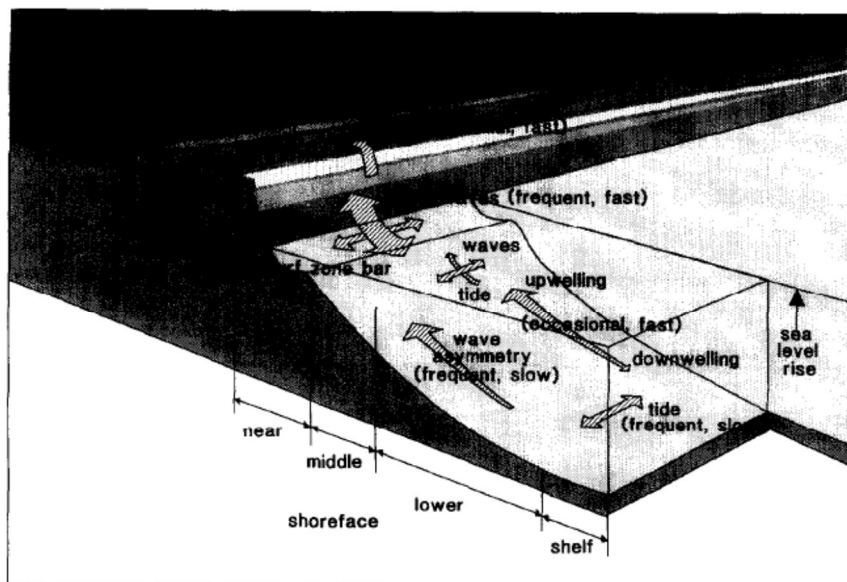
Fig. 1. Overview of hydrodynamic processes on the shoreface (modified after Stive et al., 1990).

Figure 2.3 Hydrodynamic processes on the shoreface (Stive and de Vriend, 1995)

The shape of the shoreface profile differs along the entire Dutch coast. For instance, the shoreface profile along tidal deltas has a convex shape, while the shoreface profile along the Holland coast has a concave shape. However, the convex profiles along the Holland coast vary also. These shoreface profiles can either be stable or evolving, which indicates sedimentation or erosion of the shoreface, see figure 2.4. The upper-, middle- and lower shoreface all have different slopes, between which transports take place. A steeper middle

shoreface represents an accreting (prograding) upper shoreface, but a gentle middle shoreface represents erosion (Stive et al., 1990). The lower shoreface mainly provides the upper shoreface of sediment, which eventually becomes gentler. A gentle shoreface profile, thus, represents erosion, whereas a more convex curved profile represents sedimentation.
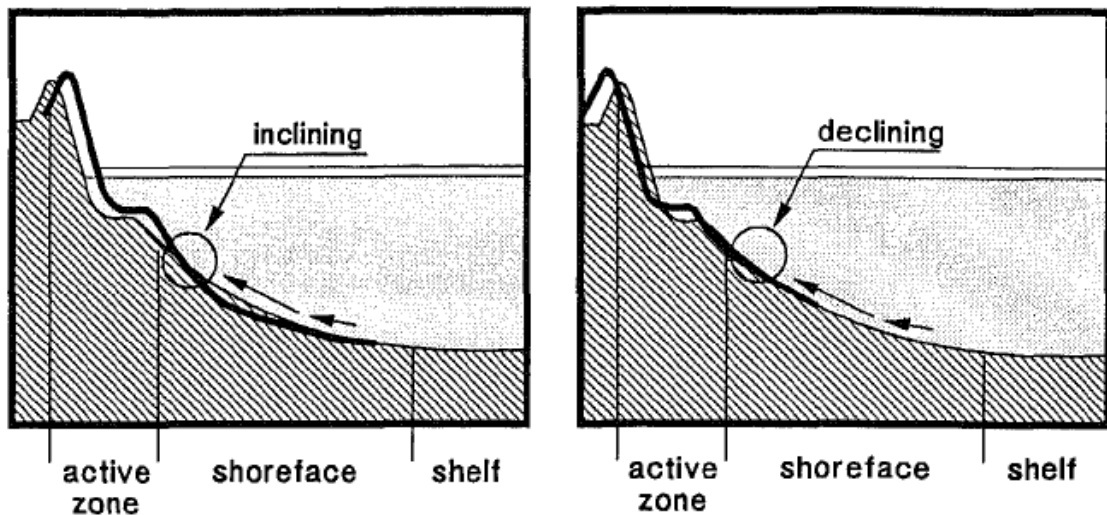
Figure 2.4 Evolving shoreface profiles (Stive et al., 1990). The left figure: upper shoreface steepening. The right figure: upper shoreface flattening.

2.2.2 Dominant processes

2.2.2.1 *Upper shoreface*

The upper shoreface is wave-dominated due to wave asymmetry, breaking waves and wave induced currents (van Alphen et al., 1990). Whereas wave asymmetry can induce an onshore transport of sediment during calm periods, the undertow causes a transport of sediment offshore during storm events. Obliquely incident-breaking waves also induce longshore sediment transport. The cross-shore and longshore transport of sediment is therefore dominated by waves. Although considering short, incident waves, infra-gravity waves should be regarded as well. Before waves break, the bound long waves cause an offshore transport of sediment, because the trough of the bound long waves coincides with the highest waves of the wave group. High wave stir up more sediment, while the long wave trough velocities are offshore directed. The long wave contribution is directed offshore until the correlation between the short wave variance and long wave become positive in the surfzone (Roelvink and Stive, 1989). The long wave contributions can be both onshore and offshore directed on the upper shoreface.

Cyclic breaker bar behaviour is present as well on the upper shoreface. The residual effect of calm and storm periods cause an offshore migration of these breaker bars. Obliquely incident waves stimulate the growth of bars, whereas storms and normal incident waves flatten the bars. Whether cyclic bar behaviour on the upper shoreface contributes to the long-term shoreface is not clear.

Storm events induce higher waves and waves break at larger depth. This influences the 'active zone' of sediment transport and accordingly the seaward extension of the upper shoreface. Because waves break at larger depth, sediment is mobilized farther offshore. Besides, higher and shoaling waves can also stir up sediment more intense and the influence is extending farther offshore during extreme events. As storm events differ in intensity and occurrence, the seaward extension of the 'active zone' is therefore time-scale dependent as well. So, the occurrence of extreme events widens the offshore extension of sediment transport and thus influence the middle/lower shoreface as well.

2.2.2.2   *Middle/lower shoreface*
The lower shoreface is tide-dominated, where a mix of waves and tides dominates the middle shoreface. A variety of processes is present on the middle/lower shoreface. The tide dominates the alongshore transport on the lower shoreface due to the fact that tidal currents are mainly alongshore directed (van Alphen et al., 1990). The shoaling waves stir up the sediment, which consequently is transported alongshore by the current. Cross-shore transport is induced by positively skewed (asymmetric), shoaling waves (Stive and de Vriend, 1995). As mentioned above, bound long waves mainly cause an offshore transport on the middle shoreface (Roelvink and Stive, 1989).

The wave boundary layer, see figure 2.5, is the transition layer between the bed and the layer of 'normal' oscillating flow. In this layer, water moving along the bed incurs a shear stress on the bed and can set sediment grains into motion. Besides a purely oscillatory flow, a non-zero wave-averaged horizontal flow, which is called streaming, is found (Longuet-Higgins, 1953). For linear waves the streaming is directed in wave propagation direction. Bowen (1980) stated that the effect of wave asymmetry in deep water is negligible in the wave boundary layer streaming. The relative dominance of the wave boundary layer streaming should be regarded in cross-shore sediment transport.
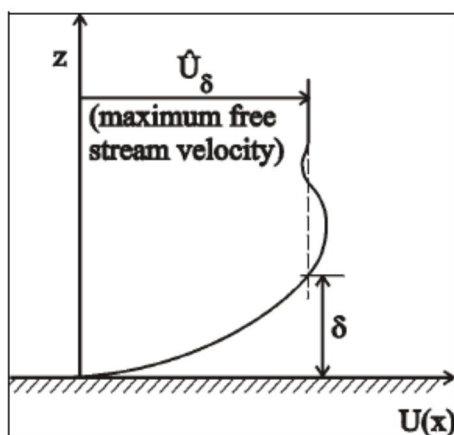
Figure 2.5 δ is the wave boundary thickness (Bosboom and Stive, 2011)

Besides tidal and wave action, several other processes contribute to sediment transport on the lower shoreface. For instance, parallel wind causes a cross-shore current along the bottom (Niedoroda et al., 1985). Other processes involved are pressure gradients, density currents, upwelling and downwelling. Up- and downwelling are large-scale circulations caused by counteracting the pressure gradients and possibly contribute to the transport on the middle/lower shoreface.

Another interesting phenomenon is the presence of sand waves bordering the toe of the shoreface. Sand waves have a length of a few kilometres, a width of a few hundred meters

and a height in the order of meters. These sand waves propagate with a velocity of approximately 100m/year along the shoreline. It is questionable, according to past research, whether these sand waves are involved with the erosion or accretion of the shoreface and influencing the shoreface profile evolution.

As a general note, it can be said that the bathymetry of the shoreface is important and hard erodible sediments impede transports on the shoreface.

2.3 Model Unibest-TC

To investigate the offshore-extending sediment transport on certain depth contours and considering an alongshore uniform coast, a cross-shore sediment transport model is best to be used. As stated before, an alongshore uniform beach will be assumed to examine these phenomena. According to Roelvink and Stive (1989), a 1D model should be used in case this assumption is made. These assumptions imply the deep water wave and current conditions to vary slowly along the Holland coast and that on an alongshore scale of tens of kilometres the depth contours are approximately parallel. Under these conditions, the problem is assumed to reduce to a one-dimensional problem.

A model that fits best with the above conditions is Unibest-TC. Unibest-TC represents ''UNIform BEach Sediment Transport (Time-dependent Cross-shore)''. This model performs well regarding cross-shore transport dominated cases, but performs less in case 3D-phenomena become dominant. The predecessor of Unibest-TC is CROSTRAN, which has been used multiple times in similar past research. Van Rijn et al. (1995) also used Unibest-TC to assess the yearly-averaged sand transport at the -20m and -8m NAP depth contours. Although Unibest-TC is designed to assess the morphodynamics in the surfzone, the study of Van Rijn et al. (1995) proves that modelling of sediment transport on the lower shoreface is possible. Additional, much historical research has been performed, but mainly in the form of behaviour based models. On the other hand, a model like Delft3D would be too comprehensive and that is completely unnecessary considering the scope of this investigation.

Unibest-TC is a process-based one dimensional model, which makes use of the (upgraded) Bailard-Bagnold sediment transport formulation. This formulation is used considerably in similar past researches and seems to perform well. In Unibest-TC, instead of the Bailard formulation, a new transport formulation according to Van Rijn (1995) is used, because it is able to separate the bed-load and suspended transport. The instantaneous bed-load transport and the non-instantaneous can now have different directions, where it was impossible in previous versions of the formulation. According to Stive and De Vriend (1995), suspended load is dominant on the middle shoreface of the Holland coast and bed load is disregarded. With the division of the different sediment transport modes, this hypothesis can be investigated with this model.

The non-instantaneous suspended transport is approximated by the product of the mean current and mean concentration integrated over the vertical. The vertical velocity distribution, to determine the mean current, is determined by solving the horizontal momentum balance. Using a quasi-3D model, according to Roelvink and Reniers (1994), in which effects of wind stress, breaking-induced forcing, surface slope and the wave boundary layer are taken into account. A parabolic distribution of the eddy viscosity is implemented in which effects of turbulence are included. In fact, the vertical can be divided in three layers, namely:

- the surface or trough-to-crest layer,
- the middle layer and
- the bottom boundary layer.

The mean current is known via the condition that the mean flow in the middle layer and the bottom boundary layer must compensate for the mass flux in the surface layer. The mass flux is determined by using a wave model, whereas the bottom boundary layer is included in the momentum balance. Calculation of the mean concentration will be elaborated in chapter 3. Regarding the wave model, it consists of three equations, namely:

- The energy balance equation (Battjes and Janssen, 1978)
- The balance equation for the energy contained in surface rollers (Nairn et al., 1990)
- The horizontal momentum balance
-

The energy balance equation, the balance equation regarding surface rollers and horizontal momentum balance are differential equations, in which the energy balance equation entails:

$$\frac{\partial}{\partial x}\left(E C_g cos\theta\right) = -D_w - D_f \tag{2.1}$$

In which E is the organised wave energy, C_g is the wave group velocity, θ is the incident wave angle. D_w represents the dissipation of wave energy due to breaking and D_f is the dissipation due to bottom friction. Subsequently, the balance equation for the energy contained in surface rollers reads:

$$\frac{\partial}{\partial x}\left(2E_r Ccos\theta\right) = -D_w - D_{diss} \tag{2.2}$$

In which E_r is the energy contained in surface rollers and D_{diss} represents the dissipation of roller energy. Finally, the horizontal momentum balance entails:

$$\frac{\partial \bar{\eta}}{\partial x} = -\frac{1}{\rho g h}\frac{\partial S_{xx}}{\partial x} \tag{2.3}$$

η is the mean wave set-up, h is the local water depth, g is the gravitational force, ρ is the density of the water and finally S_{xx} is the cross-shore radiation stress. So, by solving these equations, the mean current can be determined.

The instantaneous bed load transport is calculated by using a shear stress dependent formulation. Shear stress of the mean current and stirring of waves induces sediment transport along the bed. The classical Shields curve is used calculating the threshold of motion parameter, which entails that the shear stress should be large enough to initiate bed load transport. The mean current shear stress is determined by using the mean current as described in the this section. The magnitude of the wave orbital velocity determines the shear stress due to waves. The wave orbital velocity can be derived from the bottom friction dissipation, D_f, which reads:

$$D_f = \frac{f_w \rho}{\sqrt{\pi}} u_{orb}^3 \tag{2.4}$$

Where f_w is a friction factor and u_{orb} is the amplitude of the wave orbital velocity.

After elaborating upon the transport formulations and equations, some model properties and limitations will be described.

Unibest-TC includes many of parameters. That means that simulations can be adjusted until the required results are obtained. However, it also means the outcome can be unrealistic when parameters are chosen incorrectly. Though, by performing a sensitivity analysis the model results can be validated (see appendix 7). The model also includes a morphological 'switch' with which sediment transport due to a certain forcing can be investigation without a changing profile. Furthermore it allows changing the median grain size with depth, which is present in reality. The internal angle of friction, some dissipation parameters, shear stress parameters, wave asymmetry parameters and mean current parameters can all be adjusted to let the model perform well.

Besides the ability to change formulation parameters, cross-shore profiles, wave, wind and tide climates can be assigned to the model. Varying the grid size is possible as well, for instance to investigate the propagation of an excavation pit by decreasing the grid size. Higher resolution results can be obtained in that way. A big advantage of the model is that certain processes can be 'switched off' in the model and therefore e.g. sediment transport due to waves or tide only can be examined. Furthermore, as the model only calculates sediment transport in wet points, an extrapolation of sediment transport at the last wet point over the dry points is included to cope with sediment transport over the dry points.

The tidal velocity is calculated using the Shields formulation:

$$\overline{v_{tide}} = C \sqrt{h \frac{\partial h}{\partial y}} \qquad (2.5)$$

Equation (2.5) indicates that the tidal velocity increases with the square-root of the depth. Besides, the Unibest-TC can include alongshore water level gradients ($\partial h/\partial y$), to cope with the alongshore tidal current.

Unibest-TC is proven to be a robust model considering short term time scales, say in the order of years (Walstra et al., 2012). For this research the long term time scale will be considered (100 yrs.). The question arises how the model will deal with long term simulations.

Sediment transport on various depth contours of the 'Holland Coast' shoreface

3 Identification of dominant processes

Regarding sediment transport on certain depth contours along the Holland coast, one should first understand the physics behind the transports. To do so, an analysis will be performed to examine the response of certain types of transports regarding variable conditions. Using the model Unibest-TC, simulations will be made and analysed.

The analysis focusses on onshore/offshore transport on various depth contours. This will be done by evaluating the dominance and directed of sediment transport components. On the basis of varying parameters e.g. slope steepness or wave height, the onshore/offshore direction of sediment transport will be examined.

First, a description of this analysis will be presented, which is mainly intended for section 3.2 and 3.3. Assumptions will be listed and the different transport components will be described shortly. Subsequently, transport components will be introduced and analysed regarding their response to various conditions. To examine whether transport components are dependent of certain parameters, dimensionless numbers are introduced in section 3.3 to possibly discover trend lines. In section 3.4, sediment transport equations are examined to validate the results from the first three sections of this chapter.

3.1 Approach

First sediment transport due to varying all parameters (discussed in section 3.1.1) will be considered. By first obtaining some possible trends, parameters can be varied and fixed accordingly. In this way, the analysis might be executed more efficiently. Subsequently, the dominance and dependencies of sediment transport can be evaluated.

In the next section, the varying parameters and the assumptions will be presented. Subsequently a description of the different transport modes will be discussed briefly. To analyse the transports, one should be familiar with the different parts and what driving forces are causing it. Supplementary, the default settings of the model Unibest-TC that will be used in the simulations are presented in appendix 1.

3.1.1 Assumptions and parameters

The profiles consist of a straight, gentle slope from -50m NAP until 0m NAP. However, the interest area for this research lies between -25m NAP and -5m NAP and will be regarded. The water level will be set at 0m NAP and the profile is assumed to be alongshore uniform. Furthermore, it is assumed that there are no wind influences.

For this analysis 6 parameters will be varied. Variable wave heights and periods from daily calm conditions to once in a thousand year storm events are simulated accordingly. Subsequently, the grain size, slope steepness and Longuet-Higgins streaming are variable. Finally, these variable parameters are considered for various depths. The assumptions and parameters are listed below.
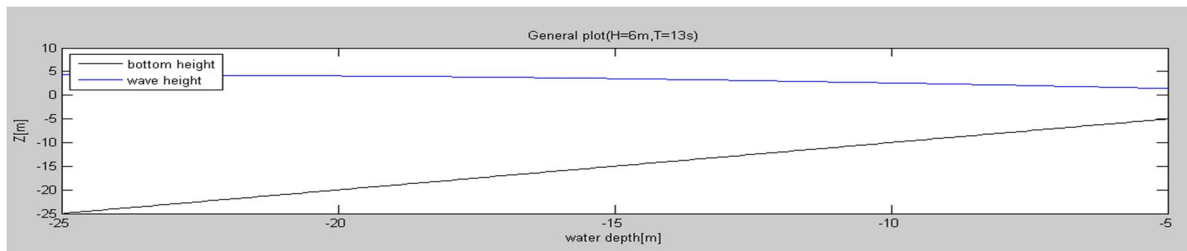
Figure 3.1 Cross-shore straight profile

3.1.1.1   Assumptions:

- Straight slope
- Interest area: -25m NAP till -5m NAP
- Water level: 0m NAP
- No wind influences
- Alongshore uniform
- No tide
- Normal incident waves
- Ignoring Aeolian transport
- Ignoring up- and down welling

Firstly, a straight slope, see figure 3.1, will be assumed to investigate the influence of steepness. Steep slopes, for instance, can cause different transport modes than very gentle slopes. Secondly, the interest area lies between -25m NAP and -5m NAP, because the scope of this project is mainly to examine the response time scale in deep water, say deeper than -10m NAP. Additional, wind influences are disregarded, to make this analysis not too complicated and comprehensive. The model that is being used is one-dimensional, so cannot include alongshore variability. Therefore, an alongshore uniform coast is assumed. Because sediment transport due to waves only will be investigated first, the horizontal and vertical tide is assumed to be zero too. Besides, the waves are assumed to be normal incident waves. The zero tide and normal incident waves assumptions are for the sake of simplicity and to make this first analysis not too extensively. Omitting Aeolian transport and up- and down welling is considered for this entire research, again for reason mentioned above.

3.1.1.2   *Parameters:*

- Wave height (H_{rms}):   H = 1 – 6m
- Wave period (T):   T = 3 – 13sec
- Grain size (D_{50}):   D50 = 100, 200 and 400mu
- Slope: Slope = 1:1000, 1:500, 1:100 and 1:50
- Longuet-Higgins streaming scaling factor: LH = 0, 1, 5
- Depth: d = -5m NAP till -25m NAP

For this analysis, the above listed parameters are being varied. The wave height and wave period are correlated. Higher waves, in case of a storm, are able to move more sediment than very low amplitude waves. It is therefore interesting to investigate this effect. The wave height given here is the root-mean-square wave height (H_{rms}) which is ($1/\sqrt{2}$) times smaller than the significant wave height (H_s). A wave height of 1m is approximately the yearly averaged wave condition along the Holland coast, according to Stive et al. (1990). The higher wave conditions are the 1/10 to 1/1000 year storm wave conditions. The wave periods are consistent with the wave heights. Furthermore, the variable slope and grain size, too, have effect on the transport modes. Increasing grain size straightforwardly decreases the transport rates and increasing the slope steepness could enhance the wave breaking induced

undertow and therefore the offshore suspended transport. The considered values of the slope steepness are present on the shoreface from -5m to -25m NAP (Stolk, 1989). The variable Longuet-Higgins streaming (LH-streaming) scaling factor can affect the dominance of the undertow and therefore the direction of the transport, which will be elaborated upon later. The value of 1, regarding the Longuet-Higgins streaming scaling factor is the default value. Setting the scaling factor to zero means that the LH-streaming is turned off and a value of 5 means an enhanced LH-streaming.

3.1.2 Description bed load and suspended load transport

The different transport components, which will be used to analyse sediment transport, are described briefly in this section. A more elaborately description including equations can be found in section 3.4, in which the transport components and its equations will be examined in detail.

Both the bed load and suspended transport can be subdivided in a wave related and a current related component. The bed load transport depends on the shear stress of the mean current and stirring of waves along the bed and can be calculated separately. Suspended load transport is calculated by the product of the mean current and mean concentration integrated over the vertical (see section 2.3). This product can subsequently be divided in an average velocity component ($\int_a^h \bar{u}\bar{c}dz$, see section 3.4) and an oscillating component ($\int_a^h \tilde{u}\tilde{c}dz$, see section 3.4). Thus, the four sediment transport components can be calculated separately from each other.

3.1.2.1 *Wave related bed load transport (S_{bw})*

Wave related transport is caused by the asymmetry of waves. In case of shoaling waves, higher peak velocities at the wave crest than at the wave trough are causing a residual velocity. This transport type is also seen as the stirring part. Figure 3.2 depicts the orbital velocity for harmonic waves in shallow water. Additional, the stirring mechanism of the waves close to the bed is visible.
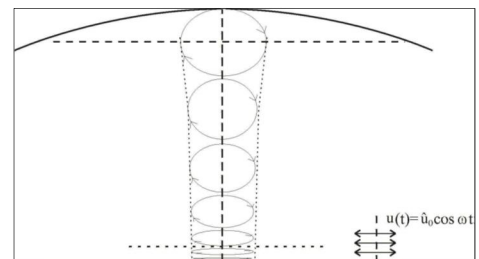
Figure 3.2 Wave orbital motion (Bosboom and Stive, 2011)

3.1.2.2 *Wave related suspended transport (S_{sw})*

S_{sw} is similar to S_{bw}, only the sediment is in suspension now. Higher peak velocities at the wave crest cause an onshore-directed residual velocity/transport. For suspended transport, the concentration is an important factor. Higher waves with a higher orbital velocity are able to enhance the stirring and increase sediment suspension.

3.1.2.3 *Current related bed load transport (S_{bc})*

In breaking waves, the mass flux has to be opposed by other forces to gain equilibrium. These are the undertow and Longuet-Higgins streaming. The undertow is predominantly offshore whereas the bottom streaming mainly is onshore directed. The dominance of these processes determines the direction of the bed transport. The velocity profile changes in case of non-breaking waves, which means that there is a reduced return current and makes the bottom streaming, therefore, dominant.

3.1.2.4 Current related suspended transport (S_{sc})

The velocity profile multiplied with the concentration profile causes the S_{sc}. In accordance with the current related bed transport, the undertow is assumed to be the dominant process.

3.1.2.5 Longuet-Higgins streaming (LH-streaming)

The LH-streaming is only present in the wave boundary layer and is predominantly onshore directed. It is caused by the horizontal and vertical velocity being out of phase. The LH-streaming is present along the bottom where the velocity is in the wave propagation direction (see figure 3.3). An increasing or decreasing LH-streaming is therefore able to influence the magnitude of the undertow.
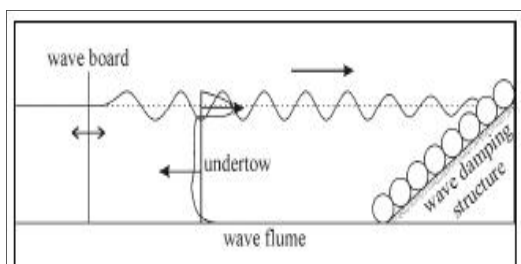
Figure 3.3 Vertical velocity profile (Bosboom and Stive, 2011)

3.2 Dependencies onshore/offshore transport

As can be seen in figure 3.4, in which all parameters (section 3.1.1) are varied, no evident dependencies are visible. Albeit that large amplitude waves result in a large offshore sediment transport. Another interesting observation is that suspended load transport is much larger than bed load transport for the highest waves. To be able to examine onshore/offshore sediment transport, certain parameters will be fixed. A reference scenario will be introduced first in which only the wave height and period are variable. Subsequently, slope steepness, grain size and LH-streaming scaling factor will be varied on turns.
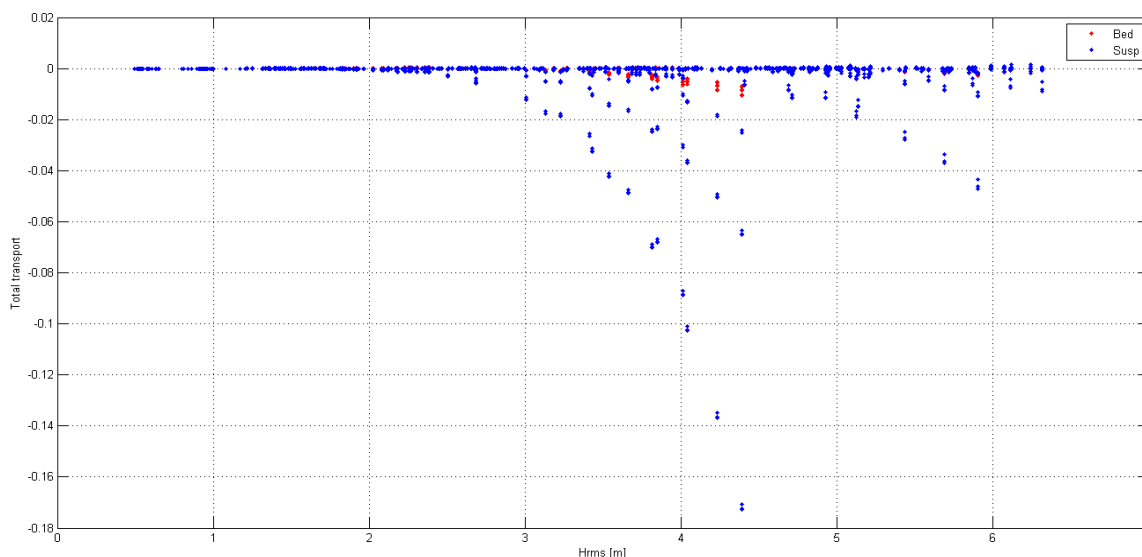
Figure 3.4 Sediment transport (all parameters variable). Bed = bed load transport, Susp = suspended load transport. Sediment transport is plotted over the offshore root-mean-square wave height H_{rms}. The blue dots: suspended transport, the red dots: bed load transport.

3.2.1 Reference scenario

As can be seen in figure 3.4, the wave height shows some dependency regarding sediment transport. Because the wave height and wave period are correlated, both parameters will be varied in this reference scenario. Therefore, the observed transports will be related to the change in wave height and period. Furthermore, a slope of 1:1000 is assumed as a reference, because this research focuses itself on the lower shoreface, which has a gentle slope of approximately 1:1000. The waves are assumed to be normal incident for this reference scenario. The grain size is stated at $D_{50} = 200\mu m$, because it is the average grain size for the North Sea (Stolk, 1989).

Used parameters:

- Slope 1:1000
- H_{rms} = 1-6m
- T = 3-13s
- D_{50} = 200 µm
- LH streaming = 1
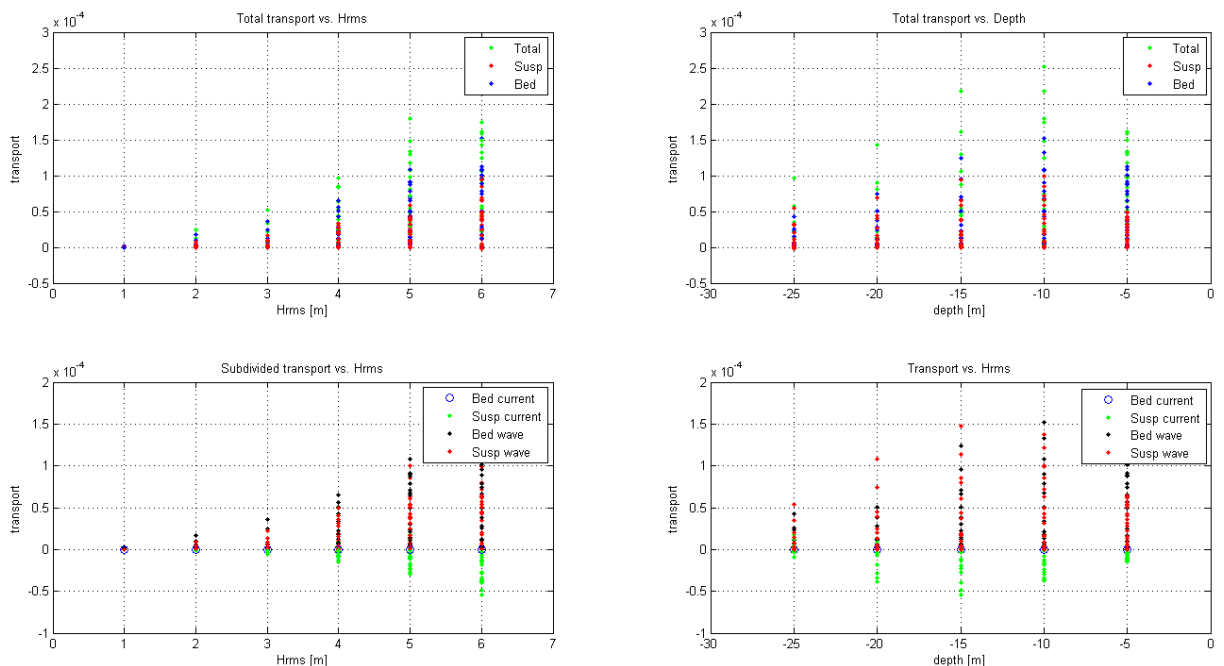
Figure 3.5 Reference scenario. The upper two plots: total, bed load and suspended load transport versus the wave height (H_{rms}) or depth. The lower plots: subdivided bed load and suspended load transport. The slope is 1:1000, grain size is 200 µm and the wave height and period are variable.

3.2.2 Analysis of reference scenario

3.2.2.1 *Total transport*

From the reference scenario (figure 3.5) it can be concluded that the total transport is onshore directed for any wave height and depth contour. An increase in transport is visible for higher waves and longer periods. Bed load transport is generally larger than suspended load transport, in contrast to what was found in figure 3.4. The steep slope of 1:50 is responsible for the largest sediment transport and suspended transport dominance. At -20m NAP, see figure 3.5, suspended load becomes more dominant. Deeper than -10m NAP, the orbital

velocity has a reduced effect, the critical shear stress will not be exceeded, and the undertow becomes the dominant mechanism.

The slope of the reference scenario is very gentle, which induces a gradually energy decay of the waves. This means that there is only a weak undertow. Hence, the Longuet-Higgins streaming and wave related suspended load transport dominate the undertow and are onshore directed.

3.2.2.2 Bed load and suspended load transport

The wave related bed load transport is predominantly onshore directed and is increasing with increasing wave height and period, whereas the current related bed load transport remains zero. As stated before, bed load transport increases in deep water for high amplitude waves. In case of increasing amplitude, the orbital velocities increase as well and are able to stir up sediment more effectively at deep water. Without any current, apart from the undertow, no current related bed load transport takes place in this case.

S_{sw} is similar to S_{bw} onshore directed. For higher waves ($H_{rms} > 3m$), current related suspended load transport becomes dominant at deep water (-25m NAP). Because large amplitude waves are breaking more heavily and cause a stronger undertow, which can reach farther offshore. Comparing S_{sw} and S_{bw}, the suspended load transport is slightly less. This can be explained by the sediment concentration being higher near the bed.

In contrast to the wave related transport, the current related suspended load transport is generally offshore directed. When waves are breaking, they cause an undertow current which is in offshore direction. Since small amplitude waves are not able to induce a strong undertow, sediment transport is less than in case of high amplitude waves.

3.2.3 Variable parameters

In the following section, more parameters will be varied and be compared with the reference scenario. A variable grain size will be treated first, before a variable LH-streaming and slope are considered.

3.2.3.1 Variable grain size

To investigate the effect of increasing and decreasing grain size, the grain size is either twice the size (400mu), in comparison with the reference scenario (200um) or half of the size (100mu). The effect of variable grain size can be explained by the different transports modes which can become dominant. Small grains induce a more suspended load transport mode; less energy is required to bring them into suspension. Furthermore, large grains are heavier, which indicates bed load transport will become the dominant transport mode.

As stated above, large grains do induce a large bed load transport in comparison with small grains. Compared to the reference scenario however, bed load transport slightly diminishes. Suspended load transport decreases as well for the wave related part as for the current related part. The large grains decrease the amount of sediment getting into suspension, which probably cause this phenomenon (see figure 3.6).

Bed load transport increases as well as the suspended load transport for smaller grains compared to the reference scenario. The bed load transport is predominantly onshore directed, while the suspended load transport is variable.

The model performs as to be expected, for small grains the both bed load and suspended load increases and for large grains bed load transport becomes the dominant mechanism.
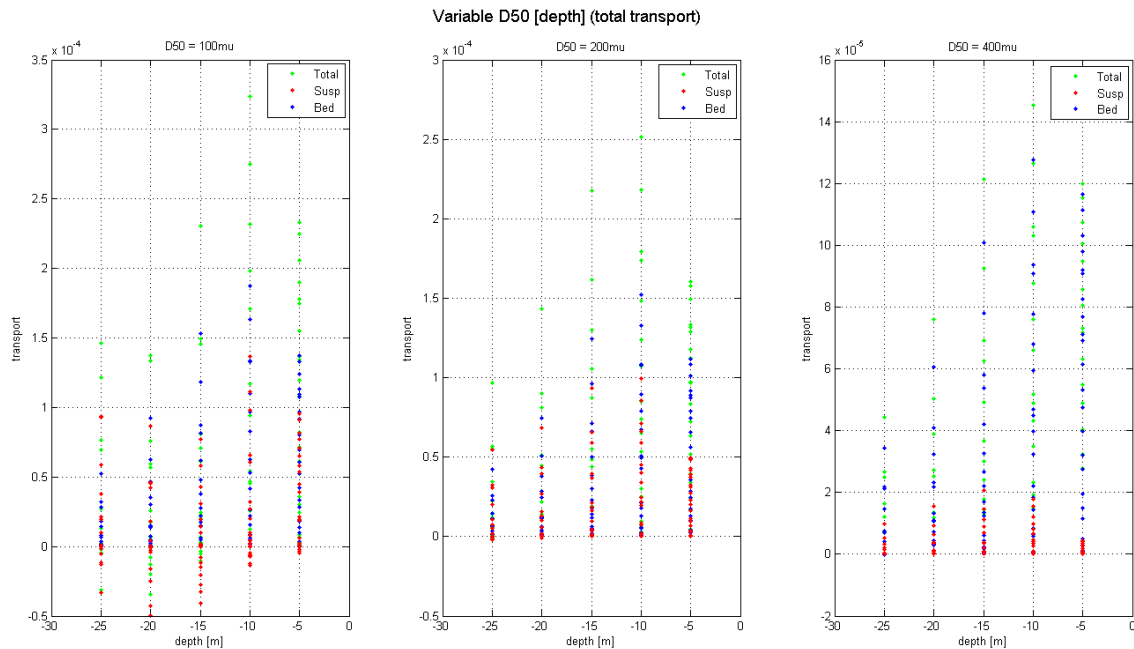
*Figure 3.6 Variable D$_{50}$. The suspended load transport is abbreviated by **susp**, the bed load transport by **bed** and the total transport by **total**. Slope steepness: 1:1000, grain size: 200 µm.*

3.2.3.2 LH-streaming

To examine the importance of the Longuet-Higgins streaming, the streaming scaling factor will be varied. This implies an increase in LH-streaming or a zero LH-streaming. Setting the streaming scaling factor to zero, the transports become more offshore directed. The suspended current related transport increases offshore, because there is no streaming present which opposes it. The S$_{sw}$ remains, on the other hand, unchanged. Streaming has no influence on the S$_{sw}$. Nevertheless, S$_{bw}$ does get affected by the zero-streaming along the bed. Transports become more offshore directed due to the absence of the onshore directed streaming. Therefore, it gets affected by the undertow current, which is the dominant mechanism of the mean velocity.

Increasing the Longuet-Higgins streaming scaling factor, in contrast to a zero-streaming, sediment transport becomes more onshore directed. Once more, it affects the mean velocity, which becomes more onshore directed as well, see figure 3.7. Therefore, S$_{sc}$ becomes more onshore directed as well as S$_{bw}$. S$_{sw}$ remains unchanged again, because the changing velocity vertical has no influence on the wave orbital velocity.

Therefore, the Longuet-Higgins streaming influences the vertical velocity profile. In case of a clearly present streaming along the bed, the undertow current reduces. Sediment transport is more onshore directed. Without any streaming along the bed, transport rates change in offshore direction.
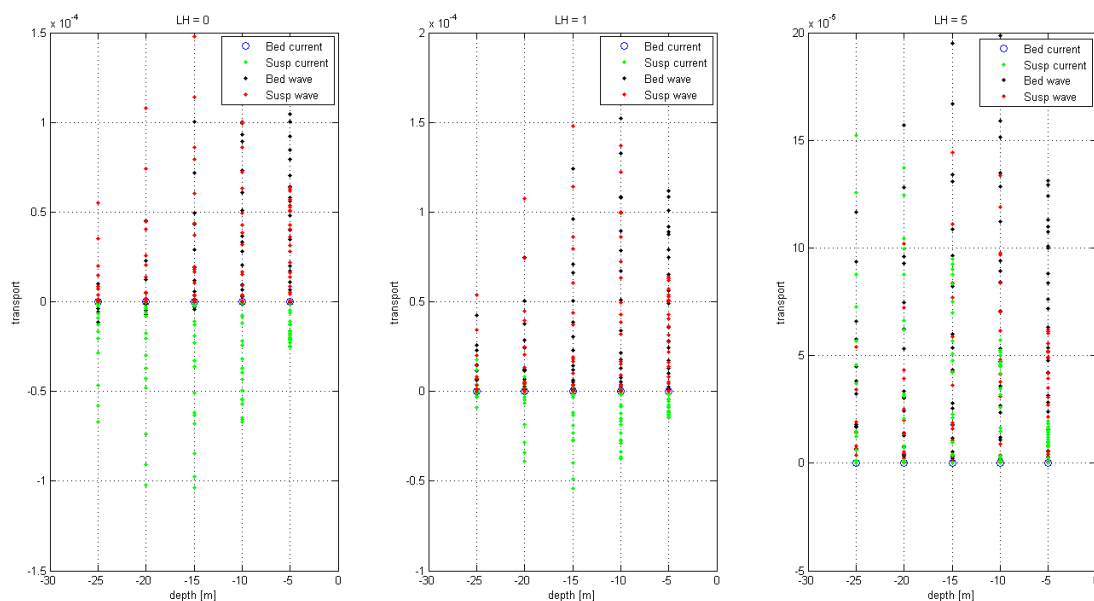
Figure 3.7 Variable value of the LH-streaming. Bed current = S_{bc}, Susp current = S_{sc}, Bed wave = S_{bw}, Susp wave = S_{sw}. Slope steepness: 1:1000, grain size: 200 µm.

3.2.3.3 Variable slope

Considering a real profile along the Holland coast, the steepness of the slopes varies considerably. Therefore, sediment transport on slopes with different steepness will be investigated. The bottom of the North Sea consists of a steepness of approximately 1:1000, whereas the steepness at -5m NAP can be up to 1:50 along the Holland coast (Stolk, 1989). So, the steepness will be varied within this range, starting with 1:50.

A slope of 1:50 induces more shoaling and more energetic breaking of waves in comparison with the reference slope of 1:1000. In case of a steep slope, bed load transport and S_{sc} are offshore directed, whereas S_{sw} is onshore directed (figure 3.8). Because of the strong effect of shoaling waves, S_{sw} is onshore directed. A steep slope not only causes strongly shoaling waves, but also more intense breaking waves. This enhances the resulting undertow and therefore the S_{sc} in offshore direction. Besides, the undertow also affects the bed load transport, which becomes offshore directed due to the dominance of the undertow.

For a gentler slope, 1:100, the transport pattern is similar, though it's slightly different. Only the bed load transport is variable. In deep water (deeper than -10m NAP) the bed load transport is onshore directed due to the diminished effect of the undertow in comparison with a slope of 1:50 and in shallow the undertow becomes more dominant again which induces an offshore transport of bed load transport.

Considering an even gentler slope, 1:500, results in a more similar transport pattern compared to a 1:1000 slope. Because 1:500 is steeper, the shoaling effect is slightly stronger as well, which results in an increased S_{sw} in onshore direction comparing to a slope of 1:1000. Furthermore, S_{bw} is also somewhat larger. Due to the presence of streaming in case of gentle slopes, wave–induced bed transport is onshore directed in deep water. Moreover, the presence of streaming reduces the undertow as well. On the other hand, a steeper slope enhances the undertow due to the stronger effect of wave breaking. So, sediment transport is variable considering different depth contours on which different mechanisms are dominant.
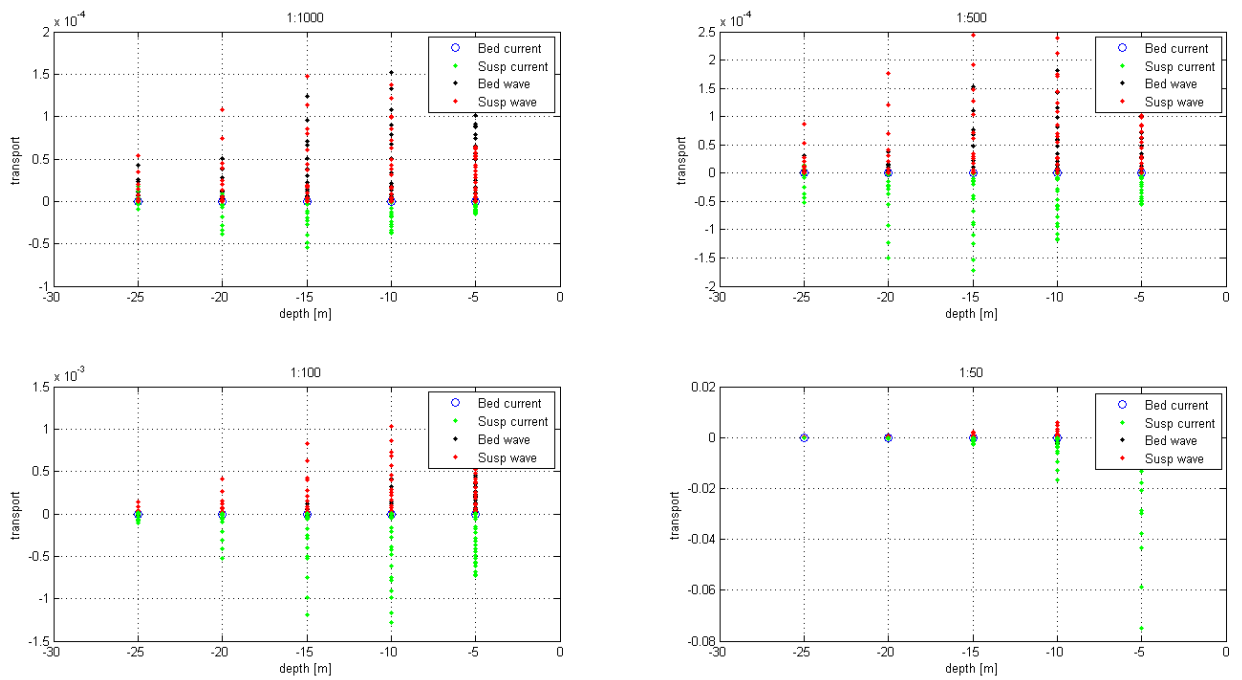
Figure 3.8 Variable slope. Bed current = S_{bc}, Susp current = S_{sc}, Bed wave = S_{bw}, Susp wave = S_{sw}. Grain size: 200 µm, the wave height and period are variable.

For gentle slopes, sediment transport is highly variable considering various wave heights and periods (see figure 3.8), whereas for steep slopes suspended transport becomes dominant.

3.2.4 Findings

Some conclusions can be drawn, which are listed according to their importance:

- Sediment transport is depth dependent

- Sediment transports is slope dependent

- Grain size increase/decrease sediment transport

- LH-streaming can become important

- Sediment transport increases with wave height and period

Sediment transport strongly varies for specific depth contours. For instance on a gentle slope, 1:1000, it is not straightforward that the largest transport is present in shallow water. The variable offshore wave height H_{rms} is responsible for this. Large amplitude waves are breaking and dissipating more energy in deeper water comparing to lower amplitude waves. Closer to the shoreline waves already lost all their energy, which lead to a reduced sediment transport. It can be concluded that the largest transport occur when the dissipation is the largest. Regarding the steepness of the slopes, an increase in steepness changes the magnitude of sediment transport as well. Especially for the steepest slope, 1:50, some transport components become more dominant, for instance S_{sc} is extremely dominant in shallow water.

Furthermore, a variable grain size and LH-streaming increase or decrease sediment transport. A variable grain size is as important as a variable depth and slope, whereas a variable LH-streaming only slightly increases/decreases sediment transport. A larger grain size reduces the sediment transport, whereas a smaller grain causes an increase in transport. Streaming mainly affects bed load transport and the undertow. An increase in streaming along the bed reduces the undertow and enhances onshore bed transport.

Finally, increasing the wave height and period predominantly increases sediment transport, but can also cause different transport components to become dominant.

3.3 Dimensionless numbers

The analysis of sediment transport in Unibest-TC shows some dependencies and trends. However, there still is a considerable variance in the transport rates. A way to reduce the scatter and to fix some variable parameter is to make them dimensionless. Section 3.2 showed that sediment transport in Unibest-TC is dependent of for instance the wave height, slope steepness, depth and grain size. By choosing the non-dimensional numbers in such a way that these parameters are included, perhaps more clear trends could be found. Using dimensionless numbers will give more insight in evaluating sediment transport on various depth contours and physical processes driven it and will therefore help to answer the hypotheses stated in section 1.2.

Regarding section 3.2, the slope steepness, water depth and wave height and period indicated the largest dependency. These parameters could be found in certain dimensionless numbers. Bowen (1980), introduces the non-dimensional depth parameter k_0h, which includes the variable depth and wave period. The Iribarren parameter includes the slope and wave steepness. Finally, the dimensionless fall velocity contains the wave height and period and grain size.

In the next sections, these dimensionless numbers will be introduced and described, and subsequently transports will be analysed.

3.3.1 Dimensionless numbers

3.3.1.1 *Non-dimensional depth*
As stated before, Bowen (1980) introduced the non-dimensional depth parameter k_0h, which reads:

$$k_0h = \frac{4\pi^2 h}{gT^2} \tag{3.1}$$

K_0 ($k_0 = \omega^2/g$) is the deep water wave-number and h is the local depth. The deep water wave-number is derived from the wave dispersion relation and depends on the frequency/period of the waves. This parameter was actually meant to investigate the importance of wave asymmetry versus the 'drift' velocity for a variable depth. The non-dimensional depth can in this research, therefore, possibly be used to investigate the importance of transport components for various depths. Considering this parameter, a large value represents deep water, whereas a small value corresponds to shallow water. Similar a large value characterises a small wave period (T is located in the denominator) and a small value a long wave period.

3.3.1.2 *Iribarren number*
The Iribarren parameter represents the ratio of the slope steepness and the wave steepness (Battjes, 1974) and entails:

$$\xi = \frac{\tan \alpha}{\sqrt{H_s/L_0}} \text{ , with tan } \alpha = \text{slope steepness and } L_0 = \frac{gT^2}{2\pi}. \tag{3.2}$$

H_s is the local significant wave height and L_0 is the deep water wave length, hence the local steepness is represented in equation 3.2. Besides the slope steepness and wave height, the

wave period is included as well by means of the wave length. The Iribarren number is able to divide certain types of wave breaking, thus regards the effect of the bed slope on the wave breaking process. It can therefore be seen as relative steepness parameter. The effect of the relative steepness on different components of sediment transport can, therefore, be investigated.

3.3.1.3 Dimensionless fall velocity

A more or less equivalent parameter to the Iribarren number is the dimensionless fall velocity:

$$\Omega_0 = \frac{H_0}{w_s T} \tag{3.3}$$

Opposite to the Iribarren number, the slope steepness is excluded and the fall velocity is included in equation 3.3. Besides, the deep water wave height is used. The dimensionless fall velocity parameter includes the fall velocity and therefore it is grain size depend. In this way the influence of variable grain sizes on different transport components can be investigated. This dimensionless parameter represents actually the ratio between sediment settling and sediment stirred up by the increased wave height and period. The interaction between wave energy and grain size is put inside this parameter. Although this non-dimensional parameter is originally thought to explain the beach state (dissipative or reflective), it could represent some clear dependencies for different transport components.

3.3.2 Analysis of sediment transport using dimensionless numbers

Similar to section 3.2, all parameters (section 3.1) are taken into account. Due to the usage of non-dimensionless numbers, some parameters are already fixed, less scatter is expected and more clear trends can possibly be indicated. First, a figure representing all transports will be illustrated to already discover certain trends and to aim for a more direct next step varying certain parameters.

3.3.2.1 Non-dimensional depth
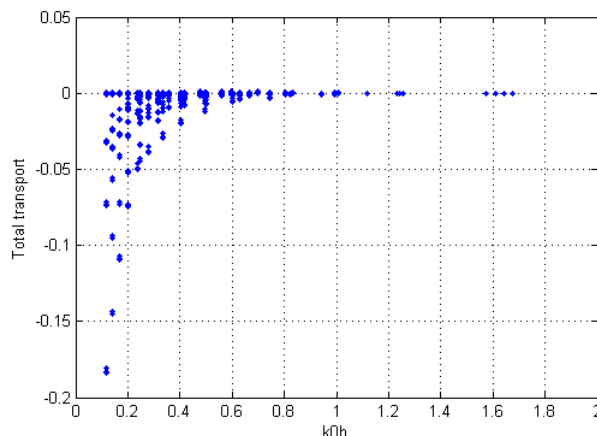
Figure 3.9 Sediment transport versus the non-dimensional depth. Variable slope steepness, wave height, wave period, grain size and water depth.

As explained before, $k_0 h$ is wave period and water depth dependent. Therefore, $k_0 h$ is large for large water depths and $k_0 h$ is small in case of large wave period. It can be seen that the largest sediment transport occurs in shallow water (figure 3.9). As was shown in section 3.2, it

can be assumed that the slope steepness is important as well. Therefore, the sensitivity of sediment transport on variable slope steepness will be examined too.

Subdividing this plot in fixed steepness of the slopes show that sediment transport indeed is slope dependent and that different patterns are visible. Sediment transport patterns and magnitudes change in case the slope becomes steeper, the steepest slope cause the largest sediment transport, see figure 3.10. The gentler slopes induce relative small transports comparing to the steepest slope. A reasonable distinction can be made for various slopes; however there still is much scatter and multiple lines are perceptible.
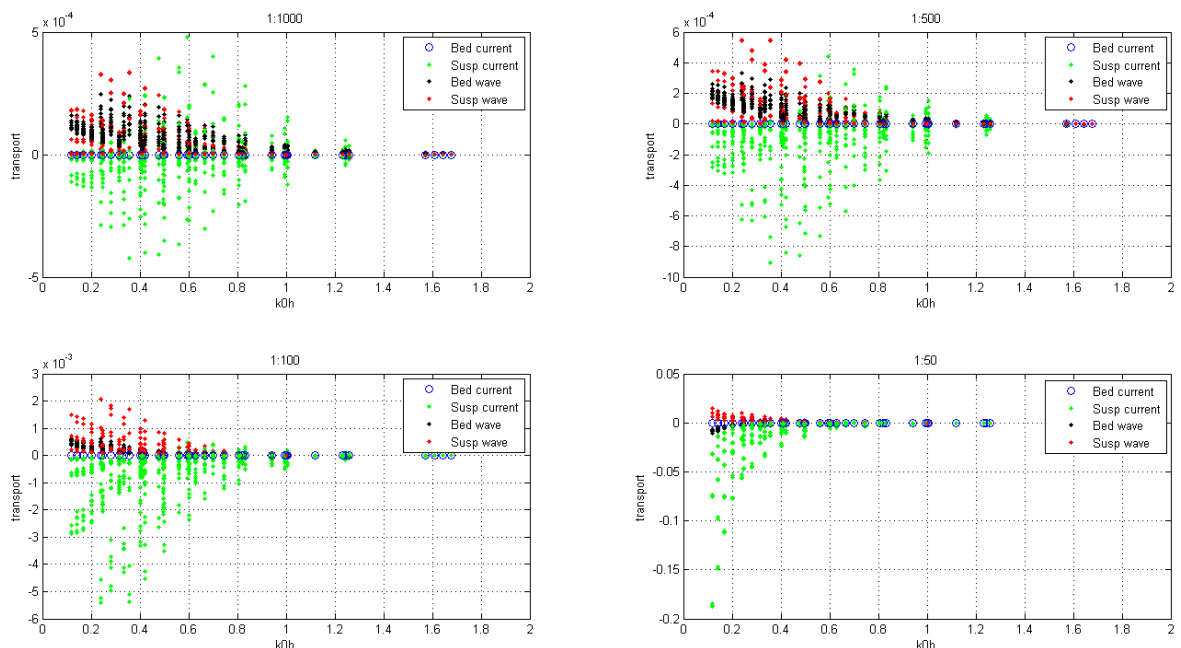
Figure 3.10 Sediment transport including a variable slope versus k_0h. Bed current = S_{bc}, Susp current = S_{sc}, bed wave = S_{bw}, susp wave = S_{sw}.. Wave height, wave period, grain size and magnitude of LH-streaming are variable.

Regarding a fixed grain size or Longuet-Higgins streaming, it reduces the scatter for both cases. Sediment transport change for a smaller or larger grain size and variable LH-streaming. Though, the pattern of sediment transport versus k_0h is quite similar and does not explain the scatter. Smaller grains induce a larger suspended transport than in case of large grains, a high value of the LH-streaming induces a larger bed load transport and a low value of the streaming enhances the suspended load transport. Though, this could already be derived in the section 3.2.

Next, a fixed depth will be considered in this case and the dominance and direction of sediment transport on fixed depth contours will be investigated. A variable kh-value is caused by including various depth contours, see figure 3.11. For deep water, the kh-value lies around 1 in case of a slope of 1:500 and for shallow water this value lies between 0.5 and 0.1. As stated before, the scatter is predominantly caused by the variable grain size and LH-streaming. However, variable wave height cause the different trends visible in figure 3.11 and 3.12. For instance at -10m NAP in figure 3.12 a few trends are noticeable which can be explained by the varying wave height.

As well as a fixed depth, a fixed wave period visualises the k_0h dependency. For large amplitude and waves with a longer period, sediment transport increases and simultaneously the k_0h-value decreases (figure 3.12). The five subdivided depth contours are also clearly visible, with the largest depth containing the largest k_0h-value. Remarkable is that for long wave periods the largest transports occur around -10m and -20m NAP. Because long wave periods are correlated with high amplitude waves, waves already break at deeper water and causing the largest transport.
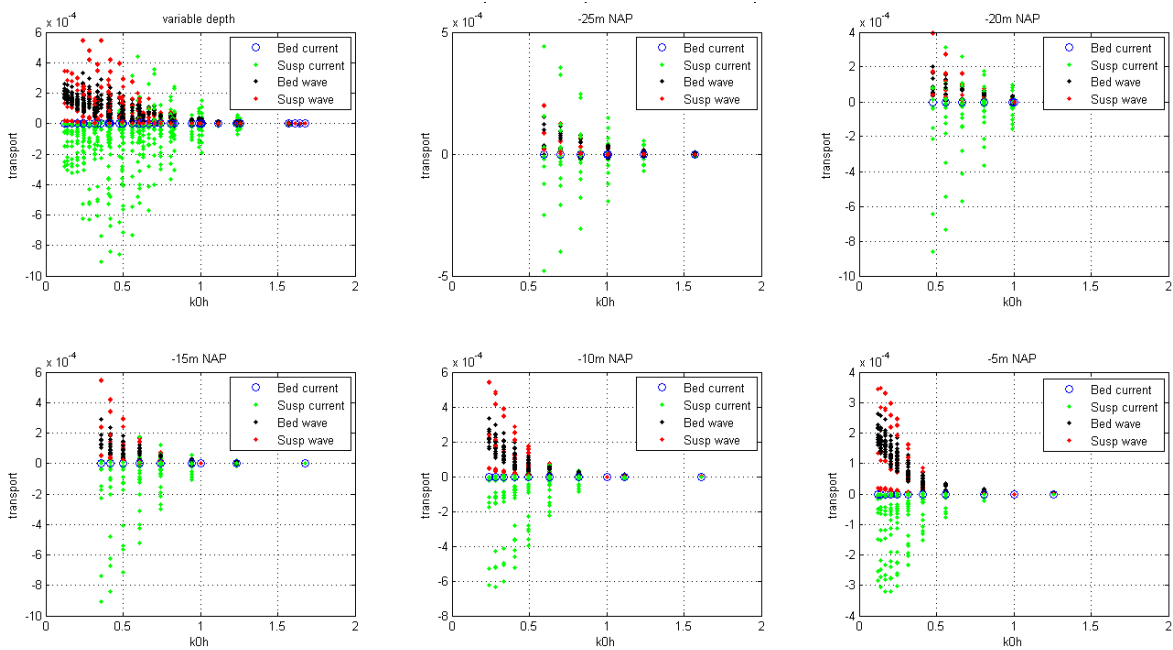
Figure 3.11 Sediment transport including a slope of 1:500 versus k_0h. Fixed water depth per subplot, except for the first subplot. Bed current = S_{bc}, Susp current = S_{sc}, bed wave = S_{bw}, susp wave = S_{sw}.
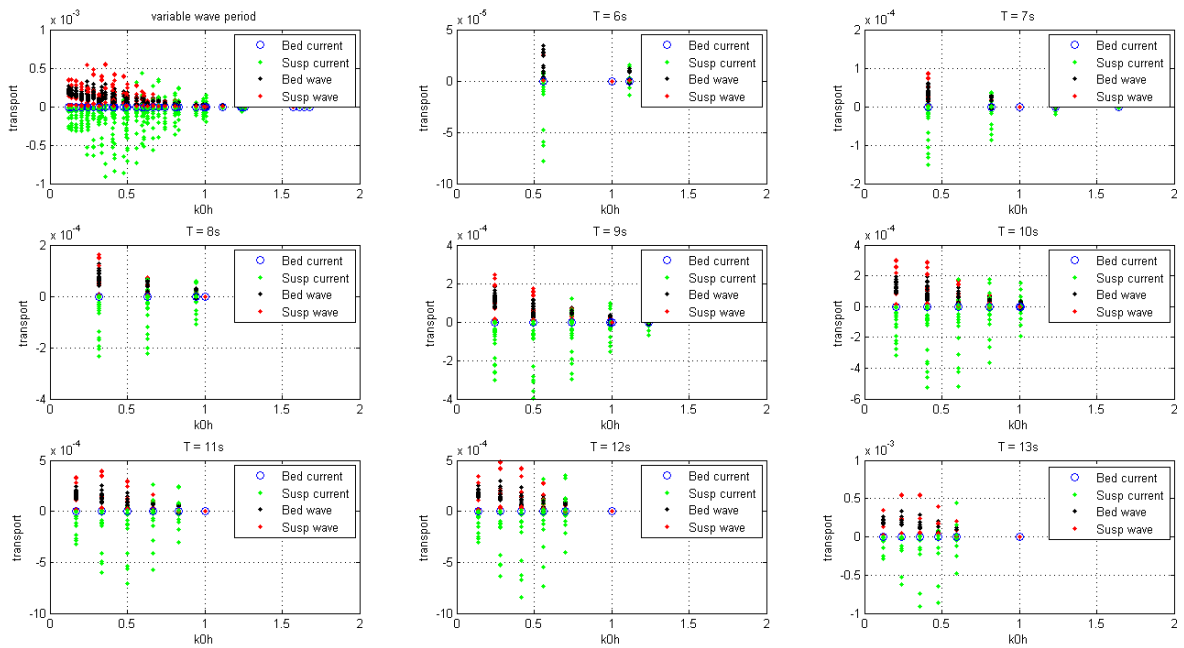
Figure 3.12 Sediment transport including a slope of 1:500 versus k_0h. Fixed wave period per subplot, except for the first subplot. Bed current = S_{bc}, Susp current = S_{sc}, bed wave = S_{bw}, susp wave = S_{sw}.

The dimensionless depth parameter (k_0h) entails that the steepness of a slope has large effect on the transport components. S_{sc} is dominant for steep slopes (1:50), while for gentle slopes the wave related transport components are becoming more dominant. Moreover, this parameter entails that the depth and wave height and period are influencing sediment transport. Sediment transport increases with increasing wave period, trends change for different wave heights and different transport components increasing in dominance regarding various depth contours.

3.3.2.2 Iribarren number
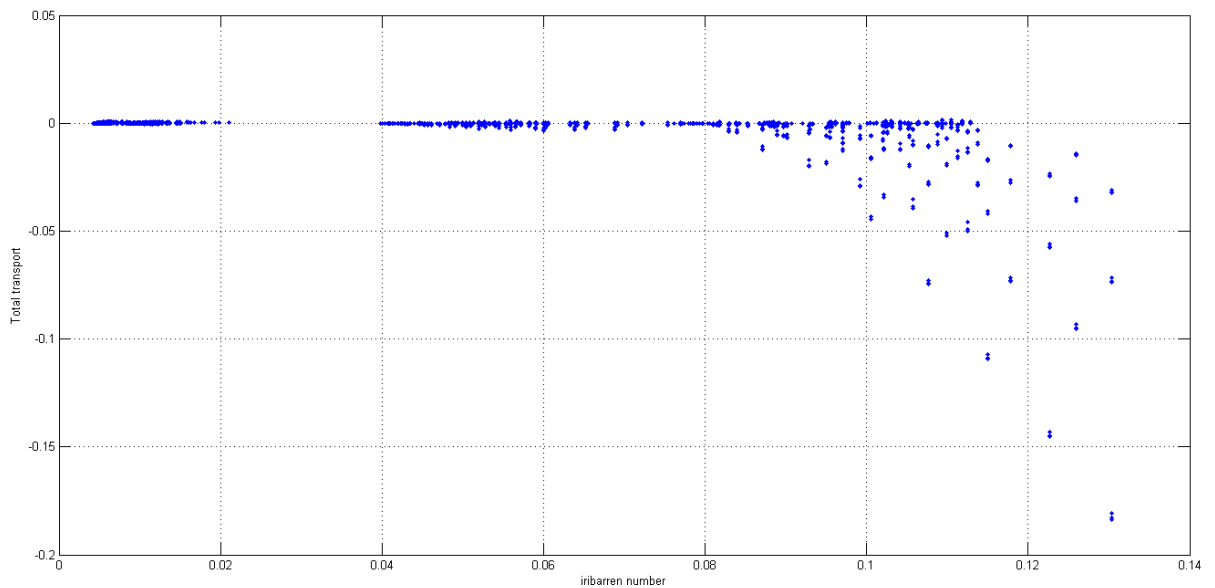
Figure 3.13 Sediment transport versus the iribarren number. All parameters (section 3.1.1) are varied.

There are at least 3 different regions distinguishable, see figure 3.13. The Iribarren number is slope, wave height and length dependent. So, the different regions could be explained by regarding, for instance, fixed slopes. In case of a steep slope, the Iribarren number, correspondingly, will be large too. Therefore, this dependence will be regarded first.

The iribarren number for a slope steepness of 1:50 is the largest (see figure 3.14). The gentler the slope, the smaller the Iribarren number. Considering a different steepness of slopes, S_{sc} increases largely for the steepest slope. Using the Iribarren number shows a clearer dependency, regarding different slopes, than in case of using the dimensionless depth parameter. It is noticeable that for gentle slopes the wave related transport is predominantly onshore and the suspended related transport is offshore. Only for a slope of 1: 50 S_{bw} is offshore directed.

Once more, multiple trend lines are noticeable including some scatter. Regarding a fixed grain size and Longuet-Higgins streaming only slightly reduces the scatter. Considering fixed depth contours on the other hand, does explain the scatter more explicitly. This can possibly be explained

Figure 3.14 Iribarren number versus slope steepness

by considering the Iribarren number as a relative steepness parameter. The higher the Iribarren number, the higher the relative steepness. Since the relative steepness between slope and waves is relatively small in deep water, the scatter is not large. If that is true, the same dependencies should become visible for fixed wave heights and wave lengths. The wave length and wave period are correlated by L = c*T and subsequently the wave height and wave period are therefore correlated considering this relative steepness parameter.

Figure 3.15 Sediment transport versus iribarren number. Fixed slope steepness per subplot. The wave height and wave period are variable. Bed current = S_{bc}, Susp current = S_{sc}, bed wave = S_{bw}, susp wave = S_{sw}.

This shows that the steepness of the slopes is responsible for the largest differences, a steep slope causes large transport, see figure 3.15. Ignoring the steepness of the slope, the relative wave steepness and depth are then responsible for the largest transport. The highest waves combined with the shallowest depth are causing the largest transports. For gentle slopes, where the steepness of the slopes has less influence on the relative wave steepness, the ratio between the wave length and wave height becomes important. So, the Iribarren number reflects the importance of the wave steepness, the steepness of the slope and depth contour.

3.3.2.3 *Dimensionless fall velocity*
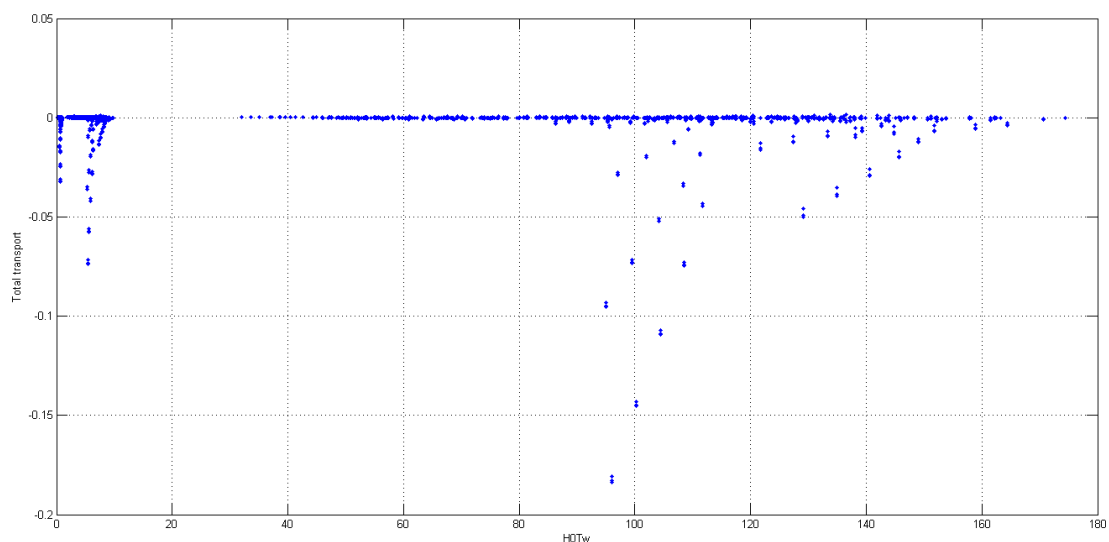
Figure 3.16 Sediment transport versus the dimensionless fall velocity (All parameters as described in section 3.1.1 are varied).

The dimensionless fall velocity depends to a large extend on the grain size. This can already be noticed by distinguishing three different regions in figure 3.16. In contrast to the other dimensionless numbers, the steepness of the slope does not result in a clear dependency. The dependency can be found by fixing the parameters which are included in the dimensionless fall velocity. In case of a fixed grain size, the three different parts are clearly depicted. For a small grain diameter, the dimensionless fall velocity parameter results in the largest value. Because the fall velocity is largest for large grains and because this parameter is located in the denominator, this results in the smallest values. The variable grain size is, therefore, responsible for the largest variation in dimensionless fall velocity value. Besides the explanation of the variance in magnitude of the dimensionless number, it does not really explain which transport is dominant on which depth contour. Though, for a fixed grain size, different regions are distinguishable (see figure 3.17). Each 'region' is represented by a different wave height H_{rms} and period T. The H_{rms}/T ratio is depth dependent, namely in deep water the wave height has not reduced much which results in a high value of this dimensionless parameter. In shallow water the wave height has decreased, where the wave period remains the same which leads to a lower value of the dimensionless fall velocity. Besides the increase and/or decrease of the dimensionless fall velocity, it results in the same dependencies as the other non-dimensional parameters.
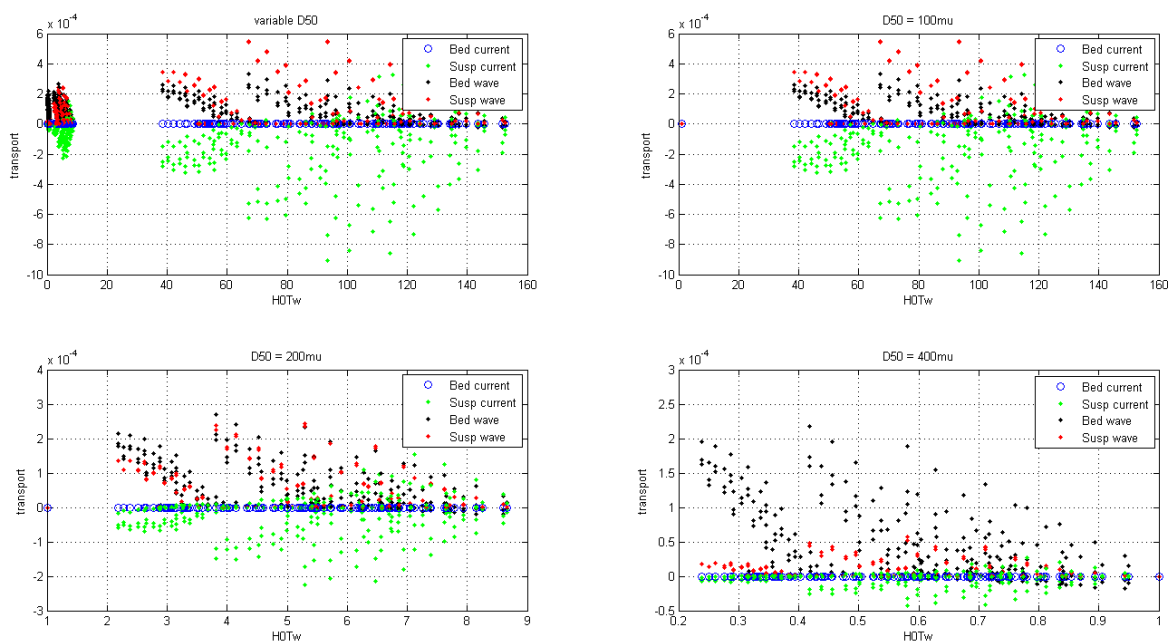
Figure 3.17 Sediment transport including a slope steepness of 1:500 versus H_0Tw. Fixed grain size per subplot, except for the first subplot. The wave height and wave period are variable. Bed current = S_{bc}, Susp current = S_{sc}, bed wave = S_{bw}, susp wave = S_{sw}.

3.3.3 Findings

Using non-dimensional numbers does, firstly, confirm the findings in section 3.2.4. Moreover, it gave more insight in the dependencies of sediment transport. The most important dependencies of the direction and magnitude of sediment transport according to the non-dimensional number are listed according to their importance:

- Based on ξ: Sediment transport is dependent of wave steepness and slope steepness for certain depth contours

- Based on Ω_0: Sediment transport is grain size dependent

- Based on K_0h: Sediment transport is slope steepness and wave period dependent (approximately similar to ξ)

Similar to the first analysis, the dimensionless numbers entail the offshore dominance of S_{sc} in offshore direction. Wave related transport is predominantly onshore directed for gentle slopes. Though, this analysis still does not presents the dominance of certain transport component for certain conditions and depth contours.

3.4 Detailed transport equations

Considering the section 3.2 and 3.3, which resulted in some dependencies, no real evident trends were observed. To further investigate sediment transport in Unibest-TC, analysing the transport equations of the different transport components would be the next step. In the first analysis, an explanation was already given (section 3.1.1), though, only briefly. By elaborating on the transport equations, working out which parameters are dependent and comparing this with simulations should give more insight in why sediment transport is onshore/offshore and why and where it is dominant.

3.4.1 Bed load transport

The bed load transport is considered the load which is more or less in continuous contact with the bed. The general equation, which is used by Unibest-TC to calculate the bed load, is (see Van Rijn et al., 1995):

$$\Phi_{bd}(t) = \frac{q_b(t)}{\sqrt{\Delta g d_{50}^3}} = 9.1 \frac{\beta_s}{(1-p)} \{|\theta'(t)| - \theta_c\}^{1.8} \frac{\theta'(t)}{|\theta'(t)|} \tag{3.4}$$

Equation (3.4) includes the in particular the median grain size (D_{50}), a slope correction factor (β_s) and the shear stress (θ). Inclusion of these parameters would suggest transport dependence. First regarding the grain size, see figure 3.18, it can be derived that sediment transport is grain size dependent as maximum sediment transport increases with decreasing grain size. As already concluded in in section 3.2 and 3.3, the smallest grains cause the largest transport and increasing the grain size decreases the transport rates.
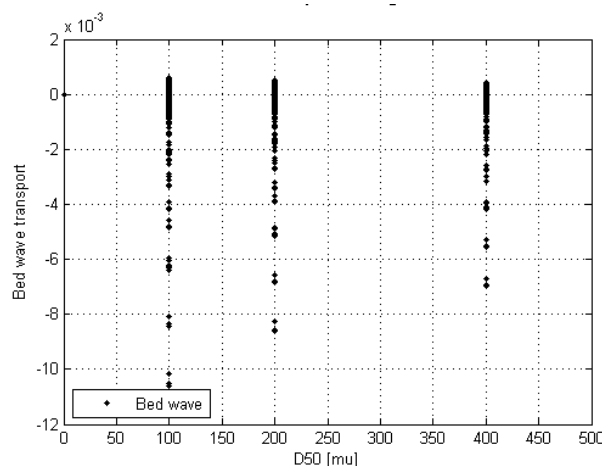
Figure 3.18 Wave related bed load transport versus grain size

Elaborating on the slope factor (βs), it is merely a factor to increase or reduce sediment transport. In case of downslope transport, the slope factor increases this transport and for upslope transport it reduces sediment transport. So, this factor is important for alongshore bars, but it is limited for gentle slopes as considered in section 3.1.1.

The shear stress is included in two ways, namely the dimensionless effective shear stress ($\theta'(t)$) and the dimensionless critical shear stress (θ_c). The non-dimensional critical shear

stress represents the threshold of motion. This parameter is calculated by the Shields curve (Van Rijn, 1993). The dimensionless effective shear stress due to currents and waves is:

$$\theta'(t) = \frac{1/2 \rho f'_{cw} |u_b(t)| u_b(t)}{(\rho_s - \rho) g d_{50}}$$ (3.5)

Equation (3.5) represents the sediment forcing as the ratio of the flow drag-force on the grains and the under-water weight of the grains (Ruessink et al., 2007). The shear stress on the grains determines whether the grains are being transported. It depends on the some friction factor, grain size, gravitational force and the time-dependent near-bottom horizontal velocity vector. The velocity vector of the combined wave-current motion is calculated on top of the wave boundary layer and is the sum of the near-bed oscillating velocity and the time-averaged velocity at 1cm from the bed. So, the bed load transport is dependent on both waves and currents.

The near-bed oscillating velocity is depends on the wave height and wave period and on the contribution due to wave asymmetry (and bound long waves). Increasing wave height and wave period increases the wave orbital velocity. The wave period, and therefore the correlated wave length, is related to the water depth and therefore whether waves start to shoal. This determines the near-bed oscillating velocity and therefore the shear stress. Shorter waves are not able to produce a shear stress over the bed, where longer waves increase this shear stress. The asymmetry of waves cause a residual velocity, which is predominantly onshore directed. Along the bed, wave asymmetry cause streaming in the wave boundary layer and is in wave propagation direction. The wave height-period combination is, therefore, important to bed load transport.

The time-averaged velocity at 1cm above the bed is determined from the depth-mean velocity profile. The depth mean-velocity is calculated by assuming equilibrium between the surface shear stress due to the dissipation of waves, streaming and return velocity. In case the surface shear stress and streaming along the bed are known, the mean velocity can rapidly be constructed. The surface shear stress is applied at mean water level and together with the bottom shear stress it is related to the velocity gradients:

$$\tau_i = \frac{\rho \nu_t}{h} \frac{\partial u_i}{\partial \sigma}$$ (3.6)

The velocity gradients are dependent on the eddy viscosity. For instance, large shear stresses at the surface cause a large velocity gradient (figure 3.19). It can be seen that for different velocity profiles, cross-shore velocity close to bed and even higher in the vertical can differ considerably. Close to the bed sediment transport can change direction for different wave conditions.
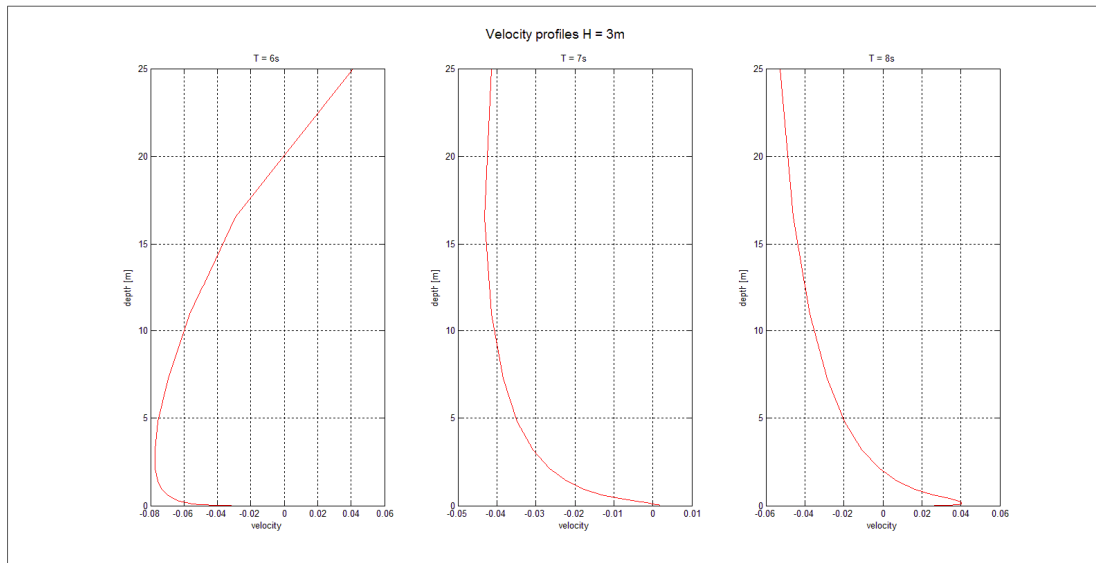
Figure 3.19 Velocity profiles (H = 3m, T = 6,7,8s)at a water depth of 25m.

3.4.1.1 Wave related bed load transport

The wave related bed load transport S_{bw} is calculated with the near-bed orbital velocity signal and thus depends on the wave height and period. In case of longer wave periods, streaming is present along the bottom on gentle slopes. For instance, a longer wave (H_{rms} = 3m, T = 8s) results in streaming along bottom, whereas no streaming is present for shorter waves (H_{rms} = 3m, T = 6s). This phenomenon is perceptible in figure 3.20 which is displayed to illustrate the relative importance of the wave length. Considering the different slopes, steep slopes induces more energetic wave breaking and enhances the return current, which opposes the streaming along the bottom. Figure 3.20 A illustrates that for steep slopes S_{bw} is predominantly offshore. Figure 3.20 B demonstrates that S_{bw} increases in case of increasing the wave period on a gentle slope of 1:1000.
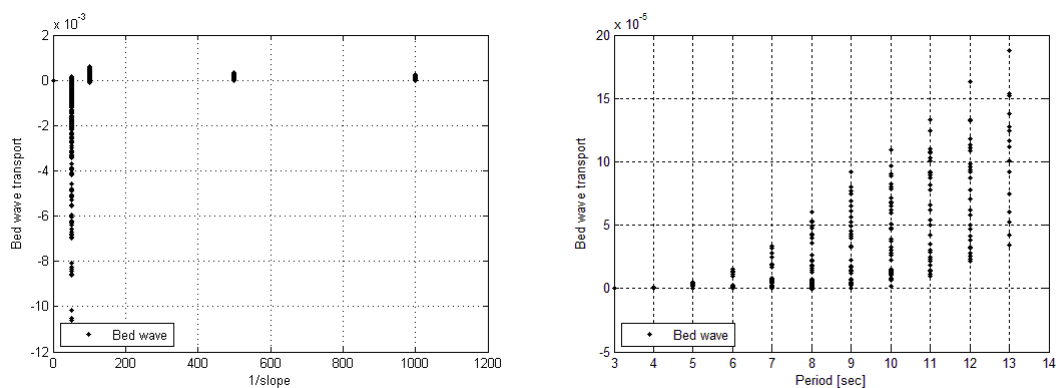
Figure 3.20 S_{bw} versus slope steepness, left figure (A) and S_{bw} versus the wave period, right figure (B).

Similar to an increasing wave period, an increasing wave height influences S_{bw} as well. Though, like the length of the wave determines the degree of streaming, the wave height more or less determines the degree of breaking. The wave height-period combination, wave steepness, is therefore the dominating factor for the onshore/offshore transport unless the slope does not become too steep (>1:50).

3.4.1.2   Current related bed load transport

The current related bed transport is calculated by considering the time-averaged mean velocity at 1cm from the bed. It is, thus, dependent on the vertical velocity profile. The surface shear stress, and therefore the degree of wave breaking, and the bottom shear stress are influencing the mean velocity profile. As indicated in the wave related bed load transport section, the wave steepness on specific slopes is the determining factor.

Regarding current related bed transport on variable slopes, it can be perceived that sediment transport is only present on a slope of 1:50. This can probably be explained by fact that no tidal velocity is included in this simulation. Obviously, the undertow is only strong enough to transport sediment in case of a slope of 1:50. In the bed load transport equation (3.4), the critical shear stress is included, see (3.7). Possibly the critical shear stress is only reached on the steepest slope.

$$\theta' = \frac{\tau'_b}{(\rho_s - \rho)gd_{50}}$$

(3.7)

3.4.2   Suspended transport

Suspended transport is the transport of sediment which is in suspension and is computed from the vertical distribution of the velocity multiplied by the vertical distribution of the sediment concentration:

$$q_s = \int_a^{h+\eta} VC dz$$

(3.8)

Equation (3.8) contains integration of the fluid velocity and sediment concentration over the vertical. The velocity and concentration can both be subdivided in an average velocity and concentration and an oscillating component of both the velocity and concentration. These represent the current related and the wave related suspended transport respectively. The computation of the suspended transport is illustrated in figure 3.21.
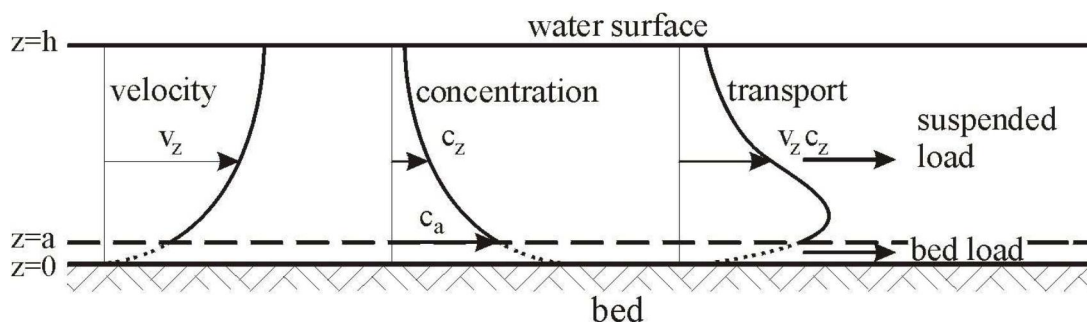
Figure 3.21 Velocity plus concentration profile is suspended load profile. (Bosboom and Stive, 2011)

Computation of the sediment concentration over the vertical for both wave-related and current-related transport is performed in the same manner. Equation (3.9) represents the main equation to compute the equilibrium concentration profile:

$$w_s c(z) + \varepsilon_s(z) \frac{dc(z)}{dz} = 0$$

(3.9)

This advection-diffusion equation (3.9) includes besides the concentration, the fall velocity and a mixing coefficient. Hence, it is a relation between the stirring/mixing and the fall velocity

of the particles. The fall velocity is computed according to Van Rijn (1993) and includes in particular the grain size. Due to a high sediment concentration, the hindered settling fall velocity is used. The mixing coefficient consists of a wave related and a current related part. Once more, the wave related part is dependent on the wave orbital velocity and therefore the wave height and period. Depth-averaged velocity induced shear stress determines the current related mixing coefficient.

3.4.1.3 Current related suspended transport

The depth-mean velocity, to compute the current related transport, is similar as described for the bed load transport. The return current is calculated by balancing the surface shear stress and bottom shear stress (figure 3.22). Opposite to the S_{bc}, the depth-mean velocity will be regarded instead of the velocity 1cm above the bed. Because the mean velocity will be considered, which is from the bed to the wave trough level, sediment transport depends on the undertow versus streaming dominance. Therefore, it's interesting to know when the undertow or streaming is dominant. In this report the shoreward velocity along the bed due to streaming will be called streaming.
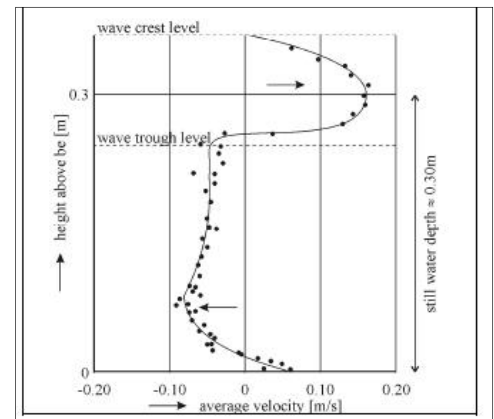
Figure 3.22 Vertical velocity profile. The vertical velocity profile consists of the surface mass flux, return current and bottom streaming (Bosboom and Stive, 2011).

Similar to the bed load transport, increasing grain size induce smaller transports. Regarding the wave period (figure 3.23), which was of influence considering the bed load transport, illustrates that S_{sc} is predominantly offshore directed. In contrast to the bed load transport, where the mean velocity was regarded at 1cm above the bed, streaming along the bottom has, therefore, less influence.
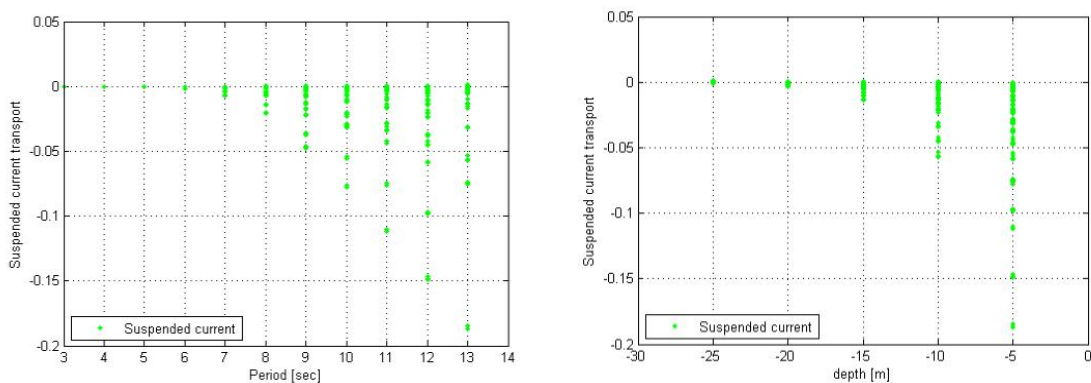
Figure 3.23 S_{sw} versus the wave period, left figure (A) and S_{sw} versus the water depth, right figure (B).

S_{sc} increases with increasing wave height and period, with decreasing depth and increasing slope steepness. More energetic waves enhance the undertow and especially on steep slopes, this effect is clearly perceptible. Especially near shore these energetic waves break and cause the largest transport in shallow water. Although, for gentle slopes the maximum transport will shift offshore as will be explained in the next section. Though, this is the case for every transport component.

3.4.1.4 *Wave related suspended transport*

Similar to S_{bw}, S_{sw} is computed by considering the orbital velocity. Although in contrast to the bed transport, streaming has no influence S_{sw}. Sediment transport is always onshore and increases with increasing wave period, see figure 3.24. Since the orbital velocity depends on the wave height, length and period, these parameters determine the wave related transport. It is therefore also straightforward that the largest sediment transport occurs on the steepest slopes. Due to the stronger effect of wave shoaling and breaking, sediment transport is larger for steep slopes.
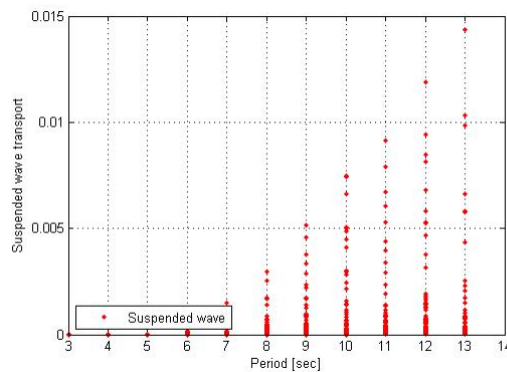
Figure 3.24 Wave related suspended transport versus the wave period

Afore mentioned influence of the slope steepness on region of maximum sediment transport can clearly be seen in figure 3.25. A gentle slope shifts the maximum transport offshore, where a steep slope induces a maximum near-shore sediment transport. In case of a gentle slope, waves are breaking more gradually. Because the orbital velocity used for computing S_{sw}, which is dependent on the mass flux, determines the transport rates, it can have its maximum farther offshore. The shear stress at the surface is larger at, for instance, -15m NAP, and is already diminished in shallow water. A steep slope induces more energetic wave breaking near-shore and thus shifting the maximum transport region shoreward. S_{sw} is therefore dependent on the degree of wave breakings and magnitude of shoaling.
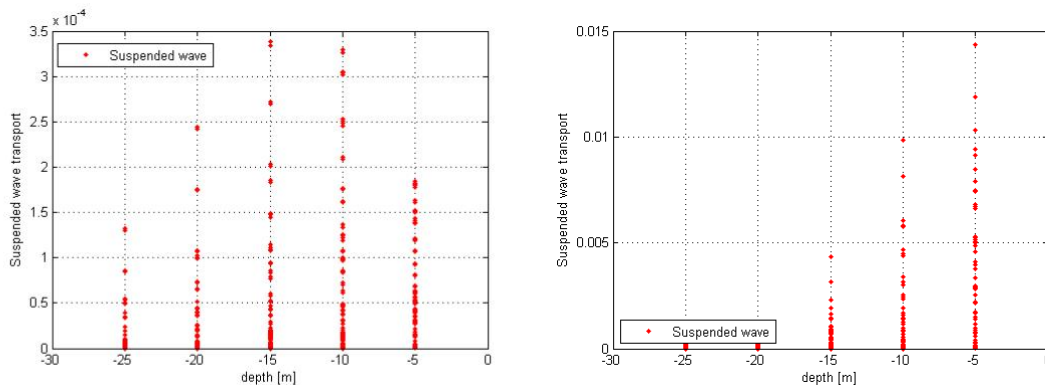
Figure 3.25 S_{sw} versus water depth with a fixed slope of 1:1000, left figure (A) and S_{sw} versus water depth with a fixed slope of 1:50, right figure (B)

3.4.2 Findings

Elaborating on the different sediment transport components, the vertical velocity profile in correspondence with the degree of wave breaking appears to be dominant. S_{bw} depends on the magnitude of streaming along the bottom and is therefore dependent on vertical velocity profile. If waves start to shoal, streaming develops and an onshore transport is perceptible. However, a strong undertow current can oppose streaming, which can change the direction of the bed transport. The magnitude of orbital velocity is important considering the magnitude of the bed load transport. This is also true for S_{sw}. Though, in this case the surface shear stress, due to shoaling and wave breaking, is of importance as well. The findings are listed below:

• Vertical velocity profile + orbital velocity + degree of wave breaking are important.
• Streaming along the bottom versus the undertow current determines the S_{sc} or S_{bw} dominance.
• S_{bw} is streaming and wave orbital velocity dependent.
• S_{sc} is depth-mean velocity dependent.
• S_{sw} is surface shear stress and wave orbital velocity dependent.
• Slope steepness + H_{rms}/T ratio determines the direction and magnitude of sediment transport.

Wave energy in correspondence with the slope steepness for various depths is responsible for the sediment transport magnitude and direction. Therefore, a real profile including fixed slopes for certain depths considering particular wave conditions would give further insight in the dominance and direction of the different transport components. Besides, this classification would make this analysis more realistic.

Sediment transport on various depth contours of the 'Holland Coast' shoreface

4 Dominant processes at different water depths

As stated in the findings of chapter 3, a classification including realistic profiles will be considered and schematised in this chapter. In that way, realistic slopes can be specified to certain depth contours and more insight will be gained in the magnitude, direction and dominance of the transport components, which will help to answer some of the hypotheses. Only realistic profiles will be considered in this chapter.

In continuance with chapter 3, only normal incident waves without horizontal and vertical tide will be considered first. Variable wave angle and tide will be included in chapter 5. Furthermore, the grain size is considered to be 200µm over the entire profile and the value of the LH-streaming is set on its default value (=1). Likewise, the same variable wave height and period will be assumed as was used in chapter 3.

First, the schematised profiles will be explained in section 4.1. Next, an analysis will be made in section 4.2. In this section, the dominant transport component and transport direction will be examined per depth contour for various profiles and will be analysed. Additionally, the direction and dominancy of the transport components per depth contour will be described in this section. Subsequently, in section 4.3 the various profiles will be compared by comparing the difference in sediment transport.

4.1 Schematised profiles

The realistic profiles are schematised according to the steepness of the slopes used in chapter 3, which were obtained from Van Alphen and Damoiseaux (1987). From this, an upper gentle slope and a lower steep slope are schematised which read:

- -25m: 1:1000 – 1:1000
- -20m: 1:1000 – 1:1000
- -15m: 1:500 – 1:1000
- -10m: 1:100 – 1:500
- -5m: 1:50 – 1:100

The first column represents the steep slope, whereas the second column represents the gentle slope. According to Van Alphen and Damoiseaux (1987), the toe of the shoreface and thereby the passage with the sea bottom is located approximately around -20m NAP. They assume that the sea bottom has a slope of 1:1000. Subsequently, they state that close to the beach the slope varies between 1:25 and 1:90 along the Holland Coast. Because a depth of -5m NAP is considered to be the most shoreward depth contour, a slightly gentler slope will be assumed. This leads to a slope of 1: 50 and 1:100 at the -5m NAP depth

Figure 4.1 Holland Coast (GoogleEarth). The yellow pins represent the city of Noordwijk and 'Meetpost-Noordwijk'.

contour and a slope of 1:1000 at -20m NAP and deeper. In between, the profiles slightly become steeper towards the shoreline.

Secondly, a realistic profile will be considered as well, namely the shoreface profile in front of Noordwijk. This profile dates from 1984 and extends to a depth of -18m NAP. The shoreface profile in front of Noordwijk is chosen, because of the usage of the available wave climate later on, which is recorded about 11 kilometres offshore of Noordwijk (figure 4.1). Besides, Noordwijk is approximately located in the middle of the southern part of the uninterrupted Holland Coast interrupted by the debouching river Rhine and harbour moles of IJmuiden. This, too, makes the alongshore uniform coastline assumption more realistic. The city Noordwijk and the recording station are marked as yellow pins.

The 'Noordwijk-profile' has a slope steepness of 1:2000 at -18m NAP, which increases towards 1:500 at -15m NAP. At -10m NAP the steepness is increased even further, namely 1:200 which is also the steepness at -5m NAP. Near the water line (0m NAP) the slope steepness is 1:50. To be able to examine sediment transport at -25m NAP, the 'Noordwijk-profile' is elongated until -30m NAP. The steepness is assumed to be constant from -18m NAP to -30m NAP, which is 1:2000.
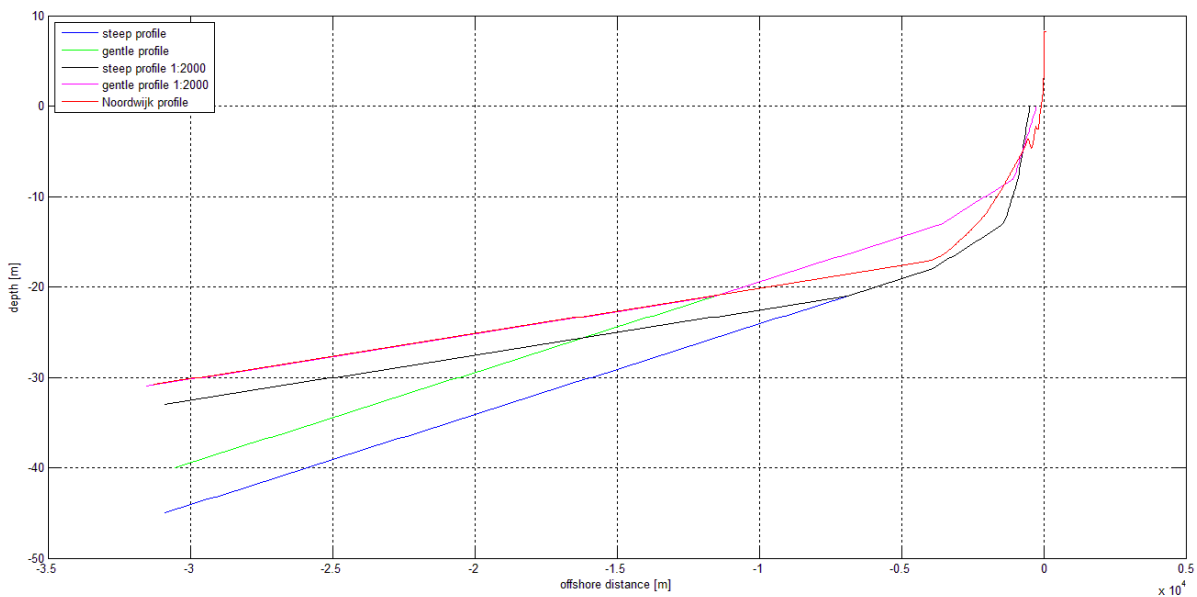
Figure 4.2 Schematized profiles.

The mentioned steep lower profile, gentle upper profile and the 'Noordwijk-profile' are included in figure 4.2. Though, it also contains two extra profiles, viz. a steep profile including a slope of 1:2000 deeper than -20m NAP and a gentle slope including a slope of 1:2000 deeper than -20m NAP as well. Because the 'Noordwijk-profile' contains a slope steepness of 1:2000 at -18m NAP, two profiles are added which contain a similar slope steepness. In this case, the 'Noordwijk-profile' is surrounded by steeper and gentler profiles and it is considered to be the average profile. In a later stadium in section 4.3, the variability of the profile will be examined in which the variability of sediment transport on different profiles will be compared and investigated. First, the dominance and direction of the transport components on the 'Noordwijk-profile' will be examined in section 4.2.

4.2 Analysis 'Noordwijk-profile'

As stated in the introduction of chapter 4, the response of transport components, considering a variable wave height and period only, will be investigated. It should be noted that only the wave related bed load and suspended load and S_{sc} will be considered in this analysis. The current related bed load transport will be ignored in this chapter. From chapter 3, it can be derived that without a 'sufficient' tidal velocity, the current related bed load transport is practically zero.

The dominance and direction of the transport components will be investigated for the 6 different wave heights. Additional, various wave periods will be regarded, given the 6 different wave heights taking into account the correlation between the wave height and period. In total 12 different conditions will be examined.

4.2.1 Analysing sediment transport per wave height

First, the dominance and direction of the transport components will be examined per wave height and will be analysed. As can be seen from appendix 3, in which all wave heights are included in contrast to figure 4.3, waves with wave height of H_{rms} = 4-6m approximately induce similar transport components to be dominant on the same depth contours. Waves with a wave height of H_{rms} = 5-6m are for that reason excluded of figure 4.3. Subsequently, a summary, including the most important conclusions derived from analysing sediment transport per wave height, will be given.

4.2.1.1 $H_{rms} = 1m$
In deep water (-25m and -20m NAP), for 5s period waves, S_{sc} is very small andoffshore directed, because the offshore depth-mean velocity is offshore directed. The orbital velocity induced shear stress of the 1m wave is too small to exceed the critical shear stress and induce an onshore streaming. At -15m, streaming starts to become important and dominating the undertow. In this region, waves start to shoal and causing streaming along the bottom. The bed load transport becomes dominant, though sediment transport is still small.

Regarding the 3s wave period, S_{sc} is very small dominant over almost the entire profile and is in offshore direction. In this case the orbital velocity induced shear stress does not exceed the critical shear stress either in deep water (-25m till -10m NAP). S_{sc} is so small, as it was for 5s waves, that it is negligible. In shallow water, the shear stress exceeds the critical shear stress, what enhances the wave related onshore transport.

4.2.1.2 $H_{rms} = 2m$
Waves with a period of 7s already start to shoal in deep water (-25m NAP), which induces an onshore streaming along the bottom. S_{sc} is affected by streaming as well, and, hence, can be in onshore direction. In shallow water (-5m NAP), S_{sw} becomes more dominant, due to an increasing surface shear stress. The undertow is equally dominant, but in opposite, offshore, direction.

In deep water (-25m and -20m NAP), the depth-mean velocity is in offshore direction, due to the absence of streaming along the bed concerning a 5s wave period. S_{sc} is dominant in this case, however, it is negligible small as it was for H_{rms} = 1m waves. Regarding less deep water (-15m and -20m NAP), streaming start to become more dominant, though, sediment transport is still offshore directed. Streaming reduces the undertow, by which the S_{bw} becomes dominant. At – 10m NAP, the S_{bw} is already dominant. A steeper slope reduces the

onshore streaming along the bottom and enhances wave breaking, which results in an offshore transport at – 5m NAP.

4.2.1.3 $H_{rms} = 3m$

In deep water (-25m NAP), streaming along the bottom is present for 8s waves, which results in a dominant onshore bed load transport. Concerning more shallow water (-10m and -15m NAP), waves start to shoal considerably, which enhances the surface shear stress and therefore the S_{sw}. Near-shore, where waves are breaking, the undertow becomes dominant in offshore direction.

Considering a 6s wave period, no effective streaming occurs until -15m NAP, which leads to a very small offshore transport. Although no effective streaming occurs, it is the effect of the streaming what reduces the return current and is enhancing the S_{bw}. At -15m NAP, the streaming becomes that effective that bed load transport becomes onshore directed. In shallow water, the wave energy dissipation becomes that effective that the compensating return current becomes dominant.

4.2.1.4 $H_{rms} = 4m$

Streaming is dominant in deep water (-25m NAP) for 10s waves as it influences S_{bw} and S_{sc}. Gradually considering shallower water, waves start to shoal more intense and enhance the onshore directed wave related transport $S_{w,on}$. In shallower water (-5m and -10m NAP), the undertow becomes more dominant due to more intense wave breaking.

In deep water (-25m NAP), streaming is not effective enough to induce an onshore transport for 7s wave periods. Hence, sediment transport is offshore directed. At -20m NAP, shoaling of waves enhance the onshore S_{bw}. Concerning shallower water (-10m and -5m NAP), S_{sw} and S_{sc} are equally dominant until waves start to break, what increases the undertow dominance.

4.2.1.5 $H_{rms} = 5-6m$

In shallow water (-10m and -5m NAP), S_{sc} and S_{sw} remain equally dominant, similar to H_{rms} =4m. The only difference with H_{rms} is present between -25m and -15m NAP, where the S_{sw} becomes more dominant on the remaining 3 depth contours. Due to an increased orbital velocity and surface shear stress S_{sw} becomes the dominant transport component.

4.2.2   Dominance per depth

4.2.2.1   -25m NAP

Waves smaller than H_{rms} =2 and shorter than T = 5s induce an offshore sediment, the undertow is predominantly dominant. Once streaming becomes important, transport can still be offshore, though the bed load transport becomes the dominant transport component. Waves longer than 7s enhance onshore bed load transport. Considering the highest waves (H_{rms} = 5-6m), $S_{sw,on}$ becomes dominant.

4.2.2.2   -20m NAP

Only for waves with a wave height smaller than 1m, S_{sc} is small and offshore directed. Waves higher than 1m induce an onshore bed load transport, provided that the waves are longer than 6 seconds. Waves higher than 4 meter, induce a S_{sw} dominance, equal to the bed load transport. Sediment transport is more onshore directed and is only for the lowest amplitude waves offshore.
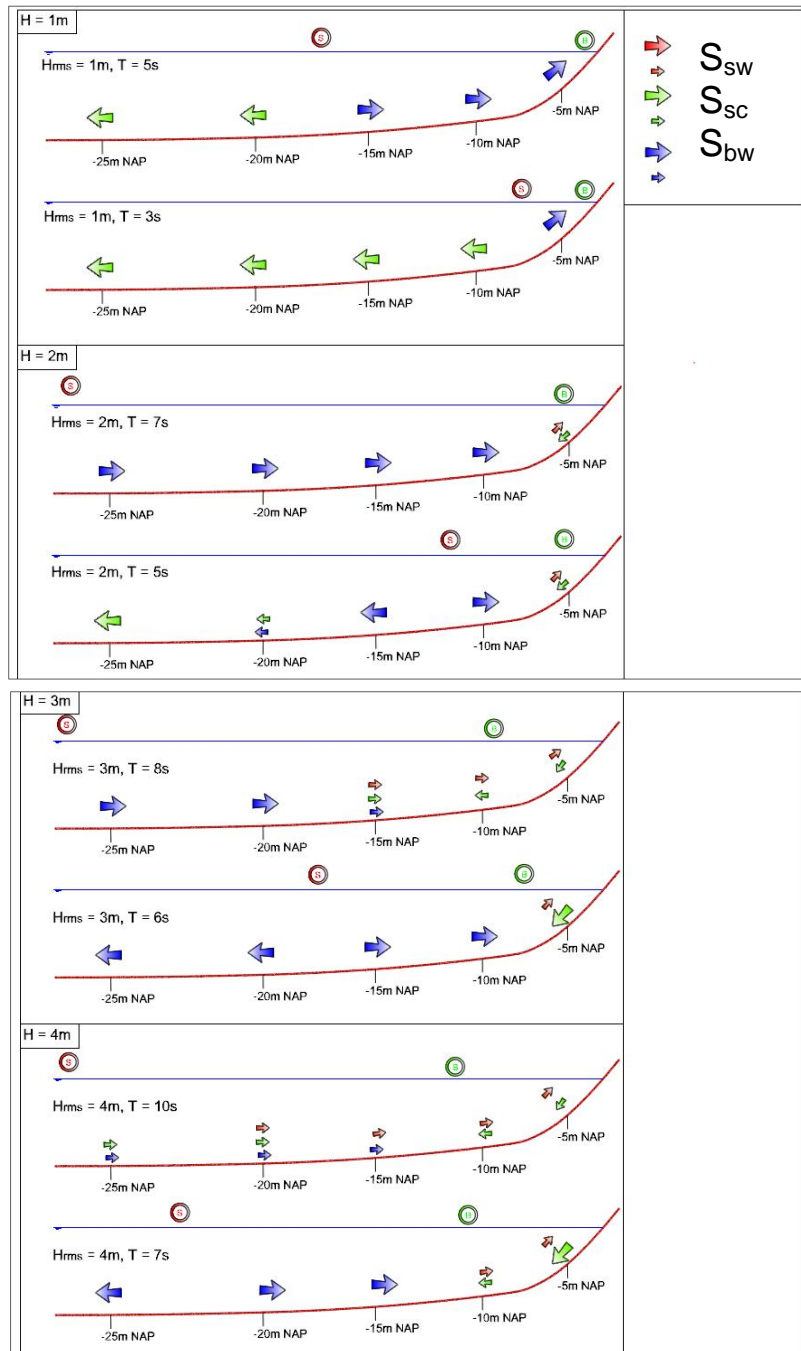
Figure 4.3 Classification profiles. 8 different conditions are depicted, including the direction and dominance of the different transport components. The green colour represents the S_{sc}, the blue colour S_{bw} and the red colour the S_{sw}. The transport components are illustrated from -25m NAP till -5m NAP, with an interval of 5 meters. Large arrows indicate the dominant transport mechanism; small arrows indicate the secondary transport mechanism. Furthermore, red and green circles are depicted near the water line in every profile. The green circle represents the offshore distance at where waves start to break. The red circle signifies the offshore distance at where waves start to shoal, so where the orbital velocity induced shear stress exceeds the critical shear stress and initiates sediment transport. This figure is subdivided in 4 subplots, each representing a different wave height. In each subplot, 2 profiles are illustrated, in which the upper profile expressing a long wave period relative to the lower profile, where the wave is shorter.

4.2.2.3   -15m NAP

Waves with a wave height smaller than 3m result in an onshore S_{bw} dominance, provided that the waves are longer than 7s. In case waves are shorter than 7s, sediment transport is offshore directed. Increasing the wave height result in a combined dominance of S_{bw} and S_{sw} in onshore direction. Sediment transport is predominantly onshore; wave related transport is the dominant mechanism.

4.2.2.4   -10m NAP

Waves with a wave height smaller than 3m show an onshore dominance of bed load transport. Increasing the wave height induces an equally onshore dominance of S_{sw} as an offshore S_{sc}. Sediment transport is onshore directed.

4.2.2.5   -5m NAP

Considering a wave height lower than 1m, reveals an onshore dominance of bed load transport. Waves higher than 1 metre lead to an equally onshore dominance of S_{sw} and an offshore dominance of the undertow. Sediment transport is predominantly in onshore direction.

4.3   Influence of profile steepness

To investigate the sensitivity of sediment transport present on various profiles, the profiles depicted in figure 4.2 will be used to examine this. Regarding sediment transport, taking into account the variable profiles, there is no difference visible considering wave heights of 1 and 2 meter. So, steeper and gentler slope have a diminished influence on low amplitude waves. For waves higher than 2 metre considering the near-shore zone, the slope steepness determines the dependence of the wave related versus S_{sc}. Steeper slopes enhance wave breaking and therefore the undertow, whereas gentle slopes reduce the undertow, which makes S_{sw} dominant.

In deep water (-15m to -25m NAP), gentle slopes enhance streaming along the bottom, resulting in a S_{bw} dominance. Though, this is only valid for higher waves higher than 3 metres. Nevertheless, the bed load transport gets affected when the slope steepness increases from 1:2000 to 1:1000. A steeper shoreface profile enhances the dissipation of wave energy which is caused by more energetic wave breaking. S_{sc} becomes dominant and reduces the bed load transport. Similar to the S_{bw}, S_{sw} does get influenced by the profile steepness. Steeper shoreface profiles enhance shoaling and, therefore, S_{sw}.

4.4   Findings

From the sections 4.2 and 4.3 the following can be concluded:

- Offshore S_{sc} is dominant, but very small, in deep water (-25m till -15m NAP) provided that the bed load related critical shear stress is not exceeded yet.
- Onshore S_{bw} dominance, provided that the orbital velocity induced shear stress exceeds the critical shear stress.
- Streaming is dominant in deep water and wave period dependent and determines the S_{sc} or S_{bw} dominance.
- S_{sc} and S_{sw} is dominant when wave-breaking occurs (-10m and -5m NAP).
- The wave orbital velocity – wave period ratio (u_{orb}/T) is important especially in deeper water.

5 Relative dominance of sediment transport per depth contour

In order to examine sediment transport and the evolution of the shoreface along the Holland Coast, a realistic wave climate should be used. Chapter 3 and 4 only included normal incident waves and the tide was ignored. Besides, the occurrence of certain wave conditions was omitted as well. In this chapter, a realistic wave climate including occurrences will be regarded. To be able to analyse sediment transport considering a realistic wave climate, sediment transport due to a variable wave angle and tidal velocity will be examined. This will be done in section 5.1. Afterwards, an analysis will be performed including a realistic wave and tidal climate. Histograms, which represent sediment transport multiplied with percentages of occurrence of wave conditions, will be used to examine the direction and relative dominance of sediment transport. Additional, in appendix 7 a sensitivity analysis is added to investigate the robustness of the model by varying certain parameters.

Including tidal current and adding percentages of occurrence of wave conditions in this chapter will contribute in answering the hypotheses stated in section 1.2. Firstly, the implementation of a tidal current in Unibest-TC can answer the question whether the suspended load transport is dominant on the lower shoreface and that bed load transport can be neglected. Secondly, adding percentages of occurrence to all wave conditions will give more insight in whether the continuous processes or the event-driven processes are responsible for the lower shoreface morphodynamics.

5.1 Wave angle and tide analysis

Prior to the response of sediment transport due to a variable wave angle and tidal velocity will be examined, the effect of a variable wave angle only will be studied first. This section will first elaborate the wave angle in 5.1.1 and afterwards the tidal velocity will be included in 5.1.2.

5.1.1 Wave angle analysis

The effect of a variable wave angle will be examined in this section, where a comparison is made with the normal incident scenarios discussed in chapter 3 and 4. The modification of the considered transport components will be examined.

Sediment transport has its maximum at a wave angle of 20 degrees (see figure 5.1). All wave heights, wave periods and depth contours, as described in section 3.1.1, are included. The S_{bw} is maximum for every depth contour, although this effect is more clearly for shallow water (-10m and -5m NAP). Similar to S_{bw}, S_{sc} and S_{sw} experience a maximum transport at a wave angle of 20 degrees as well. However, this does not apply for every depth contour, but only in shallow water (-10m and -5m NAP).

Suspended transport is not maximum at 20 degrees for every depth contour, in deep water (deeper than -15m NAP), sediment transport decreases in case the wave angle increases. Increasing the wave angle from 0 to 20degrees in deep water (-25m till -15m NAP), reduces the cross-shore return current, what enhances the bed load transport. Nevertheless, in case the wave angle is increased from 20 to 80 degrees, the cross-shore bed load transport decreases too. In shallow water (-10m and -5m NAP), obliquely incident waves drive an alongshore current. This alongshore current act as a stirring mechanism, which enhances the suspended transport and causes a maximum suspended transport for a wave angle of 20

degrees. A wave with a wave angle larger than 20 degrees subsequently decreases the cross-shore transport because less energy is dissipated in cross-shore direction.
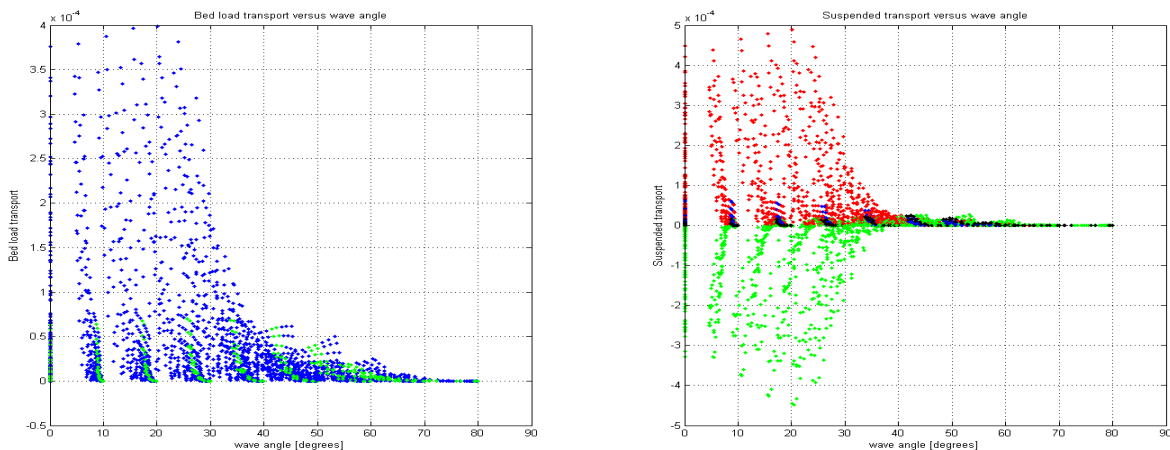
Figure 5.1 Sediment transport versus wave angle. Bed load transport versus wave angle in left subplot, suspended transport versus wave angle in right subplot. The blue dots (left plot) are bed load transport at -10m and -5m NAP, the green dots represent the bed load transport between -25m and -15m NAP. The red dots in the right subplot are the S_{sw} at -10m and -5m NAP, the green dots are the S_{sc} at the same depth contours. The remaining blue and black dots are the suspended transport between -25m and -15m NAP.

5.1.2   Wave angle and tidal velocity analysis

This section elaborates on the influence of including a variable tidal velocity in combination with obliquely incident waves. The response of the different transport components will be examined by means of including a tidal velocity, which is variable in magnitude and direction. The effect of waves and tide in the same and opposite direction will, therefore, be investigated as well.

The tidal velocity is increasing with the square-root of the depth (equation 2.5), see figure 5.2. As the tidal velocity acts as a stirring mechanism, it enhances the suspended transport. Predominantly S_{sc} is enhanced significantly. Whereas hardly any S_{sc} was present in deep water, it now is the dominant transport component, provided that the tidal velocity is strong enough. Regarding the two most columns, it is perceptible that the tide is dominant in deep water (deeper than -15m NAP). In shallow water (shallower than -10m NAP), sediment transport due to wave energy dissipation is dominant again examining the difference between the two most left columns and the right column.

Similar to S_{sc}, the S_{sw} is enhanced as well in deep water and for high amplitude waves. For waves with an amplitude of 1 metre, the S_{sw} remains negligible in deep water (figure 5.2). Stirring of the tidal velocity and high amplitude waves bring more sediment into suspension and higher into the water column, therefore, the S_{sw} is enhanced too.

Considering the bed load transport, all three columns show different patterns. In case of an insufficient tidal velocity, the bed load transport responds as derived in chapter 3 and 4. Provided a sufficient tidal velocity, the bed load transport is onshore directed when the waves and tide are in the same direction, but it is in offshore direction when waves and tidal velocity are in opposite direction. Involving the total sediment transport in deep water, an assimilated

direction of waves and tide reduces the offshore transport, whereas an opposed direction of waves and tide enhances offshore transport. This effect might influence the erosion or sedimentation of different parts of the shoreface.
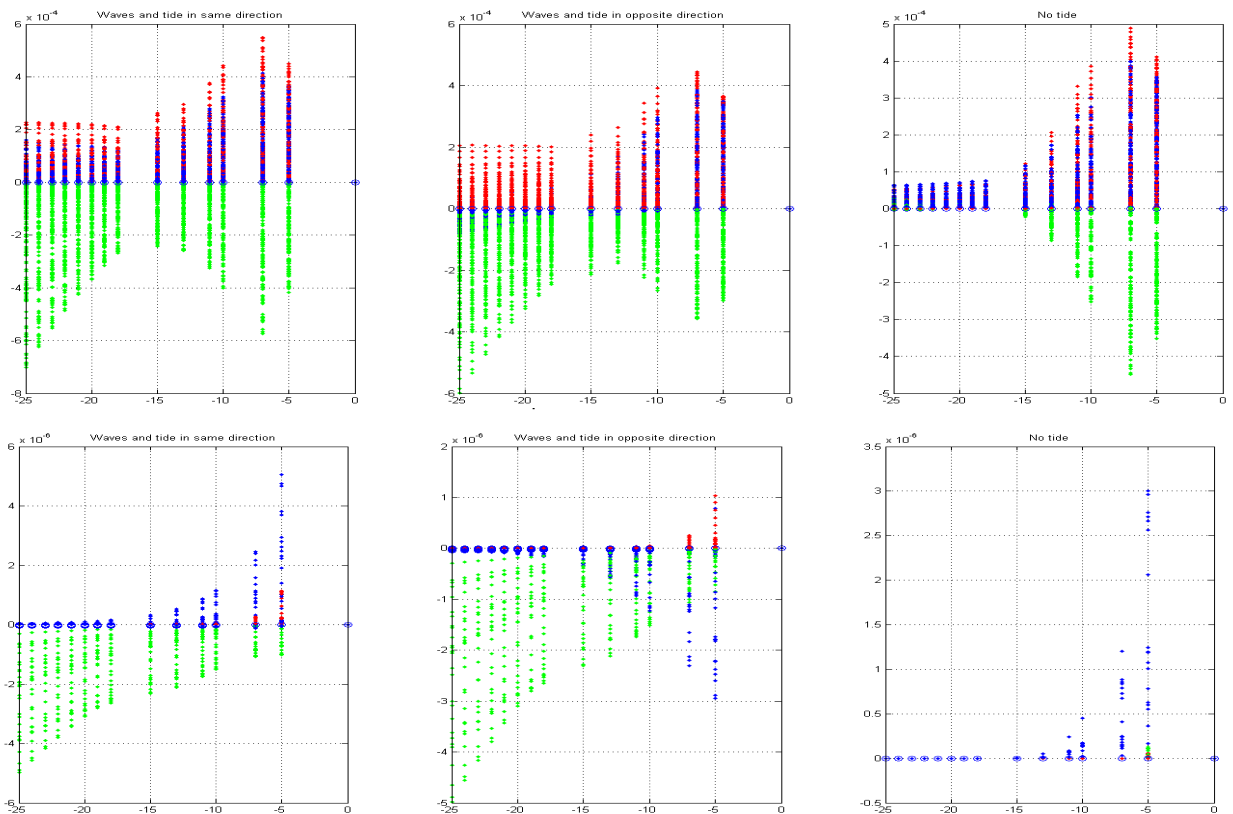
Figure 5.2 Sediment transport versus water depth. The upper subplots include all wave heights, the lower subplot include waves of 1m. In the left column the waves and the tidal current propagate in the same direction, in the middle column waves and tide are in opposite direction. The right column includes a weak tidal velocity and waves in the same and opposite direction. S_{sc} = green, S_{bw} = blue, S_{sw} = red.

A explanation for the above mentioned effect could be the tidal velocity amplifying and/or counteracting the wave orbital velocity along the bed. In case of an assimilated direction of waves and tidal current, the tidal velocity amplifies the onshore wave orbital velocity and counteracts the offshore orbital velocity, which leads to an enhance onshore velocity. Similarly, considering waves and tides in opposite direction, the tidal velocity now amplifies the offshore wave orbital velocity and counteracts the onshore orbital velocity, which lead to a bed load transport in offshore direction (figure 5.3). Although the tidal current is in alongshore direction and this effect predominantly occurs in alongshore direction, this effect is that effective that it influences the cross-shore transport as well. A similar explanation for this phenomenon is given by Groenendijk (1992), who also considered waves and tidal current in the same and opposing direction.

Regarding a variable tidal velocity once more, it should have a certain magnitude to result in a S_{sc} dominance and, therefore, enhance offshore sediment transport in deep water. In anticipation of the next section, a realistic wave climate of 24 years is already considered to examine the magnitude at which the tide becomes dominant. A tidal velocity of 0.35m/s at -5m NAP appears to be the so called 'threshold of motion' velocity at which the tide becomes

dominant. Examining the occurrence of this tidal velocity shows that 60% of the time, the tidal velocity is 0.35m/s or larger at -5m NAP. This means that this effect cannot be neglected.
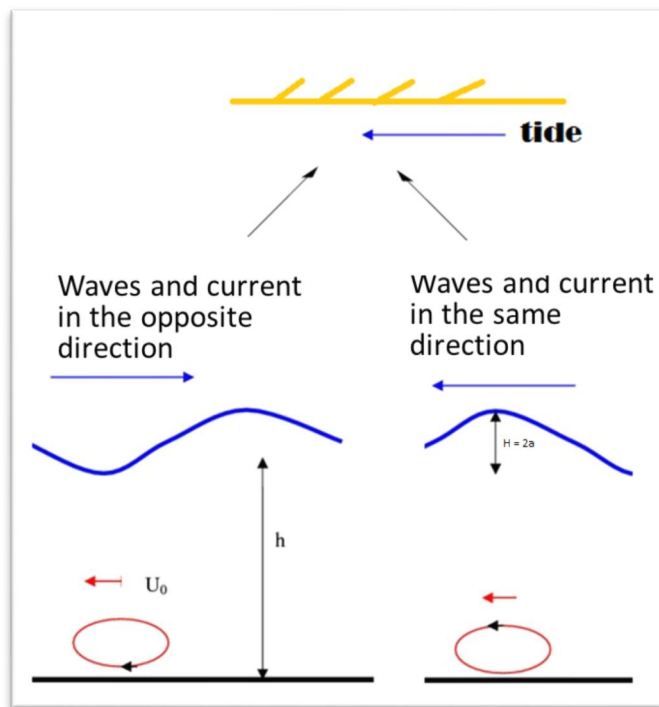
Figure 5.3 Explanation equal and opposing direction for waves and tide

5.2   Relative dominance per depth contour

For this section a reduced wave climate will be used to examine the dominance of different wave conditions and corresponding sediment transport. Applying histograms, which represent the magnitude of sediment transport multiplied with the occurrence per wave condition, will illustrate the relative importance of certain wave conditions. In that way, the dominant direction of the transport components and wave conditions can be determined per depth contour. A situation excluding and a situation including a tidal velocity will be examined, but first the wave and tidal climate will be described. Furthermore, a sensitivity analysis was performed indicating that the model Unibest-TC is robust. Varying parameters, as described in appendix 7, result in similar sediment transport dominance on various depth contours.

5.2.1   Wave and tidal climate

As stated before, a wave climate in front of the coast of Noordwijk will be used, which contains a time series of 24 years. This time series is recorded from 1979 until 2002 at 'meetpost Noordwijk', which is located 11km offshore. Every 3 hours, the significant wave height, wave period and wave angle are recorded. The tidal elevation and the gradient of the horizontal tide are derived from tidal stations at Scheveningen and IJmuiden.

The wave rose recorded at 'meetpost Noordwijk' is illustrated in figure 5.4. The shore normal of the shoreline of Noordwijk is located on 298°, considering that a shore normal of 0° is directed north and rotates clockwise. In that way, a proper wave climate for Noordwijk can be derived.

The afore mentioned wave climate, will be used to examine the dominance of certain wave conditions in relation with corresponding sediment transport. For the purpose of examining this more accurately, an occurrence table is created, which is added in the appendix 2. Three occurrence tables are being regarded, namely, wave height versus wave angle, wave height versus wave period and wave angle versus wave period. The wave height includes classes of 10cm, the wave period of 1s and the wave angle of 10 degrees. Per wave class a percentage of occurrence is given, which reduces the amount of wave conditions. The purpose of the occurrence table will be explained later.
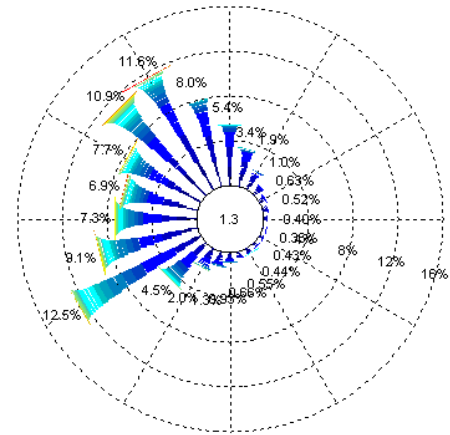
Figure 5.4 Wave rose 'Meetpost-Noordwijk', including percentages of occurrence per wave direction.

In combination with the reduced wave climate, a full tidal climate will be used (figure 5.5). By dividing the tidal climate and making multiple runs, the tidal climate will be taken into account entirely.
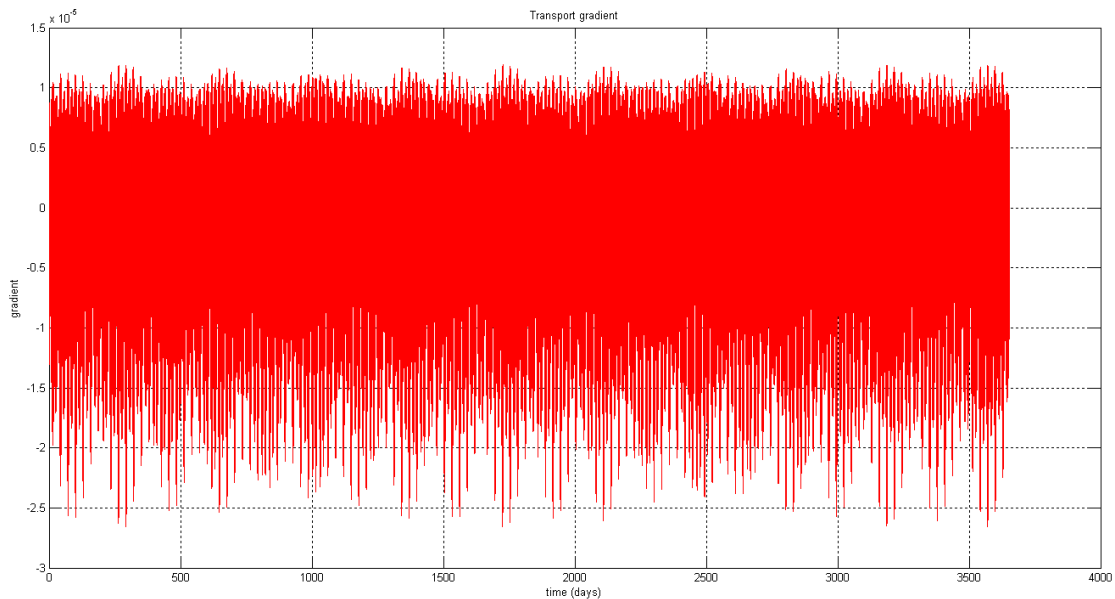
Figure 5.5 Gradients of the tidal current

5.2.2   Relative dominance per depth including waves only

In order to examine the response of sediment transport due to waves only and to study the difference between including and excluding a tidal current, a scenario including waves only will be considered first. To investigate the direction and dominance of the three transport components, histograms will be introduced. A situation for waves only is illustrated in figure 5.6, which consists of a histogram per depth contour. A histogram represents the total transport per wave condition multiplied with the percentage of occurrence, in which the occurrence of wave height, period and angle is taken into account. The occurrence tables mentioned in section 5.2.1 will be used for this purpose. The histograms, representing

sediment transport times the occurrence of wave conditions, are intended to characterise the relative importance of the dominance of the sediment transport components. In that way, it can be indicated which transport component is dominant and whether transport is in onshore or offshore direction. In continuation of chapter 4 a grain size of 200µm will be used.

Bed load transport is the dominant transport component, see figure 5.6. Furthermore, sediment transport is onshore directed over the entire shoreface profile. In section 4.3.1, it was stated that bed load transport is dominant considering depth contours deeper than -10m NAP. However, it was also said that short waves induce an offshore S_{sc} dominance. Though, as discussed in sections 3.2 – 3.4, waves with relative long periods are dominant. Low amplitude long waves are dominant on almost the entire shoreface profile (see figure 5.6). Furthermore it was described that high amplitude waves cause a suspended transport dominance regarding shallow water (shallower than -10m NAP). This fact is also illustrated in figure 5.6, in which the negative bars represent the offshore S_{sc} and the positive bars the wave related onshore transport.
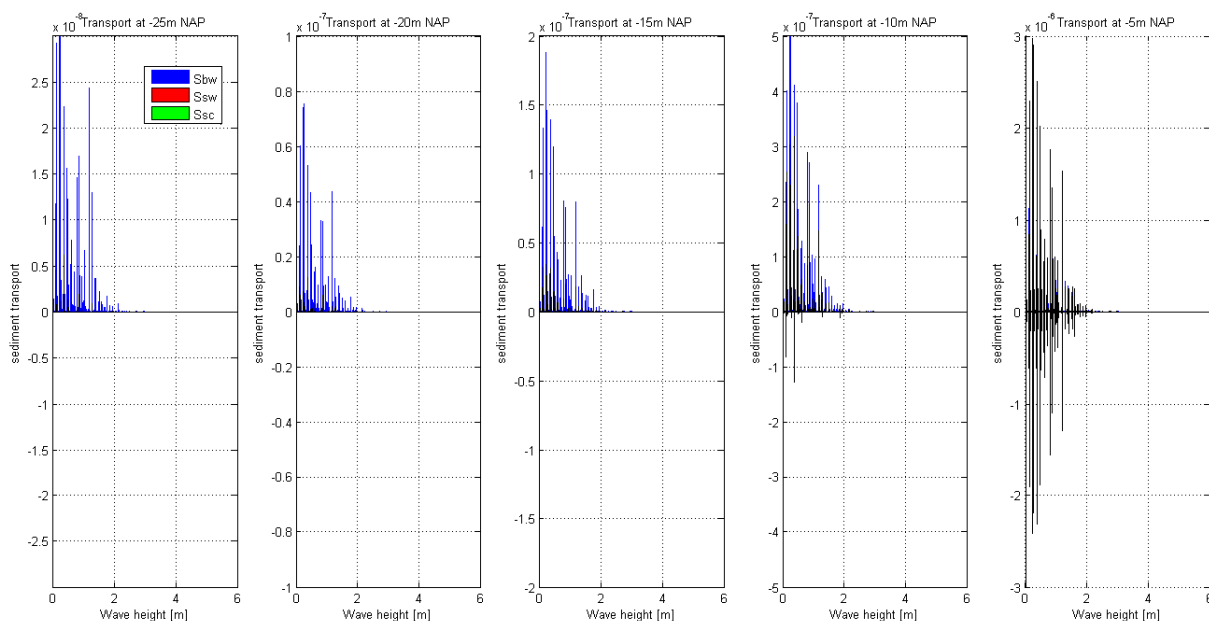
Figure 5.6 Histograms versus wave height(H_{rms})for waves only. The histograms indicate sediment transport multiplied with the percentage of occurrence per wave condition. The blue bars: bed load transport, the red bars: S_{sw} and the green bars: S_{sc}. The vertical axes are variable.

5.2.3   Relative dominance per depth including waves and a tidal velocity

Comparing a scenario including waves and a tidal velocity with a scenario without a tidal velocity, results in a different pattern, see figure 5.7. Deeper than -15m NAP, sediment transport is in offshore direction. S_{sc} is the dominant component in deep water. In shallow water, S_{sw} and S_{bw} dominate the S_{sc}. So, including a tidal velocity is responsible for offshore sediment transport dominance in deep water. Wave energy dissipation becomes more dominant in shallow water, where the wave related transport components dominate the current related transport. A sensitivity analysis (see appendix 7) confirms that varying certain important parameters result in an offshore sediment transport in deep water (-25m till -15m NAP) and an onshore transport in shallow water.

Whereas a scenario including waves only lead to accretion of the entire shoreface, a scenario including a tidal velocity results in erosion of the lower shoreface and accretion of the upper shoreface. The results of the shoreface evolution including a tidal velocity are in agreement with the description of the evolution of the shoreface in chapter 2. In this chapter, Stive and de Vriend (1995) describe the dominance of waves on the upper shoreface and of shoreface 'currents' on the lower shoreface. So, the analysed results seem to agree with the evolution of the shoreface, describe in chapter 2.
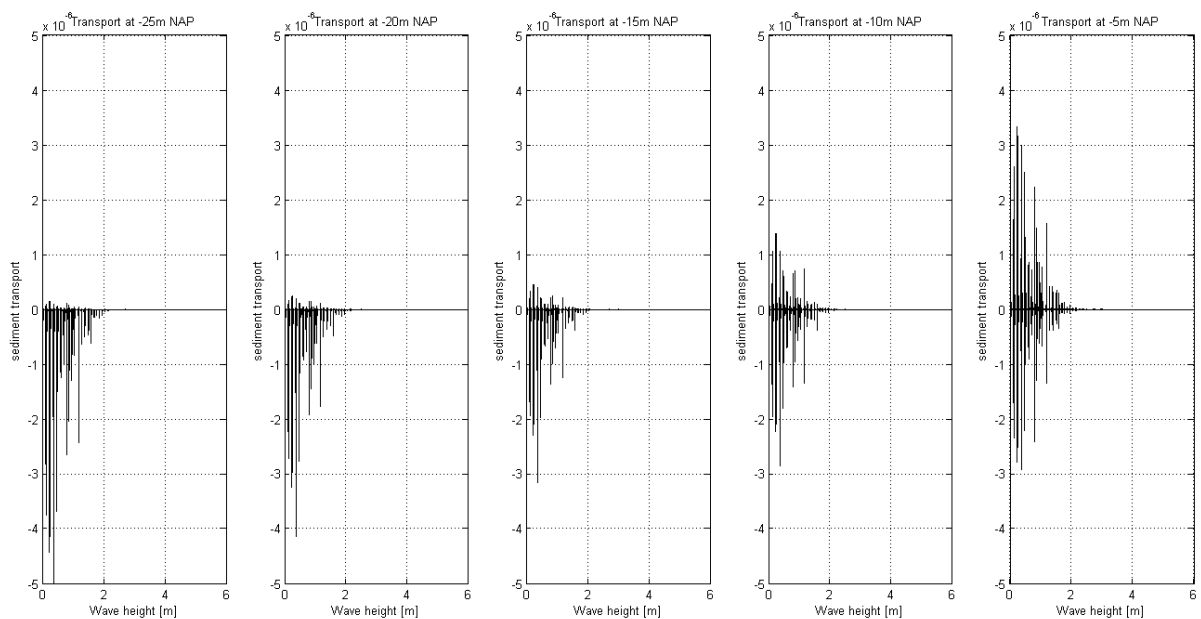
Figure 5.7 Histograms versus wave height(H_{rms}) including a tidal current. The histograms indicate sediment transport multiplied with the percentage of occurrence per wave condition. The black bars represent the total sediment transport. The vertical axes are variable.

This section includes the occurrence of wave conditions and tidal current (figure 5.7), which is done to evaluate the hypotheses stated in section 1.2. The hypothesis, stating that suspended transport is dominant on the lower shoreface and bed load transport can be neglected in case a tidal current is implemented in the model, is hereby validated. Sediment transport at -15m NAP till -25m NAP is dominated by $S_{sc,off}$, whereas S_{bw} is negligible(figure 5.7).

Wave conditions with a wave height smaller than $H_{rms} = 2m$ are responsible for the lower shoreface morphodynamics (figure 5.7). This validates the hypothesis stating that continuous processes are responsible for the lower shoreface morphodynamics, in contrast to the even-driven processes. However, amongst others, Stive and de Vriend (1995) conclude that the very event-driven processes are responsible for the lower shoreface morphodynamics. The difference with the model used by Stive and de Vriend (1995), amongst others, is the exclusion of a storm-surge level set-up and usage of different wave classes. As they used only one representative wave period assigned to one representative wave height, multiple wave periods assigned to one representative wave height is used here (see appendix 2). That means that low amplitude waves with long periods are included as well. As it was concluded in chapter 3 and 4, long wave periods induce an enhanced streaming along the bed, and therefore an enhance bed load transport, in comparison to short wave periods. Hence, the

inclusion of long waves periods assigned to waves with a wave height smaller than $H_{rms} = 2m$ are responsible for the lower shoreface morphodynamics.

6 100-year simulation of the shoreface profile

In order to investigate whether the upper shoreface is actually steepening and the lower shoreface is flattening, according to the chapter 5, morphological simulations will be performed. A 100-year simulation will be done to examine whether sediment transport at -20m NAP influences the upper shoreface. In line with the preceding chapters, a simulation with and without a tidal current will be examined to study the influence of including a tidal current.

Furthermore, profile perturbations like sand pits will be positioned on various depth contours and analysed in order to estimate timescales of the considered depth contours. The purpose of this analysis is merely to evaluate the present processes and not to examine the actual magnitude of sediment transport. First, the approach including some limitations will be explained. Subsequently, the results will be presented and analysed.

6.1 Approach

A 100-year simulation will be performed, using the realistic wave climate and tidal climate discussed in chapter 5. Because a wave and tidal climate of only 24 years has been used, the time series will be repeated about 4 times to construct a 100-year tidal cycle. Moreover, the Noordwijk profile, including a grain size of 200µm over the entire profile, will be used to examine the 100-year profile evolution.

Furthermore, in line with the scope of this investigation, excavations and nourishments located at certain water depths will be examined (see figure 6.3). The goal of this study is to investigate the different behaviour of profile perturbations near the -20m NAP depth contour. Therefore, excavations and nourishments located at -25m, -20m and -15m NAP depth contours will be considered. The sand pits and artificial ridges will have a width of 200m, a height of 1m and slopes of 1:50 (see figure 6.3). The purpose of including artificial sand ridges is to compare and validate the behaviour of the sand pits. The sand pits/artificial ridges are subtracted from the original profile to make a good comparison between several simulation years. Hence, erosion of the profile, which increases as the simulation time increases, is omitted in this way. For the purpose of examining the propagation and diffusion of the sand pits, the centre of gravity is added per simulation time step. Also, a 100-year simulation scenario including and excluding a tidal current will be examined and compared.

6.1.1 Limitations

This section will describe the following limitations:

- Overestimation of the tidal current
- Alongshore uniform coastline assumption
- A fixed grain size of 200µm

The tidal current is dominant in deep water (see section 5.2.3). Though, it should be investigated whether it is properly accounted for in the model. In open ocean waters, the tidal wave has a progressive character, which indicates that friction can be ignored and inertia is dominant. In shallow waters, the inertia effect is small and the tidal current is determined by the balance between the alongshore water level gradient and bottom friction. This can be

derived from the alongshore momentum balance in which inertia is ignored and friction is added:

$$g \frac{\partial \eta}{\partial y} = -\frac{\tau_{by}}{\rho h} \qquad (6.1)$$

If a quadratic friction law is considered, the tidal velocity is proportional to the square root of the water depth and alongshore water level gradient:

$$\tau_{by} = \rho c_f v |v| \qquad (6.2)$$

$$v \propto \sqrt{h \frac{\partial \eta}{\partial y}} \qquad (6.3)$$

This means that the tidal velocity increases with the square root of depth, which is obvious considering that bottom friction is less effective in reducing the magnitude of the tidal velocity. This equation, which includes a friction factor as well, is included in Unibest-TC (equation 2.5). Therefore, regarding the analysed results, the tidal current is implemented properly.

However, concerning water depths of about -20m and -25m NAP, it can be questioned whether bottom friction is still dominant. Straightforwardly, the influence of bottom friction diminished along with an increasing water depth. Taking that into account, the model slightly exaggerating the tidal current in deep water. Moreover, measurements performed by Rijkswaterstaat (1994) show a maximum alongshore tidal current of 0.65m/s at -20m and 0.55m/s at -8m NAP in front of the coast of Noordwijk. These measurements exclude wind influences as was done in this research and are therefore comparable. Computations show about 25% larger values for the tidal current as was measured. However, maximum tidal flow velocities are comparable to what was measured by Hisgen and Laane (2004). Therefore, it can be concluded that the model slightly overestimates the actual tidal velocity, though, its presence is dominant.

Another interesting fact is that the alongshore uniform coast assumption is not taken into account regarding the propagation of the sand pits. Actually the sand pits are sand gullies with a length of several kilometres. This is the reason that the tidal current is able to increase in magnitude inside the sand pit. Regarding a length and a width of both 200m probably reduces the tidal current inside the pit as the tidal current needs some distance to reach the bottom of the pit. In case of a reduced width and length, the alongshore tidal current is not able to stir up sediment and subsequently transport it.

Furthermore, the importance of the grain size (described in section 3.2 and 3.3) has been ignored in this chapter. However, as explained by i.e. Van Straaten (1965), the shoreface of the Holland Coast consists of different grain sizes, which does not linearly decrease along with an increasing water depth. This observation will not only influence the 100-year evolution of the shoreface, but the propagation of the sand pits as well. A different grain size probably affects the shoreward propagation and sand pit diffusion as the internal angle of friction is different too. Besides a different grain size on the lower shoreface, also a different composition of grains is present (Van Straaten, 1965) which will influence sediment transport and, therefore, sand pit propagation. Not only different compositions of grains, but also hard erodible material or mud could be present, which influences sediment transport.

6.2 Results

6.2.1 Profile evolution
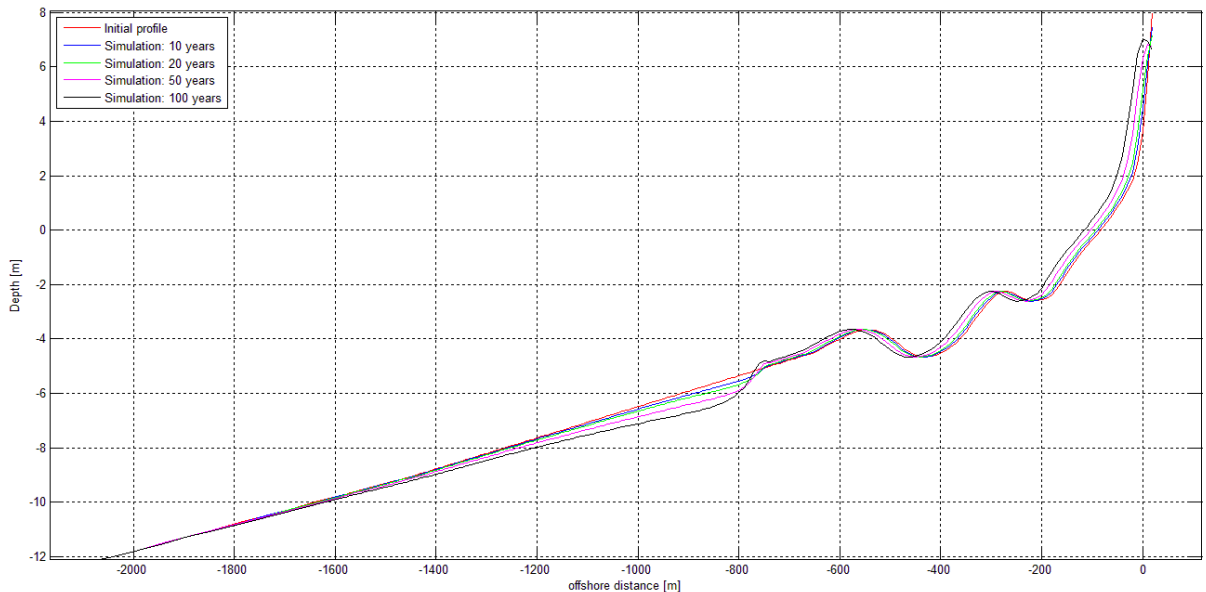
Figure 6.1 100-year simulation due to waves only.

The upper part of the Noordwijk profile after a simulation of 100 years is illustrated in figure 6.1. The depth-change below -12m NAP is considered to be negligible, see appendix 4. Only the upper shoreface shows depth changes, which seems to steepen shallower than -5m NAP. Below this depth contour, erosion appears to be present which flattens the lower part of the upper shoreface. Although the accretion near the -5m NAP depth contour is in agreement with chapter 5, the erosion at -10m NAP contradicts this analysis. However, sand present at the accreted profile above the -5m NAP depth contour finds its origin somewhere below this depth contour, namely between -10m and -5m NAP. Due to a stronger accretion rate above -5m NAP, the profile between -10m and -5m NAP experiences erosion. Even deeper than -10m NAP the transport magnitude is insufficient to cause significant depth changes.

Including a tidal current, result in a profile which can be seen in figure 6.2. The profile changes have increased considerably in comparison to figure 6.1. The upper shoreface has become steeper and has prograded even more. Deeper than -5m NAP, the profile flattens and erosion is perceptible even deeper than -15m NAP. Considering the region around the -18m NAP, the amount of erosion present here is present until -30m NAP. Thus, the erosion present at -18m NAP continuous to the seaward border of this profile, which is about 20cm over 100 years. Similar to figure 6.1, the onshore sediment transport reaching to -10m NAP causes a steepening of the upper shoreface shallower than -5m NAP. However, due to a larger offshore directed sediment transport deeper than -10m NAP, the profile flattens deeper than -5m NAP. As can be observed from sediment transport present over the entire profile, which is added in appendix 5, the onshore transport rate is dominant shallower than -10m NAP, whereas a larger offshore sediment transport is present deeper than -10m NAP.
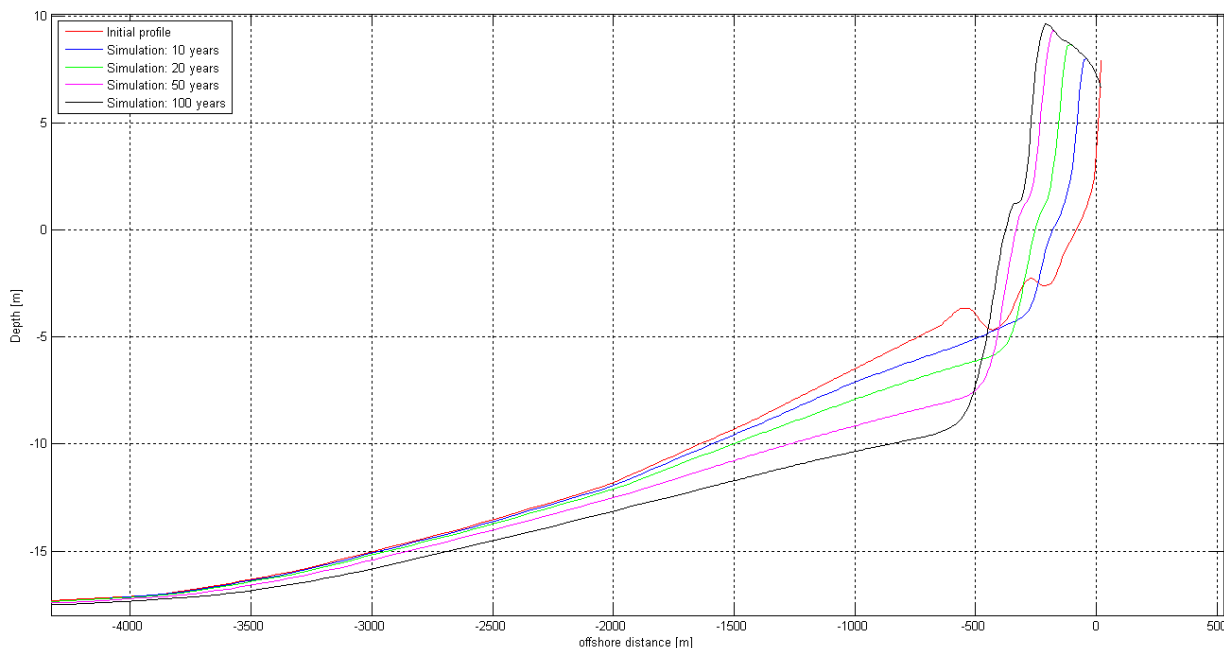
Figure 6.2 100-year simulation due to waves and a tidal current

Examining the profile evolution, an upper shoreface steepening and lower shoreface flattening is visible. Comparing a scenario excluding a tidal current with a scenario including a tidal current reveals that the tidal current is responsible for the profile changes in deep water. Furthermore, an enhanced progradation of the upper shoreface is present. These results correspond with the results from chapter 5 and confirm the stated conclusions. Evaluating the difference of figure 6.2 with figure 6.1 shows an upper shoreface regression extending farther seaward. This might suggest that including a tidal current is responsible for shifting the depth of closure, described in section 2.1.2, farther seaward.

6.2.2 Profile perturbations

All sand pits propagate in shoreward direction, see figure 6.3. However, the locations of the sand pits, location of the centre of gravity of the sand pits and shape of the sand pits after 100 years all differ. Scenarios including a tidal current, illustrate that a sand pit located at -25m NAP propagates faster shoreward than a sand pit located at -20m and -15m NAP respectively. Nonetheless, the diffusion is larger regarding the -15m NAP depth contour. The sand pit height has been reduces to almost half its original size, where considering the -25m NAP depth contour it has only reduced a quarter of its original height. Comparing the propagation of the sand pits excluding a tidal current with the sand pits including a tidal current it can be noticed that the shoreward propagation is less. Especially at -25m NAP the difference is considerable, whereas at -15m NAP it is less discernible. The dominance of the tidal current in deep water causes this difference, which will be elaborated in section 6.2.2.1. The diffusion of the sand pits, on the other hand, is comparable, which must therefore be caused by the presence of waves. Additional, artificial ridges show the same behaviour as the sand pits, namely an onshore propagation, though artificial sand ridges propagate faster. An illustration of this has been added in appendix 6, which includes the propagation of sand pits and artificial ridges.

Sediment transport on various depth contours of the 'Holland Coast' shoreface
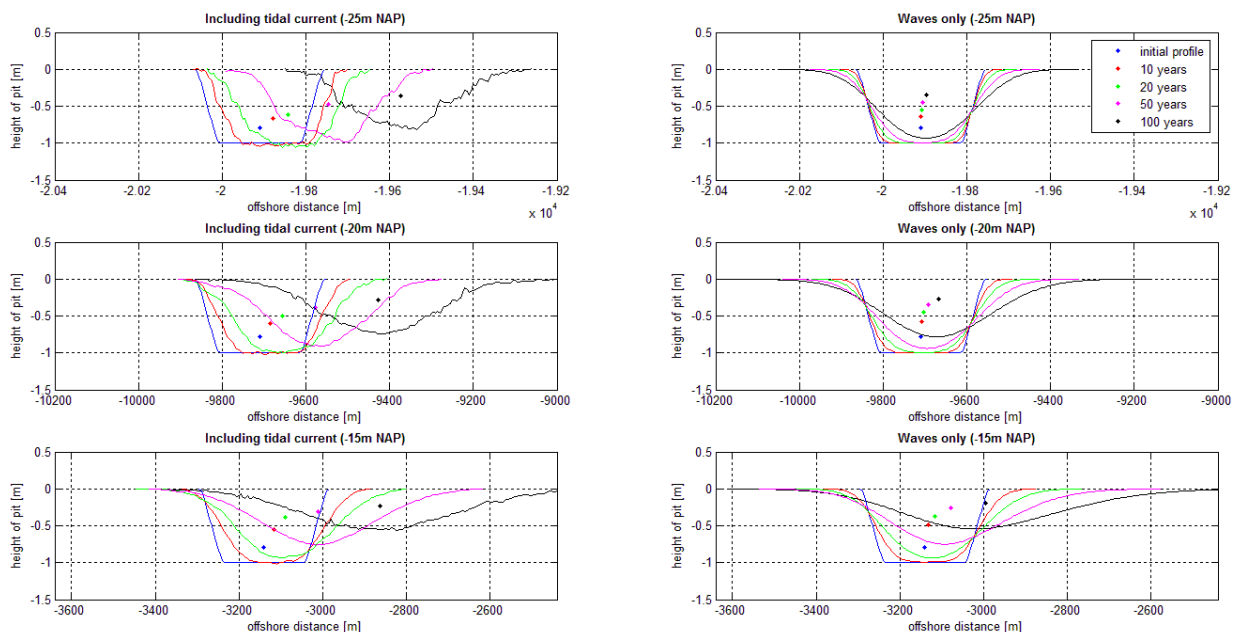
Figure 6.3 Morphology of sand pits. The left column includes a tidal current, the right column excludes a tidal current. The dots represent the centre of gravity. The shore is located at the right side of sand pits.

As can be seen in figure 6.3, all sand pits propagate onshore. First, the onshore propagation of sand pits due to including a tidal velocity will be examined. This will be done by first considering the total onshore/offshore transport and subsequently to subdivide it in the three known transport components (see figures 6.5). This means that, provided that the total sediment transport is onshore, some transport components are offshore directed. The dominant transport components which are responsible for this behaviour can be identified in this way.

6.2.2.1 Elaborating profile perturbations

The average total sediment transport (depicted in figure 6.4) shows that the average transport inside the sand pit located at -25m NAP is larger than outside the sand pit and is offshore directed. Although the average transport is offshore, the propagation of the sand pits is onshore due to the transport gradient. Concerning the shoreward edge of the sand pit, sediment transport increases in offshore direction (see figure 6.4), what means erosion is present here. Subsequently regarding the seaward edge of the sand pit, sediment transport is decreasing, what results in deposition. So, the sand pit is eroding at the shoreward edge and accreting near the seaward boundary, which results in a shoreward shifting of the sand pit. It should be mentioned that the average total sediment behaviour is similar regarding the -20m and -15m NAP depth contours. However, the transport gradient is reduced compared to the gradient at -25m NAP. By considering the different transport components the reduced transport gradient might be explained.
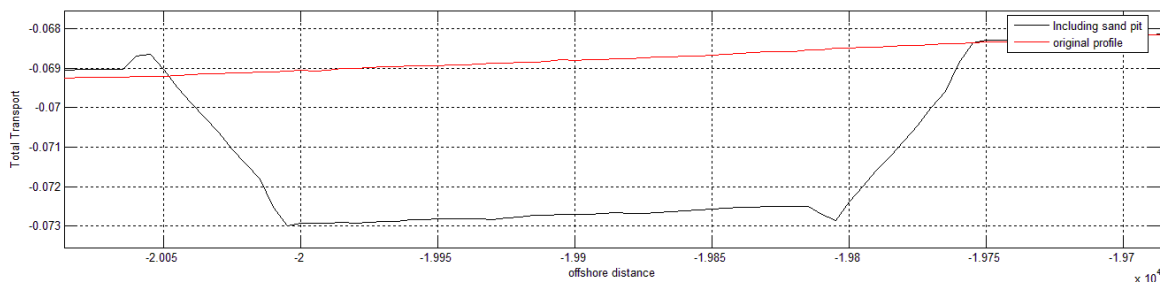
Figure 6.4 Average total sediment transport (sand pit at -25m NAP). Red is original profile, black is including profile perturbation.

The average onshore and offshore transport is shown in figure 6.5. It also includes the average total transport and average suspended transport. The onshore transport is dominated by the bed load transport, which has approximately the same pattern as the average total transport gradient. Inside the sand pit sediment transport is less, because the wave orbital velocity is reduced when the water depth is increased and is therefore less able to transport sediment. Near the boundaries of the sand pit, a slight increase (seaward side) and decrease (shoreward side) of sediment transport is visible (see figure 6.5). The gradients near the head and toe of the sand pit boundaries are responsible for diffusion of the sand pits: a negative gradient near the head induces erosion, whereas a positive gradient near the toe induces deposition at the shoreward boundary.

S_{sc} is the dominant offshore sediment transport component. Inside the sand pit, S_{sc} transport increases, because it is tidal current-dependent, which increases with the square root of the water depth. Due to an increase in sediment transport inside the sand pit, transport gradients are present which induce sand pit propagation (see figure 6.5). Both the average onshore and offshore transport show a similar transport pattern as the average total transport and its gradients explain the onshore propagation of the sand pits.

Concerning sand pits at -20m and -15m NAP, show reduced transport gradients which result in a reduced onshore propagation of the sand pits. The reduced transport gradients can be explained by the fact that it regards shallower water, which enhances wave related transport and reduces the tidal current magnitude. Due to less intensive stirring of the tidal current in shallower water, S_{sc} is reduced as is the transport gradient which is still dominated by the tidal current. The increased wave related transport at -15m NAP, on the other hand, causes a larger diffusion of the sand pit. Regarding the scenarios without a tidal current in figure 6.3, confirms this phenomenon. As the offset of the bed load gradient near the boundaries of the sand pit increases concerning shallower water, it possibly explains the larger diffusion of the sand pits at -15m NAP.
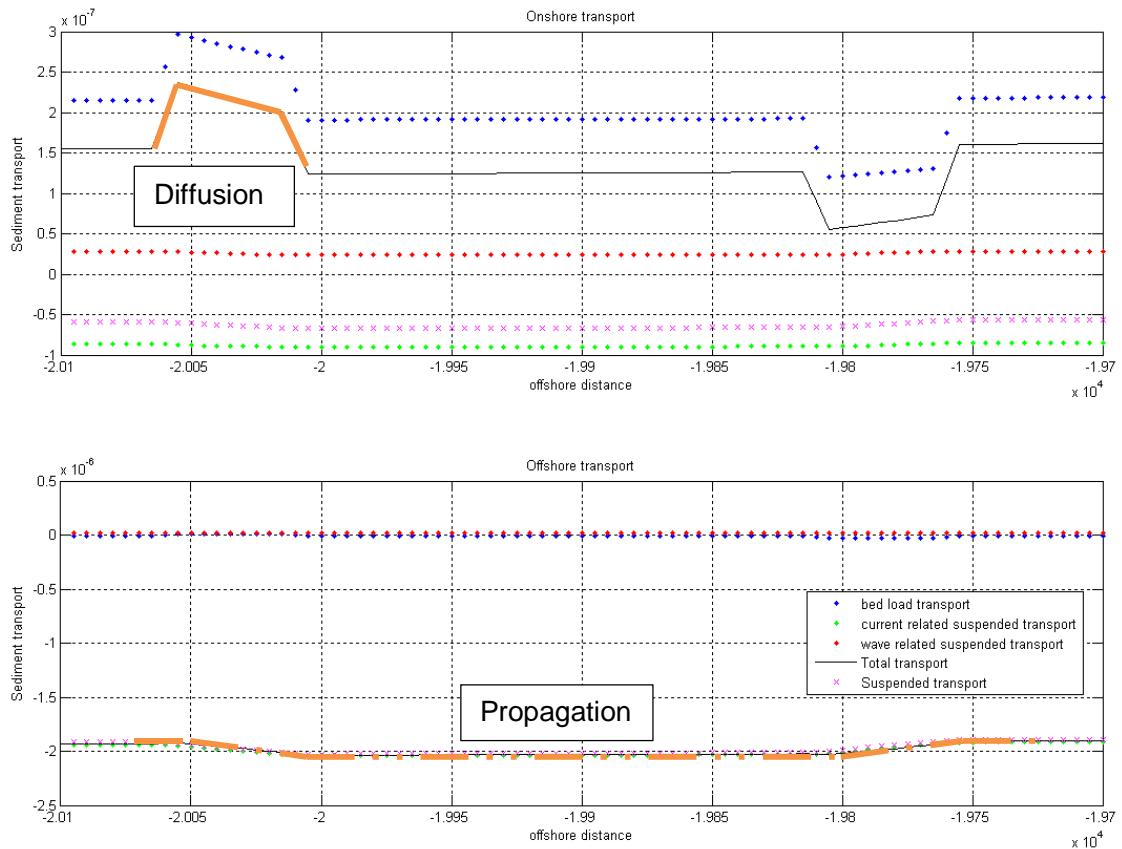
Figure 6.5 Average onshore and offshore transports (sand pit -25m NAP)

6.3 Findings

Diffusion of the sand pits at various depths are comparable, see figure 6.3. Nevertheless, the difference in sand pit propagation is different per depth contour, concerning the scenarios including and excluding a tidal current. At -25m NAP the sand pit propagates the farthest shoreward in case a tidal current is included, whereas excluding a tidal current the sand pit hardly propagates. Figure 6.6, illustrates the trend lines of the propagation (left plot) and diffusion (right plot) of the sand pits and artificial ridges. No distinction has been made upon sand pits and artificial ridges in this figure. Although, the steepest trend line represent the artificial ridge as the water depth is less on top of the ridge.

Not only the difference in shoreward propagation and diffusion per depth contour are visible in figure 6.6, it also reproduces the difference including and excluding a tidal current. Considering the propagation of profile perturbations first, shows that a perturbation located at -25m NAP propagates the farthest onshore and that excluding the tidal current it propagates the least. At -15m NAP, profile perturbations excluding a tidal current propagate more than half of the distance of the perturbations including a tidal current. So, in deep water (-25m NAP) the tidal current is dominant, whereas regarding less deep water (-15m NAP) waves become approximately equally dominant. This means that the interaction between waves and tidal currents may be of great importance and may have large impact on cross-shore sediment transport patterns.

Finally, considering the diffusion of the sand pits and artificial ridges, it is observable that diffusion of profile perturbations located at -15m is the largest. In most cases, the diffusion is large in the first 20 years and reduces after that. The diffusion reduces with increasing water depth, as was already concluded before. Furthermore, the difference between including and excluding a tidal velocity, regarding diffusion of profile perturbations, is very small.

The most important findings are listed below:

- Diffusion of sand pits due to waves (S_{bw}).
- Tidal current induced (S_{sc}) gradients cause a shoreward propagation of sand pits.
- Interaction between waves and tidal currents may be of great importance
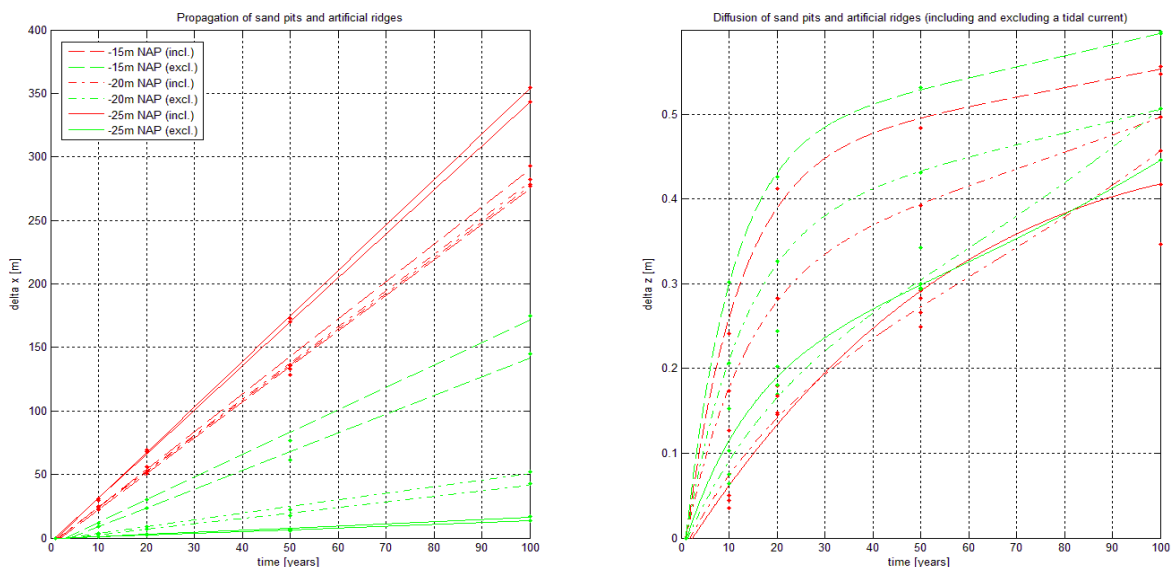
Figure 6.6 Trend lines of sand pits/artificial ridges. Left plot: propagation of the centre of gravity of the sand pits and artificial ridges. Right plot: diffusion of the sand pits and artificial ridges. The red colour is propagation and diffusion with a tidal current, the green colour is when the tidal current is excluded.

7 Conclusions and recommendations

7.1 Conclusion and hypotheses

In this section the hypotheses, introduced in section 1.2, will be discussed. Based on the insights obtained with this thesis, conclusions on sediment transport dynamics will be given first.

7.1.1 Conclusions

Evaluating the dominant processes on the shoreface by varying essential parameters (e.g. wave height, wave period, grain size, slope steepness and water depth) shows that sediment transports vary as expected. A smaller grain size induces larger sediment transport, the magnitude and directions of sediment transport are positive related to slope steepness, wave height and water depth. The magnitude of the LH-streaming is determinative for the direction of sediment transport in a situation without tide. The wave steepness in combination with the slope steepness for certain depth contours determines the direction and magnitude of sediment transport.

Elaborating on the transport equations show that the vertical velocity profile, wave orbital velocity and degree of wave breaking are important in determining the dominant transport component. Wave orbital velocity induced streaming along the bed versus the vertical velocity dependent return current determine whether the onshore directed S_{bw} or offshore directed S_{sc} is dominant. In addition, the slope steepness in combination with the wave height – period ratio determines which transport component is dominant.

Considering a realistic shoreface profile to gain insight in the dominant processes per water depth indicates that, for a situation including only waves, S_{bw} is dominant on the lower shoreface, whereas suspended transport is dominant on the upper shoreface. The onshore directed S_{bw} is dominant on the lower shoreface, provided that the orbital velocity induced shear stress exceeds the critical shear stress. On the upper shoreface, the in offshore direction S_{sc} and S_{sw} are dominant, because the turbulence generated by breaking waves is very effective in keeping sediment into suspension.

Adding a variable wave angle and tidal velocity shows that the additional stirring due to the tidal current causes the offshore S_{sc} dominance on the lower shoreface. Onshore wave related sediment transport is dominant on the upper shoreface. The direction of the waves in combination with the tidal current influences S_{bw} the most; S_{bw} is onshore when waves and tide are in the same direction and is offshore in case of opposite direction. So, the interaction between tidal currents and waves is of great importance and may have large impact on cross-shore sediment transport patterns.

7.1.2 Hypotheses

By examining the 100-year shoreface evolution and profile perturbations located at certain depth contours, the first three hypotheses, stated in section 1.2, are evaluated:

- Within a time scale of 100 years, there's no substantial sediment transport at -20m NAP that influences the upper shoreface.

- Both a situation including only waves and a situation including a tidal current confirm this hypothesis. A profile degradation of 20cm over 100 years is present on the lower shoreface (-25m till -15m NAP). Sand pits and artificial ridges on the -20m depth contour propagate shoreward approximately 400m over 100 years. As the -20m NAP depth contour is located between 5 and 15km offshore (Stolk, 1989), sand pits do not affect the upper shoreface at a time scale of 100 years.

- Sand borrowing pits between -20m NAP and -18m NAP affect the upper shoreface within a time scale of 100 years.
  - In response to the above hypothesis, this hypothesis should be rejected. Comparing profile perturbations on the -15m and -25m NAP depth contours result in similar shoreward propagation rates. Assuming an average shoreward propagation of sand pits between -25m and -15m NAP of 400m would imply sand pits eventually do affect the upper shoreface (-10m NAP), but not within a time scale of 100 years.

- Sand pits and artificial ridges located on various depth contours have different time scales.
  - Profile perturbations on various depth contours of the lower shoreface do have different time scales, what makes this hypothesis valid. However, it was expected that sediment transport at -15m NAP would be larger than -20m NAP and subsequently -25m NAP. Moreover, sand pits propagate about 600m shoreward at -25m NAP and only 400m at -15m NAP. Sand pits at -20m NAP propagate only slightly farther onshore. The tidal current induced stirring is responsible for the different propagation of sand pits on various depth contours. As the tidal current depends on the square root of depth, it induces larger gradients at -25m NAP than at -15m NAP, which explains the farther propagation at -25m NAP.

Through analysing the relative dominance of sediment transport on various depth contours, including occurrences of wave conditions and tidal current, the last two hypotheses can be discussed:

- The continuous processes, in contrast to event driven processes, are responsible for the lower shoreface morphodynamics.
  - Wave conditions with a wave height smaller than $H_{rms} = 2m$ are responsible for the lower shoreface morphodynamics (figure 5.6 and 5.7). This validates the hypothesis stating that continuous processes are responsible for the lower shoreface morphodynamics, in contrast to the even-driven processes. However, this result can be questioned as, amongst others, Stive and de Vriend (1995) conclude that the very event-driven processes are responsible for the lower shoreface morphodynamics. As they used only one representative wave period assigned to one representative wave height, multiple wave periods assigned to one representative wave height is used here (see appendix 2). This means that low amplitude waves with long periods are included as well. As concluded in chapter 3 and 4, long wave periods induce an enhanced streaming along the bed, and therefore enhance bed load transport, in comparison to short wave periods. Hence, the inclusion of long wave periods assigned to waves with a wave height smaller than $H_{rms} = 2m$ are responsible for the lower shoreface morphodynamics.

- Implementation of a tidal current in Unibest-TC makes the suspended load transport dominant on the lower shoreface.
    - The hypothesis, stating that suspended transport is dominant on the lower shoreface and bed load transport can be neglected in case a tidal current is implemented in the model, is can be validated: Sediment transport at -15m NAP till -25m NAP is dominated by offshore directed S_{sc}, whereas S_{bw} is negligible (see figure 5.7). Tidal current induced sediment transport is, thus, dominant on the lower shoreface.

7.2 Discussion

Tidal current induced suspended sediment transport is dominant on the lower shoreface. However, the implemented tidal velocity is overestimated by Unibest-TC, hence sediment transport is exaggerated. The magnitude of the depth-average tidal velocity at -20m NAP simulated by the model is about 25% as large as was measured (Rijkswaterstaat, 1994). The 100-year simulation of the Noordwijk-profile could therefore be exaggerated as well is the suspended transport gradient induced sand pit propagation. However, in case deeper sand pits are considered, say 5m, the same results could be obtained. Nevertheless, the tidal current dominance on the lower shoreface appears to be of great importance.

Omitting certain physical processes and only including waves and a tidal current in examining sediment transport resulted in a seaward (tidal current induced) sediment transport on the lower shoreface. However, Borst (1987) concluded that a residual flow due to upwelling is present on the lower shoreface. As sediment transport is in the direction of the current, sediment transport is onshore directed. Also the influence of the river Rhine is important considering cross-shore sediment transport along the Holland Coast. The freshwater debouching from the river Rhine into the North Sea and the presence of Coriolis, which is caused by the earth's rotation, cause that the fresh water that enters the North Sea in the south bends towards the north. As a result salinity gradients over depth are present on the shoreface (especially along the southern Holland Coast which may cause an onshore net flow component (De Boer, 2008)).

7.3 Recommendations

In response with the given conclusions and discussion, some recommendations will be presented. First some recommendations to Unibest-TC, concerning long term simulations, will be given. Subsequently, recommendations how to improve or extend this research will be presented.

The model Unibest-TC should be calibrated or the settings should be adjusted such that the alongshore tidal velocity represents realistic values and such that a realistic behaviour of alongshore bars is present running a 100-year simulation. By adding boundary conditions to the calculation of the water depth dependent alongshore tidal velocity for instance, the alongshore tidal velocity in deeper water can be reduced. Another interesting adjustment to the model would be the implementation of a variable grain size per depth contour and variable grain size layers. As investigated by Van Straaten (1965) the shoreface of the Holland Coast roughly consists of a different grain size per depth contour (per meter water depth). Considering the 100-year evolution of the shoreface profile, a degradation of 20cm is

present at e.g. -20m NAP. Including variable grain size layers can take into account hard erodible layers, which might be present at -20m NAP and influence sediment transport such that the erosion is reduced.

Evaluating the propagation of sand pits is affected by the uniform profile assumption and overestimation of the tidal current. To examine the influence of the shoreward sand pit propagation caused by an alongshore uniform profile assumption, the alongshore length of the sand pit at which the tidal current related sediment transport S_{tide} becomes dominant inside the sand pit should be investigated. As it was concluded to be the tidal current influence that predominantly causes an onshore sand pit propagation in deep water, it is interesting to investigate the alongshore length of the sand pit at which the tidal current has no influence on a shoreward propagation. Furthermore, using variable geometry of the sand pit can change the behaviour of the sand pit due to changing sediment transport gradients. Also a different or a variable grain size can affect the propagation of the sand pits.

To extend the investigation of profile perturbations on the shoreface profile, one can use different shoreface profiles. For instance, a shoreface profile including sand banks on the lower shoreface can be used to examine the propagation of sand pits and compare this with the results of this research. Moreover, instead of examining profile perturbations on the lower shoreface, one could investigate perturbations located on the upper shoreface and evaluate its response.

Recommendations using Unibest-TC:

- Adjustment of the model Unibest-TC:
  - Proper inclusion of the tidal velocity
  - Including variable grain size layers
- Use a different geometry of the profile perturbations.
- Investigate the influence of sand banks, present on the lower shoreface, on the time scale of sediment transport on various depth contours.

Finally, some physical processes have been excluded in this research. However, as concluded by Borst (1987) upwelling causes an onshore residual flow. So, physical processes like up- and downwelling and sediment transport due to wind should be taken into account in investigating sediment transport on various depth contours and the shoreface profile evolution. At last, model results should be compared with recorded data to actually verify its outcome.

Other recommendations (using a 3D model):

- Investigate the tidal current dominance on the lower shoreface more elaborately.
- Investigate the interaction between waves and tidal currents on the lower shoreface more elaborately.
- Investigate the alongshore length of the sand pit at which the tidal current has no influence on a shoreward propagation.
- Investigate the influence of including wind, up- and downwelling and density gradients with respect to cross-shore sediment transport.
- Verify results with recorded data.

8 Summary

The scientific foundation to maintain the Holland Coast shoreward of the -20m depth contour is limited. It is assumed that profile perturbations shoreward of the -20m depth contour influence the coast within a time scale of 50 to 200 years. Hence, seaward of -20m NAP dredging companies are allowed to dredge, and apply dredged material in nourishments near the beach to naturally preserve the shoreface of the Dutch Coast. It would be economically beneficial for dredging companies to dredge closer to coast, because the -20m NAP depth contour is located 5 -20km offshore. Secondly, as Dutch Coastal policy prescribes the sediment volume of Holland Coast should be preserved shoreward of the -20m depth contour. The required volume to achieve this can be significantly reduced in case a shallower depth contour is assumed. In order to investigate the influence of profile perturbations shoreward of -20m NAP and to validate the scientific foundation of the -20m depth contour, sediment transport on various depth contours will be analysed in this thesis. The emphasis will lie on sediment transport on the lower shoreface (deeper than -10m NAP).

To gain insight in sediment transport on various depth contours, the model Unibest-TC will be used to examine sediment transport sensitivity for a range of parameter settings. Hence, to identify the dominant processes on the shoreface (see chapter 3). First, a straight gentle slope steepness of 1:1000 (for all depth contours) including a fixed grain size of 200µm, normal incident waves and variable wave height H_{rms}, period T and water depth will be assumed. By examining the dominance, direction and magnitude of four different sediment transport components (S_{sw}, S_{sc}, S_{bw} and S_{bc}), sediment transport on various depth contours will be analysed. Subsequently, sediment transport due to a variable slope steepness, grain size and magnitude of the Longuet-Higgins streaming (LH-streaming) will be evaluated. Sediment transport responds as expected, for instance a smaller grain size induces larger sediment transport. Furthermore, sediment transport is slope steepness and water depth dependent, and the magnitude of the LH-streaming is determinative for the direction of sediment transport.

Elaborating on transport equations and using non-dimensional numbers, to further analyse sediment transport on various depth contours, will give more insight in sediment transport dependencies. Evaluating sediment transport processes indicate that the direction, dominance and magnitude of sediment transport depends on the wave steepness in combinations with the slope steepness for certain depth contours. Furthermore, transport equations signify that the vertical velocity profile, wave orbital velocity and degree of wave breaking are important in determining the dominant transport component. Wave orbital velocity induced streaming along the bed versus the vertical velocity dependent return current determine whether onshore directed S_{bw} or the offshore directed S_{sc} is dominant.

As it was concluded that sediment transport i.e. slope steepness and water depth dependent, a realistic shoreface profile (Noordwijk) will be considered to analyse sediment transport (in contrast to the assumption of a fixed slope steepness for all depth contours in chapter 3). Using a fixed grain size of 200µm and a variable wave height and period to gain more insight in the dominant processes per water depth indicate that, S_{bw} is dominant on the lower shoreface, whereas suspended transport is dominant on the upper shoreface. The onshore directed S_{bw} is dominant on the lower shoreface, provided that the orbital velocity induced shear stress exceeds the critical shear stress. On the upper shoreface, the in offshore direction S_{sc} and S_{sw} are dominant, because the turbulence generated by breaking waves is very effective in keeping sediment into suspension.

After evaluating sediment transport due to waves only, the analysis of sediment transport on the shoreface will be extended by adding a variable wave angle and a tidal current. The underlying idea is to check the hypothesis stating that suspended load transport is dominant on the lower shoreface and the hypothesis stating that continuous processes are responsible for the lower shoreface morphodynamics. To examine the latter hypothesis, percentages of occurrence per wave conditions will be multiplied with sediment transport, which will reveal the relative dominance of certain wave conditions. However, sediment transport due to obliquely incident waves and including a tidal current will be analysed. Adding a variable wave angle and tidal current indicates a tidal current induced offshore S_{sc} dominance on the lower shoreface. Onshore wave related sediment transport is dominant on the upper shoreface. The direction of the waves in combination with the tidal current influences S_{bw} the most, S_{bw} is onshore when waves and tide are in the same direction and is offshore in case of opposite direction.

Examining sediment transport on the shoreface profile validates the statement that suspended transport is dominant on the lower shoreface and bed load transport can be neglected in case a tidal current is implemented in the model. Sediment transport at -15m NAP till -25m NAP is dominated by the offshore directed S_{sc}, whereas S_{bw} is negligible (figure 5.7). Subsequently, evaluating the hypothesis stating that continuous processes are responsible for the lower shoreface morphodynamics, in contrast to the even-driven processes can be confirmed as well. Wave conditions with a wave height smaller than $H_{rms} = 2m$ are responsible for the lower shoreface morphodynamics (figure 5.7). However, this result can be questioned as, amongst others, Stive and de Vriend (1995) conclude that the very event-driven processes are responsible for the lower shoreface morphodynamics. As they used only one representative wave period assigned to one representative wave height, multiple wave periods assigned to one representative wave height is used here (see appendix 2). That means that low amplitude waves with long periods are included as well. As it was concluded in chapter 3 and 4, long wave periods induce an enhanced streaming along the bed, and therefore an enhance bed load transport, in comparison to short wave periods. Hence, the inclusion of long waves periods assigned to waves with a wave height smaller than $H_{rms} = 2m$ are responsible for the lower shoreface morphodynamics.

Finally, morphological simulations will be performed to investigate the 100-year evolution of the shoreface profile of Noordwijk. In addition, the effect of profile perturbations located at -15m, -20m and -25m NAP will be examined. A situation including waves and a tidal current and a situation including only waves will be considered in analysing morphological simulations. Comparing a situation including and excluding a tidal current result in a tidal current induced offshore S_{sc} on the lower shoreface, which flattens. Wave action on the upper shoreface induces a steeper upper shoreface profile for both situations. Concerning perturbations on the lower shoreface, tidal current induced sediment transport gradients cause shoreward sand pit propagation. The depth dependent tidal velocity stirs up more sediment inside the sand pit, by which the induced gradients cause shoreward sand pit propagation. Also in case of artificial ridges, a shoreward propagation is present. A situation including a tidal current results in a farther shoreward propagation of the perturbations at -25m than at -15m NAP. An explanation for this phenomenon is that larger sediment transport gradients are present at -25m NAP which are induced by the square root of depth dependent tidal velocity. So, the interaction of waves and tidal currents is of great importance on the entire shoreface profile and may have a large impact on cross-shore sediment transport. In particular tidal currents are dominant in transporting sediment on the lower shoreface.

References

Alphen, J.S.L.J. van and M.A. Damoiseaux, 1987. A morphological map of the Dutch shoreface and adjacent part of the continental shelf (1:250000). Nota NZ-N-87.21/MDLK-R-87.18. Rijkswaterstaat Directie Noordzee/Meekundige Dienst

Alphen, J.S.L.J. van, F.P. Hallie, J.S. Ribberink, J.A. Roelvink and C.J. Louisse, 1990. Offshore sand extraction and nearshore profile nourishment (The Dutch Coast: Paper No. 12)

Battjes, J.A. and Janssen, J.P.F.M., 1978. Energy loss and set-up due to breaking in random waves. Proc. 16th Int. Conf. On Coastal Eng., ASCE, pp. 569-587.

Battjes, J.A., 1974. Surf similarity: Proceedings of the 14th International Conference on Coastal Engineering, Copenhagen, Vol. 1, pp. 467-479.

Beets, D.J., Van der Valk, L. and Stive, M.J.F., 1992. Holocene evolution of the coast of Holland. Mar. Geol., 103: 423-443

Beets, D.J., Van der Spek, A.J.F., 2000. The Holocene evolution of the barrier and the back-barrier basins of Belgium and the Netherlands as a function of late Weichselian morphology, relative sea-level rise and sediment supply. Geologie en Mijnbouw / Netherlands Journal of Geosciences 79(1) 2000.

Boer, G.J. de, 2008. On the interaction between tides and stratification in the Rhine Region of Freshwater Influence. Proefschrift. ISBN 978-90-9023848-7

Borst, J.C., 1987. Verkennende beschrijving van het stroomklimaat in het kustvak Delfland (in Dutch). Rijkswaterstaat, Nota GWAO-87.477, The Hague, The Netherlands.

Bosboom, J. and Stive, M.J.F., 2011. Coastal Dynamics ι lecture notes CT4305 version 0.2. Delft University of Technology

Bowen, A.J., 1980. Simple models of nearshore sedimentation; beach profiles and longshore bars. In: S.B. McCann (Editor), The Coastline of Canada. Geol. Surv. Can. Pap., 80-10: 1-11.

Groenendijk, F.C., 1992. T0-berekening, Status quo van Unibest-TC. Ministerie van Verkeer en Waterstaat. Dictoraat-Generaal Rijkswaterstaat.

Hallermeier, R.J., 1981. A profile zonation for seasonal sand beaches from wave climate. J. Coastal Eng., 4: 253-277.

Hisgen, R.G.W. and Laane, R.W.P.M., 2004. Geheim van het Getij. Sdu uitgevers bv, Den Haag.

Rijkswaterstaat, 1989. Kustverdediging na 1990: Discussienota and Technish rapport 0. Rijkswaterstaat.

Kragtwijk, N.G., 2001. Aggregated scale modelling of tidal inlets of the Wadden Sea. Morphological response to the closure of the Zuiderzee. Delft.

Longuet-Higgins, M.S., 1953. Mass transport in water waves. Philos. Trans. R. Soc., Ser. A, 245: 535-581.

Nairn, R.B., Roelvink, J.A. and Southgate, H.N., 1990. Transition zone width and implications for modelling surfzone hydrodynamics. Proceedings of the Int. Conf. Coastal Eng. Conference, Delft, The Netherlands, pp. 68-82.

Nicols R.J., Larson, M., Capobianco, M. and Birkemeier, W.A., 1998. Depth of closure: Improving understand and prediction. Coastal Engineering 1998: 2888-2901.

Niedoroda, A.W., D.J.P. Swift and T.S. Hopkins (1985), The shoreface. In: R.A. Davis jr. (ed.) Coastal sedimentary environments. 2nd ed. Springer-Verlag, New York, pp. 533-624.

Rijkswaterstaat, 1994. Validation of TRIWAQ-computations (in Dutch), Note RIKZ/OS-94.111, The Hague, The Netherlands.

Rijn, L.C. van, 1994. Principles of sediment transport in rivers, estuaries and coastal seas. Aqua Publ. (The Netherlands).

Rijn, L.C. van, A.J.H.M. Reniers, T.J. Zitman, J.S. Ribberink, 1995. Yearly-averaged sand transport at the -20m and -8m NAP depth contours of the JARKUS profiles 14, 40, 76 and 103. Rijkswaterstaat, Project Kustgenese.

Roelvink, J.A. and M.J.F. Stive, 1989. Bar-generating cross-shore flow mechanisms on a beach, Journal of Geophysical Research, Vol. 94, pp. 4785-4800.

Roelvink, J.A. and Reniers, A.J.H.M., 1994. Upgrading of a quasi-3D hydrodynamic model. Abstracts-in-depth, MAST G8-M overall workshop, Gregynog.

Roskamp, A.P., 1988. Golfklimaten voor de Nederlandse kust, Nota GWAO-88.046. Rijkswaterstaat, Den Haag.

Ruessink, B.G., Y. Kuriyama, A.J.H.M. Reniers, J.A. Roelvink and D.J.R. Walstra, 2007. Modeling cross-shore sandbar behavior on the timescale of weeks. Journal of Geophysical Research, Vol. 112, F03010, pp. 1-15.

Stive, M.J.F., D.A. Roelvink and H.J. de Vriend, 1990. Large-scale coastal evolution concept. (The   Dutch Coast: Paper No. 9)

Stive, M.J.F. and H.J. de Vriend, 1995. Modelling shoreface profile evolution, Marine Geology 126 (1995) 235-248.

Stolk, A., 1989. Zandsysteem kust, een morfologische karakterisering. Technisch rapport 1. Rijksuniversiteit Utrecht, Vakgroep Fysische Geografie. Rapport GEOPRO 1989.02. Kustverdediging na 1990.

Straaten, L.M.J.U. van, 1965. Coastal barrier deposits in South- and North-Holland; in particular in the areas around Scheveningen and Ijmuiden. Geologisch instituut; Melkweg 1; Groningen, Netherlands. Mededelingen van de Geologisch Stichting, Nieuwe serie no. 17.

Valk, L van der, 1996. Geology and sedimentology of Late Atlantic, wave-dominated deposits near The Hague (South-Holland, the Netherlands): a reconstruction of an early prograding coastal sequence. Mededelingen Rijks Geologische Dienst 57: 201-228.

Walstra, D.J.R., Reniers, A.J.H.M., Ranasinghe, R., Roelvink, J.A. and Ruessink, B.G., 2012. On bar growth and decay during interannual net offshore migration. Coastal Engineering 60 (2012) 190-200

List of figures

Appendix 1:   Unibest-TC settings

Unibest-TC settings Chapter 3-4			
Grid	IBOD	0	Calculate bottom change
	USTRA	0	Transport at shoreward boundary
	TW_W	10	Water temperature [°C]
	SALIN	0	Salinity
	TDRY	40	Maximum relative wave period
	ZUV	0.1	Height at which ux and uy are extracted
Waves	ALFAC	1	Wave breaking parameter
	GAMMA	0	Wave breaking parameter (H_{max})
	BETD	0.1	Slope of wave front
	FWEE	0.01	Friction factor for bottom
	C_R	0.25	Correlation coefficient bound long waves
	K_IJL	1	Breaker delay
	F_LAM	2	Number of wave lengths for depth integration
	POW	1	Power in weighting function
	DEEP_V	-5000	Seaward boundary for reduction factor
	SHALL_V	-5000	Seaward boundary for reduction factor
Currents	FCVISC	0.1	Viscosity coefficient
	RKVAL	0.01	Friction factor for mean current
	DIEPV	5	Reference depth for tidal velocity
Sediment:	D50	0.0002	Median grain size
	D90	0.0003	Grain size
	DSS	0.00017	Grain size for suspended sediment
	DVAR	1	Cross-shore varying grain size
Transport:	RC	0.01	current related roughness
	RW	0.002	Wae related roughness
	REMLG	0.1	Fixed bottom layer (zero transport)
	TANPH1	0.3	Internal friction angle at location X1
	TANPH2	0.3	Internal friction angle at location X2
	XF1	-10000	Most seaward loction
	XF2	-5000	Most seaward loction
	ZDRY	2	Extrapolation of transport over dry part of profile
	FACQB	0	Reduction factor on fraction of breaking waves
	ASFAC	0.2	Wave-related suspended transport phase lag coefficient
	FACDEL	20	Thickness of wave boundary layer
	FACDS	1	Streaming factor

Unibest-TC settings Chapter 5-6			
Grid	IBOD	1	Calculate bottom change
	USTRA	0	Transport at shoreward boundary
	TW_W	10	Water temperature [°C]
	SALIN	0	Salinity
	TDRY	40	Maximum relative wave period
	ZUV	0.1	Height at which ux and uy are extracted
Waves	ALFAC	1	Wave breaking parameter
	GAMMA	0	Wave breaking parameter (H_{max})
	BETD	0.1	Slope of wave front
	FWEE	0.01	Friction factor for bottom
	C_R	0.25	Correlation coefficient bound long waves
	K_IJL	1	Breaker delay
	F_LAM	2	Number of wave lengths for depth integration
	POW	1	Power in weighting function
	DEEP_V	-5000	Seaward boundary for reduction factor
	SHALL_V	-5000	Seaward boundary for reduction factor
Currents	FCVISC	0.1	Viscosity coefficient
	RKVAL	0.01	Friction factor for mean current
	DIEPV	5	Reference depth for tidal velocity
Sediment:	D50	0.0002	Median grain size
	D90	0.0003	Grain size
	DSS	0.00017	Grain size for suspended sediment
	DVAR	0	Cross-shore varying grain size
Transport:	RC	0.01	current related roughness
	RW	0.002	Wae related roughness
	REMLG	0.1	Fixed bottom layer (zero transport)
	TANPH1	0.15	Internal friction angle at location X1
	TANPH2	0.15	Internal friction angle at location X2
	XF1	-750	Most seaward loction
	XF2	-120	Most seaward loction
	ZDRY	2	Extrapolation of transport over dry part of profile
	FACQB	0	Reduction factor on fraction of breaking waves
	ASFAC	0.2	Wave-related suspended transport phase lag coefficient
	FACDEL	20	Thickness of wave boundary layer
	FACDS	1	Streaming factor

Sediment transport on various depth contours of the 'Holland Coast' shoreface

Appendix 2: Occurrence tables


```
              1      2      3      4      5      6      7      8      9     10     11     12
            2.5    3.5    4.5    5.5    6.5    7.5    8.5    9.5   10.5   11.5   12.5   13.5
Hs \ Tp     3.5    4.5    5.5    6.5    7.5    8.5    9.5   10.5   11.5   12.5   13.5   13.7
0.05  0.15  0.11   0.58   0.49   0.11   0.02   0.01   0.00   0.00   0.00   0.00   0.00   0.00    1.32
0.15  0.25  1.35   4.82   3.21   0.98   0.31   0.11   0.04   0.01   0.00   0.00   0.00   0.00   10.83
0.25  0.35  2.15   4.72   3.21   1.50   0.42   0.12   0.05   0.02   0.00   0.00   0.00   0.00   12.20
0.35  0.45  1.51   4.23   3.33   1.90   0.57   0.10   0.02   0.01   0.00   0.00   0.00   0.00   11.68
0.45  0.55  0.66   3.76   3.76   2.06   0.63   0.12   0.01   0.01   0.00   0.00   0.00   0.00   11.01
0.55  0.65  0.18   2.45   3.99   1.89   0.60   0.09   0.01   0.00   0.00   0.00   0.00   0.00    9.20
0.65  0.75  0.04   1.47   4.02   1.87   0.45   0.07   0.00   0.00   0.00   0.00   0.00   0.00    7.94
0.75  0.85  0.01   0.66   3.58   1.67   0.40   0.06   0.00   0.00   0.00   0.00   0.00   0.00    6.39
0.85  0.95  0.00   0.23   3.12   1.99   0.40   0.05   0.01   0.00   0.00   0.00   0.00   0.00    5.80
0.95  1.05  0.00   0.05   1.94   2.03   0.32   0.04   0.00   0.00   0.00   0.00   0.00   0.00    4.38
1.05  1.15  0.00   0.02   1.19   2.03   0.33   0.04   0.01   0.00   0.00   0.00   0.00   0.00    3.63
1.15  1.25  0.00   0.01   0.70   1.99   0.33   0.04   0.00   0.00   0.00   0.00   0.00   0.00    3.08
1.25  1.35  0.00   0.00   0.26   1.84   0.37   0.04   0.01   0.00   0.00   0.00   0.00   0.00    2.52
1.35  1.45  0.00   0.00   0.11   1.35   0.45   0.06   0.01   0.00   0.00   0.00   0.00   0.00    1.98
1.45  1.55  0.00   0.00   0.03   1.05   0.52   0.04   0.00   0.00   0.00   0.00   0.00   0.00    1.65
1.55  1.65  0.00   0.00   0.01   0.70   0.56   0.06   0.01   0.00   0.00   0.00   0.00   0.00    1.33
1.65  1.75  0.00   0.00   0.00   0.41   0.58   0.09   0.01   0.00   0.00   0.00   0.00   0.00    1.09
1.75  1.85  0.00   0.00   0.00   0.23   0.53   0.09   0.01   0.00   0.00   0.00   0.00   0.00    0.86
1.85  1.95  0.00   0.00   0.00   0.09   0.43   0.09   0.01   0.00   0.00   0.00   0.00   0.00    0.62
1.95  2.05  0.00   0.00   0.00   0.05   0.37   0.12   0.02   0.00   0.00   0.00   0.00   0.00    0.56
2.05  2.15  0.00   0.00   0.00   0.01   0.26   0.11   0.02   0.00   0.00   0.00   0.00   0.00    0.40
2.15  2.25  0.00   0.00   0.00   0.00   0.21   0.13   0.01   0.00   0.00   0.00   0.00   0.00    0.35
2.25  2.35  0.00   0.00   0.00   0.00   0.11   0.11   0.03   0.00   0.00   0.00   0.00   0.00    0.25
2.35  2.45  0.00   0.00   0.00   0.00   0.05   0.11   0.02   0.01   0.00   0.00   0.00   0.00    0.19
2.45  2.55  0.00   0.00   0.00   0.00   0.03   0.10   0.02   0.00   0.00   0.00   0.00   0.00    0.16
2.55  2.65  0.00   0.00   0.00   0.00   0.02   0.08   0.03   0.00   0.00   0.00   0.00   0.00    0.13
2.65  2.75  0.00   0.00   0.00   0.00   0.01   0.05   0.02   0.00   0.00   0.00   0.00   0.00    0.08
2.75  2.85  0.00   0.00   0.00   0.00   0.00   0.05   0.02   0.00   0.00   0.00   0.00   0.00    0.08
2.85  2.95  0.00   0.00   0.00   0.00   0.00   0.03   0.03   0.01   0.00   0.00   0.00   0.00    0.07
2.95  3.05  0.00   0.00   0.00   0.00   0.00   0.02   0.02   0.00   0.00   0.00   0.00   0.00    0.05
3.05  3.15  0.00   0.00   0.00   0.00   0.00   0.01   0.03   0.01   0.00   0.00   0.00   0.00    0.05
3.15  3.25  0.00   0.00   0.00   0.00   0.00   0.01   0.02   0.01   0.00   0.00   0.00   0.00    0.04
3.25  3.35  0.00   0.00   0.00   0.00   0.00   0.01   0.01   0.00   0.00   0.00   0.00   0.00    0.02
3.35  3.45  0.00   0.00   0.00   0.00   0.00   0.00   0.01   0.00   0.00   0.00   0.00   0.00    0.02
3.45  3.55  0.00   0.00   0.00   0.00   0.00   0.00   0.01   0.01   0.00   0.00   0.00   0.00    0.02
3.55  3.65  0.00   0.00   0.00   0.00   0.00   0.00   0.01   0.00   0.00   0.00   0.00   0.00    0.02
3.65  3.75  0.00   0.00   0.00   0.00   0.00   0.00   0.00   0.01   0.00   0.00   0.00   0.00    0.01
3.75  3.85  0.00   0.00   0.00   0.00   0.00   0.00   0.00   0.00   0.00   0.00   0.00   0.00    0.01
3.85  3.95  0.00   0.00   0.00   0.00   0.00   0.00   0.00   0.00   0.00   0.00   0.00   0.00    0.01
3.95  4.05  0.00   0.00   0.00   0.00   0.00   0.00   0.00   0.00   0.00   0.00   0.00   0.00    0.00
4.90  5.10  0.00   0.00   0.00   0.00   0.00   0.00   0.00   0.00   0.00   0.00   0.00   0.00    0.00
            6.01  22.99  32.95  25.77   9.30   2.26   0.56   0.14   0.02   0.00   0.00   0.00  100.00
Significant wave height and peak period frequency distribution
```

Figure 2 Occurrence table. Wave height versus wave period.
Wave height classes of 10cm and wave period classes of 1s.

Appendix 3:   Classification profiles

Sediment transport on various depth contours of the 'Holland Coast' shoreface
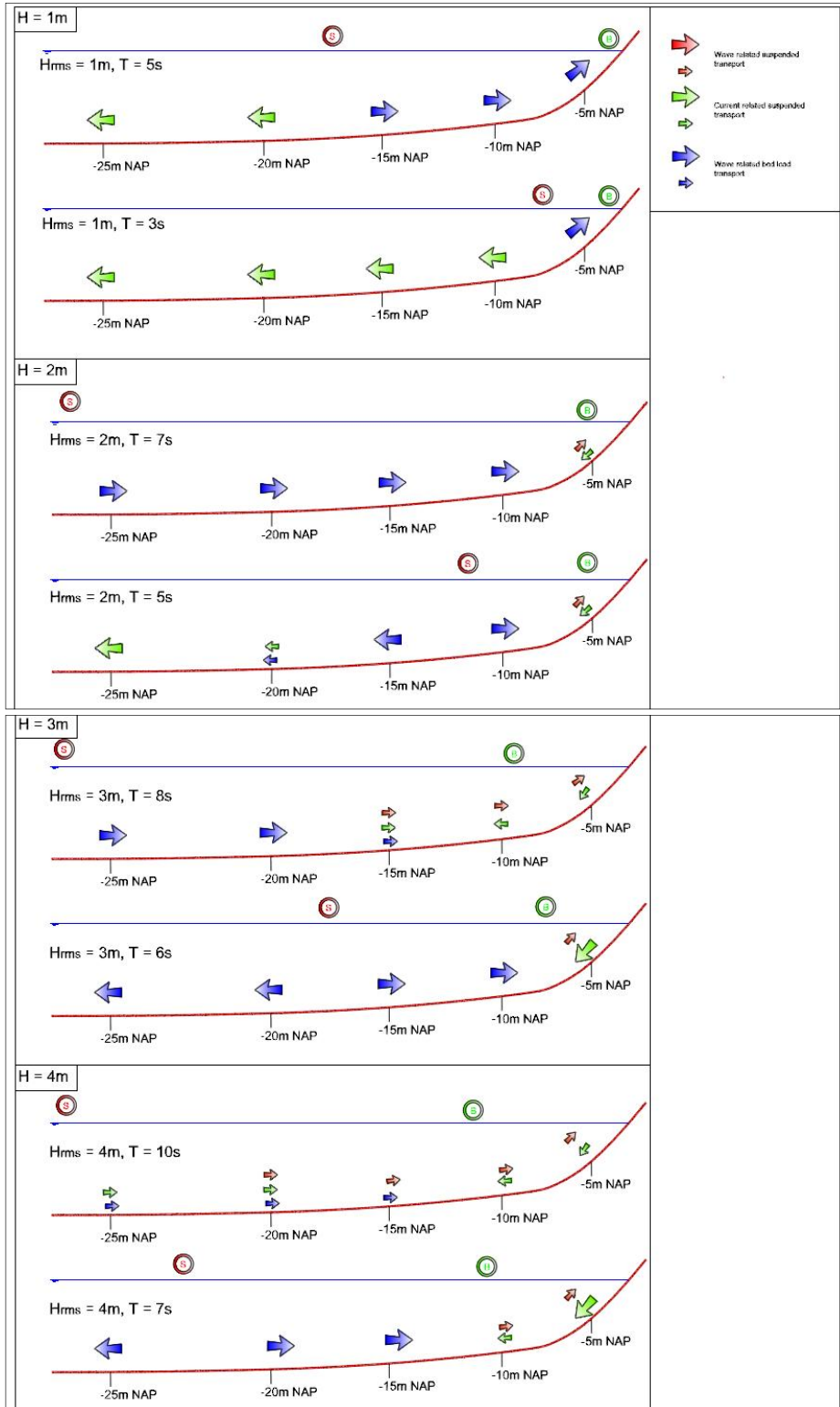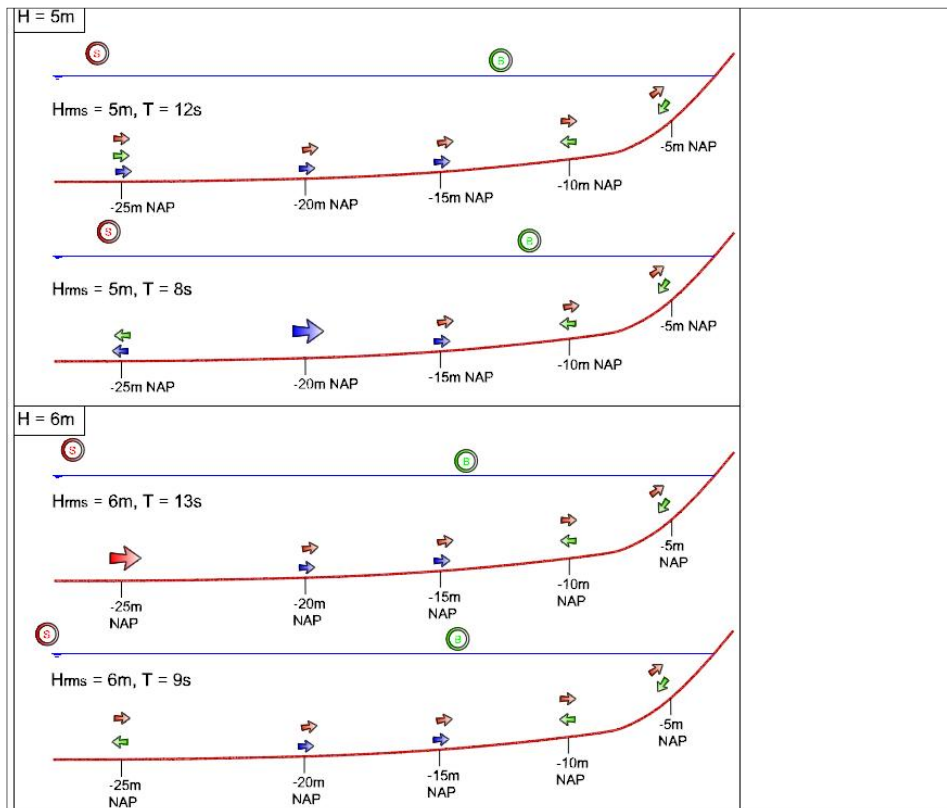
Figure 3 Classification profiles. 12 different conditions are depicted, including the direction and dominance of the different transport components. The green colour represents the S_{sc}, the blue colour S_{bw} and the red colour the S_{sw}. The transport components are illustrated from -25m NAP till -5m NAP, with an interval of 5 meters. Large arrows indicate the dominant transport mechanism; small arrows indicate the secondary transport mechanism. Furthermore, red and green circles are depicted near the water line in every subplot. The green circle represents the offshore distance at where waves start to break. The red circle signifies the offshore distance at where waves start to shoal, so where the orbital velocity induced shear stress exceeds the critical shear stress and initiates sediment transport. This figure is subdivided in 6 subplots, each representing a different wave height. In each subplot, 2 profiles are illustrated, in which the upper profile expressing a long wave period relative to the lower profile, where the wave is shorter.

Appendix 4:   100-year simulation profiles

Waves only (24yr time series)
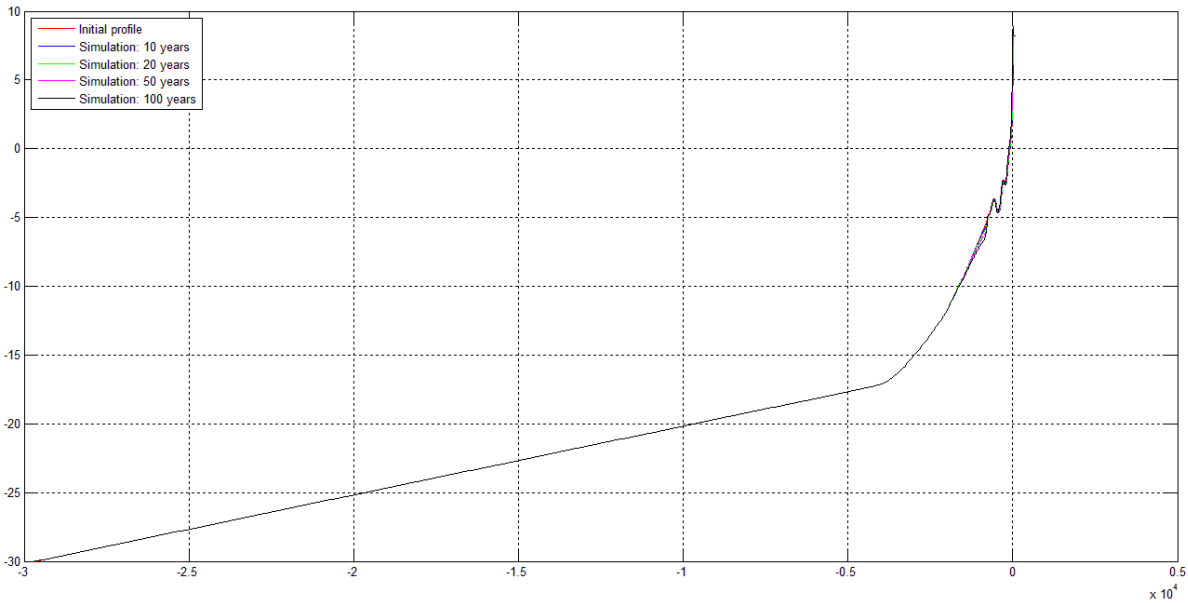
Figure 4-1 100-year simulation (excluding a tidal current)

100-year simulation (including a tidal current)
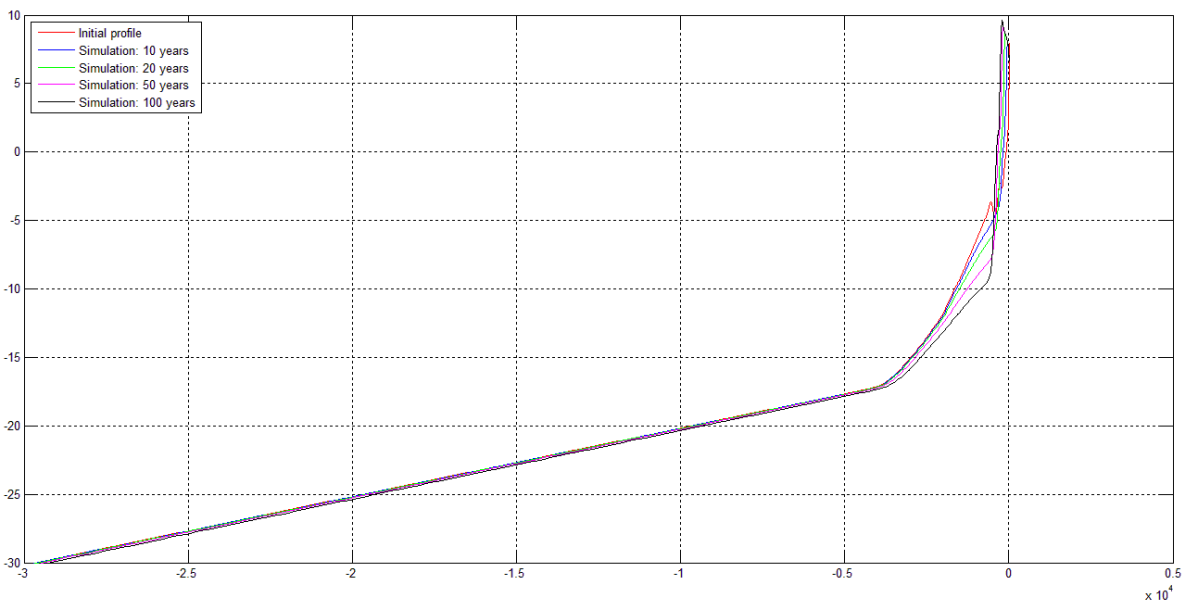
Figure 4-2 100-year simulation (including a tidal current)

Sediment transport on various depth contours of the 'Holland Coast' shoreface

Appendix 5:   Average total sediment transport
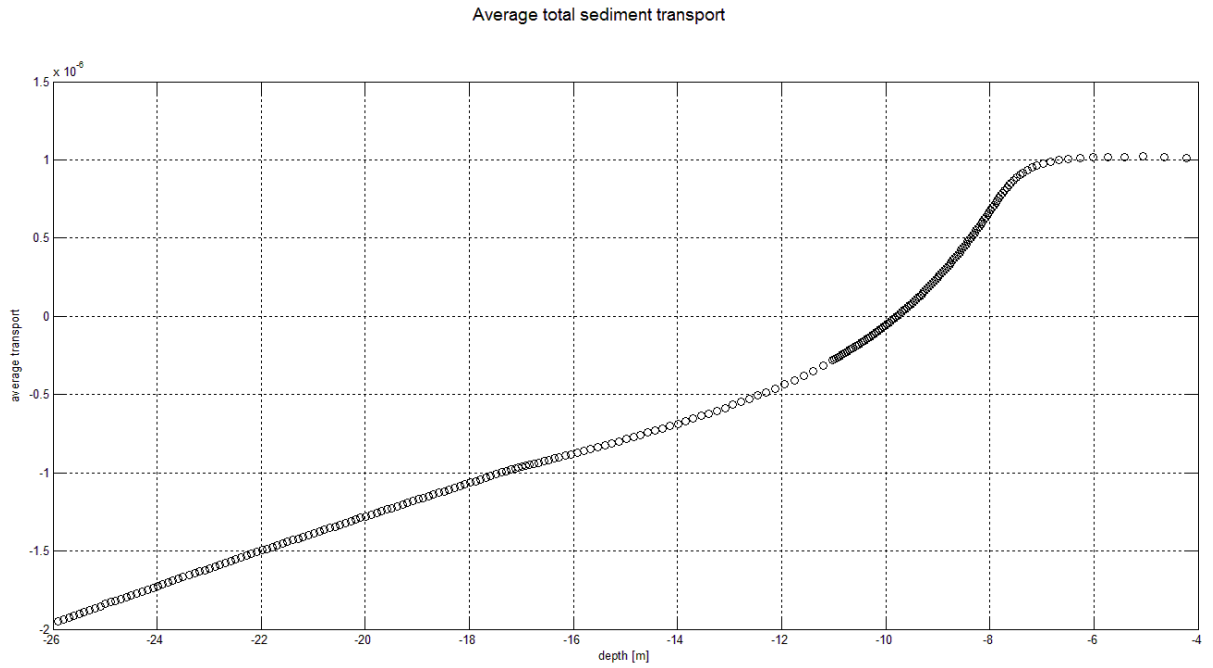
Figure 5 Average total sediment transport versus water depth

Appendix 6: Propagation of sand pits and artificial ridges
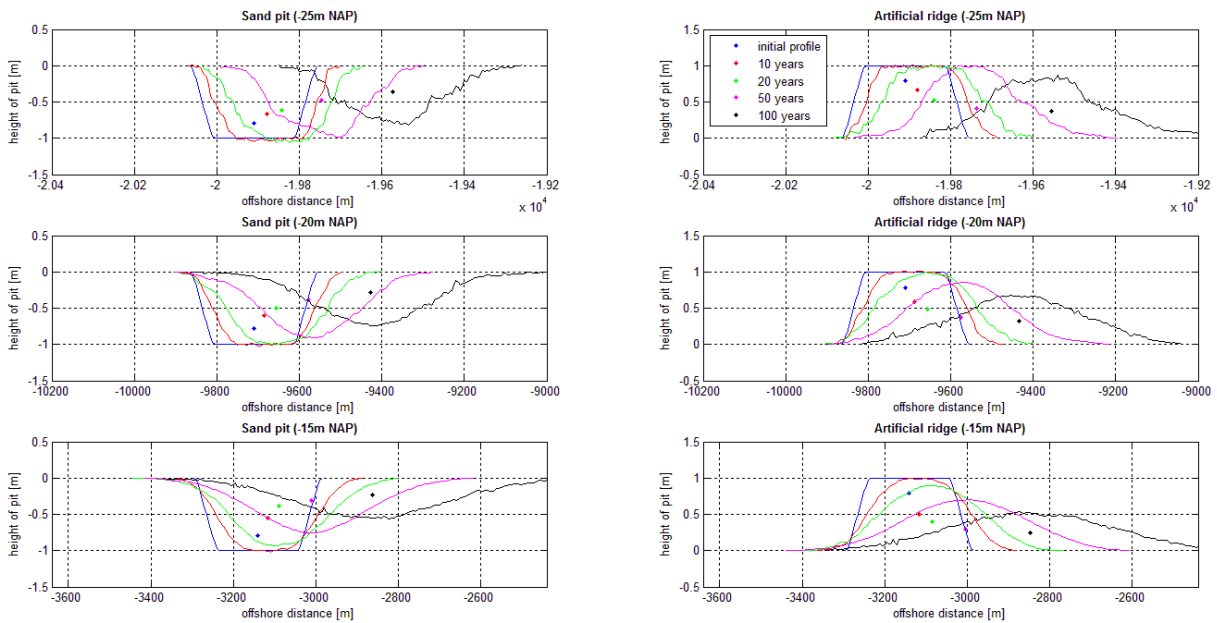
Figure 6 Propagation of sand pits and artificial ridges. The left column includes sand pits, whereas the right column includes artificial ridges. The shore is located at the right side of the sub plots.

Appendix 7: Sensitivity analysis

The model Unibest-TC includes many parameters, which all can affect sediment transport. Therefore, a sensitivity analysis will be performed to examine the robustness of the findings in section 5.2. Relevant parameters will be varied to examine whether the transport pattern will change or remain unchanged. The considered relevant parameters read:

- BETD: Roller dissipation parameter (expressing the steepness of the wave).
- FWEE: Friction factor for bed load transport.
- FCVISC: Viscosity coefficient of vertical velocity profile.
- RKVAL: Friction factor for mean current computation.
- C_R: Correlation coefficient between wave envelope and bound long waves.
- RW: Wave related roughness for sediment transport computation.
- RC: Current related roughness for sediment transport computation.

The BETD-parameter determines the cross-shore distribution of the surface shear stress due to wave breaking. This parameter influences the roller dissipation and is especially important on top or behind bars, see Walstra (2012). However, as examined in chapter 3 and 4, surface shear stress can be important regarding shallow water and is therefore taken into account. The friction factor for bed load transport (FWEE) influences the amount of wave dissipation due to bottom friction. So over a long distance the wave height may be influenced. Hence, the offshore extension of the wave related transport dominance can be affected.

Whereas the previous two parameters affect the wave forcing, the FCVISC- and RKVAL-parameters influence the mean current. The viscosity coefficient can influence the velocity profile, similar to as was explained in section 3.3. A higher viscosity coefficient results in a higher viscosity and will reduce the velocity gradient. A flatter velocity profile and therefore a reduced return current is the consequence. Likewise, the RKVAL-parameter affects the velocity profile by reducing the velocities in case higher values are used. Higher values result in a higher bed shear stress, because this parameter is in fact a roughness height.

The C_R-parameter arranges the phase shift between the long waves and short wave envelope (Roelvink and Stive, 1989). The phase shift is important, which can cause an increased offshore transport outside of the surfzone and onshore transport inside the surfzone, in case of a high value. Outside of the surfzone, the long waves are bound and sediment transport is onshore under the wave crest and offshore under the wave trough. Because the short waves are highest in the trough of the bound long wave and are able to stir up more sediment, sediment transport is offshore. Setting the C_R parameter to zero ignores this effect. Finally, the wave related and current related roughness (RW and RC) can be used to tune the transports.

Results
Similar to section 5.2, histograms will be used again to be able to perceive changes in the transport pattern. A scenario including a tidal velocity will be considered and to examine the sensitivity, the mentioned parameters will be halved and doubled regarding their default value.

Varying the roller dissipation parameter does not affect the transport rates, viz. the height of the bars of the histograms do not change. Only near-shore it has effect, though, its effect is negligibly small. Subsequently, increasing the friction factor for bed load transport decreases the transport rates in shallow water as was expected regarding the FWEE-parameter influence. Considering a low value of the friction factor results in the opposite, viz. increasing transport rates. Even though the transport rates change, the transport pattern over the entire shoreface remains unchanged. In fact, this is also the case for the remaining parameters. Locally, it affects the transport rates, but sediment transport remains offshore deeper than -15m and onshore shallower than -10m NAP.

In view of these results, which have been depicted in figure 5.8, the upper shoreface is steepening whereas the lower shoreface is flattening. Although it should be examined using morphological simulations, whether investigating sediment transport on the shoreface show similar results. Having performed an analysis, including waves and a tidal current, and a sensitivity analysis, it can be concluded that the tidal current is responsible for the offshore transport on the lower shoreface. Waves become dominant on the upper shoreface, which accretes.
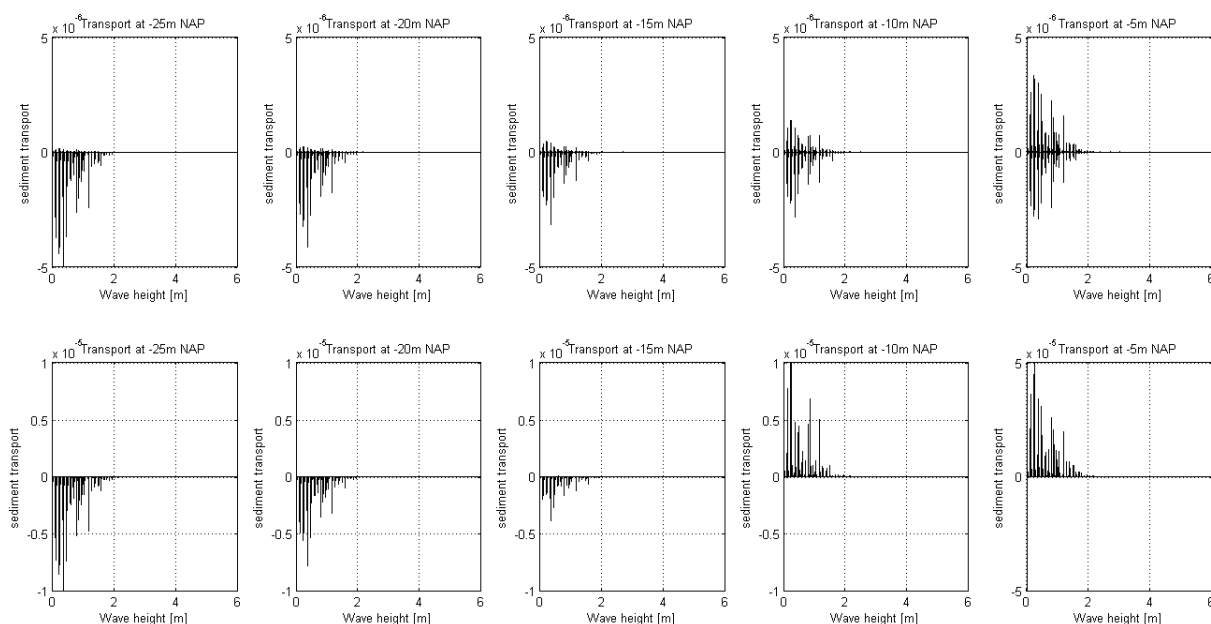
Figure 7 Histograms versus wave classes (H_{rms}) including a tidal current. The histograms indicate the sediment transport multiplied with the percentage of occurrence per wave condition. The black bars represent the total sediment transport. The upper subplots include all sediment transport components, whereas the lower subplot only includes the total transport. It should be mentioned that the vertical axes are variable.